Low-scale leptogenesis and right-handed electrons

DENNIS SCHRÖDER

Abstract

We develop a framework for obtaining rate coefficients in non-linear kinetic equations for slowly evolving quantities in a non-equilibrium system by matching real time correlation functions of thermal fluctuations computed in an effective description to those computed in thermal quantum field theory. We apply this formalism to sterile neutrino occupancies and lepton minus baryon numbers. After expanding in the sterile-neutrino Yukawa couplings, the coefficients in the equations are written as real time correlation functions of Standard Model operators. Our kinetic equations are valid for an arbitrary number of sterile neutrinos of any mass spectrum. They can be used to describe, e.g., low-scale leptogenesis via neutrino oscillations, or sterile neutrino dark matter production in the Higgs phase. We apply the formula for linear coefficients to the equilibration of right-handed electrons in the symmetric phase of the Standard Model, which happens relatively late in the history of the Universe due to the smallness of the electron Yukawa coupling. We compute the equilibration rate at leading order in the Standard Model couplings by including gauge interactions, the top Yukawa- and the Higgs self-interaction. The dominant contribution is due to $2 \to 2$ particle scattering, even though the rate of (inverse) Higgs decays is strongly enhanced by multiple soft scattering which is included by Landau-Pomeranchuk-Migdal (LPM) resummation. Our numerical result for the equilibration rate is substantially larger than approximations presented in previous literature. We find that the equilibration of right-handed electrons takes place at temperatures at which also low-scale leptogenesis can be realized, and we argue that in this case the two processes do not decouple.

Publications in this thesis

The vast majority of results in this thesis has been published before, in some parts literally, and in others according to their respective meaning.

The framework for obtaining non-linear coefficients in effective kinetic equations by using the theory of quasi-stationary fluctuations and the application to occupancies of sterile neutrinos and lepton minus baryon numbers has been obtained in

[1] D. Bödeker and D. Schröder,
Kinetic equations for sterile neutrinos from thermal fluctuations
JCAP **2002** (2020) 033
doi: 10.1088/1475-7516/2020/02/033
arXiv: 1911.05092 [hep-ph].

The equilibration rate of right-handed electrons, the corresponding leading order susceptibilities, and a brief elaboration on the connection to low-scale leptogenesis is found in

[2] D. Bödeker and D. Schröder,
Equilibration of right-handed electrons
JCAP **1905** (2019) 010
doi: 10.1088/1475-7516/2019/05/010
arXiv: 1902.07220 [hep-ph].

Declaration   The contents of this thesis have not been previously submitted to any examination office by the author. No other person's work has been used without due acknowledgment in this thesis. All sources of information have been specifically acknowledged.

Notation and conventions

We write four-vectors in lower-case italics, k, and the corresponding three-vectors in boldface, $\mathbf{k}$. Integrals over three-momentum are denoted by $\int_{\mathbf{k}} \equiv (2\pi)^{-3} \int d^3k$. When working in imaginary time we have four-vectors $k = (k^0, \mathbf{k})$ with $k^0 = in\pi T$ with n even (odd) for bosons (fermions), and T is the temperature. We denote fermionic Matsubara sums by a tilde, $\widetilde{\sum}_{k^0}$. The Bose-Einstein and Fermi-Dirac distributions are denoted by $f_{\mathrm{B}}(E) \equiv 1/(e^{E/T} - 1)$ and $f_{\mathrm{F}}(E) \equiv 1/(e^{E/T} + 1)$, respectively. We use the metric with signature $(+, -, -, -)$, and the totally antisymmetric tensor with $\varepsilon^{0123} = +1$. Covariant derivatives are $D_\mu = \partial_\mu + iy_\alpha g' B_\mu + \cdots$ with the hypercharge gauge coupling g' and gauge field B, such that $y_\varphi = 1/2$ for the Higgs field φ. The quartic term in the Higgs potential is $\lambda(\varphi^\dagger \varphi)^2$.

Contents

Introduction

1.1 Some shortcomings of the Standard Model

The Standard Models of particle physics and cosmology have been extremely successful in explaining various observations, in parts even with an outstanding precision. There are, however, some observations these widely accepted models fail to explain. We briefly review three of them here. In the following section 1.2 we introduce sterile neutrinos and outline how they could fill the corresponding gaps in our theoretical understanding.

1.1.1 Active neutrino masses

The famous Higgs mechanism, although providing masses for the weak gauge bosons as well as for most of the fermions, leaves the three left-handed Standard Model neutrinos exactly massless, and the generation of a mass term for these very light fermions requires physics beyond the Standard Model. An adequate theoretical description of neutrinos, however, requires such mass terms, because experiments with solar and atmospheric neutrinos show that there are indeed two non-zero squared mass differences [3][1]

$$\Delta m_{\text{atm}}^2 = 7.37(59) \cdot 10^{-5} \text{ eV}^2, \tag{1.1}$$

$$\Delta m_{\text{sol}}^2 = 2.56(13) \cdot 10^{-3} \text{ eV}^2. \tag{1.2}$$

These squared mass differences are inferred from neutrino oscillations which can be easily seen by a quantum mechanical argument as follows. Suppose that neutrinos have non-vanishing masses. Then there are two eigenbases which are

---

[1]The value in (1.2) assumes normal hierarchy, and differs from the one for inverted hierarchy only on the percent level.

not simultaneously diagonalizable: the eigenbasis of states produced and detected in weak interactions, and the mass eigenbasis corresponding to free propagation. Due to the misalignment of the two eigenbases, the weak interaction eigenstates $|\nu_\alpha\rangle$ with $\alpha = e, \mu, \tau$ contain a mixture of the mass eigenstates $|\nu_i\rangle$,

$$|\nu_\alpha\rangle = \sum_{i=1}^{3} U_{\alpha i}^* |\nu_i\rangle, \tag{1.3}$$

where U is the unitary Pontecorvo-Maki-Nakagawa-Sakata matrix. Free propagation implies for the mass eigenstates

$$|\nu_i(t)\rangle = e^{-iE_i(t-t_0)} |\nu_i(t_0)\rangle, \tag{1.4}$$

with $E_i = (|\mathbf{k}|^2 + m_i^2)^{1/2}$ and the momentum $\mathbf{k}$. Now consider a weak interaction eigenstate $|\nu_\alpha(t_0)\rangle$ at some initial time t_0. The amplitude for finding an interaction eigenstate β at a later time t is given by

$$\langle \nu_\beta(t) | \nu_\alpha(t_0) \rangle = \sum_{i=1}^{3} e^{iE_i(t-t_0)} U_{\beta i} U_{\alpha i}^*. \tag{1.5}$$

For ultrarelativistic neutrinos we approximate

$$E_i \approx |\mathbf{k}| + \frac{m_i^2}{2|\mathbf{k}|}, \tag{1.6}$$

which gives the probability

$$\left| \langle \nu_\beta(t) | \nu_\alpha(t_0) \rangle \right|^2 \approx \sum_{i,j=1}^{3} e^{i(t-t_0)(m_i^2 - m_j^2)/2|\mathbf{k}|} U_{\beta i} U_{\alpha i}^* U_{\beta j}^* U_{\alpha j}. \tag{1.7}$$

This implies that, given there are finite squared mass differences and a misalignment of the two eigenbases, the flavor eigenstates oscillate into each other. For solar neutrinos, e.g., this manifests as a lack of electron neutrinos arriving at earth-bound observatories, which has been known as the *solar neutrino problem*.

Neutrino oscillation experiments allow to determine only the squared mass differences, but they do not make statements about the absolute mass scale. The upper bound on the latter from measurements of the cosmic microwave background [4] reads

$$\sum_\alpha m_{\nu_\alpha} < 0.12 \text{ eV}. \tag{1.8}$$

1.1.2 Baryon asymmetry of the Universe

From anisotropies in the cosmic microwave background it has been inferred that at the decoupling temperature $T_{\text{dec}} = \mathcal{O}(\text{eV})$ the ratio of baryon density n_B to entropy density s is given by[2]

$$\frac{n_B}{s} = 8.71(4) \cdot 10^{-11}. \tag{1.9}$$

Here n_B is the net baryon density, so that the quantity in (1.9) is called the *baryon asymmetry* of the Universe. This quantity can also be probed at the much higher temperature of big bang nucleosynthesis, $T_{\text{BBN}} = \mathcal{O}(\text{MeV})$. Here the baryon to photon ratio enters the various reaction rates determining the processes of the generation of the light element abundances, and the result [6] is in agreement with (1.9), providing a robust measurement of n_B/s. Within the Standard Models of particle physics and cosmology the non-vanishing number (1.9) cannot be explained, unless one assumes initial conditions before inflation.

For a dynamic generation of a baryon asymmetry, generically called *baryogenesis*, three conditions have to be fulfilled. The so-called Sakharov conditions demand baryon number conservation as well as charge ($\mathcal{C}$) and charge-parity ($\mathcal{CP}$) symmetry to be broken in thermal non-equilibrium [7]. Within the Standard Model, baryon number is not conserved in the symmetric phase. $\mathcal{CP}$ violation appears in the Cabibbo-Kobayashi-Maskawa matrix in the quark sector which is, however, rather small and will be neglected throughout this thesis. In the thermal history of the Standard Model there is no epoch of strong non-equilibrium. For sufficiently small values of the Higgs mass $m_\varphi \lesssim 80$ GeV the electroweak transition would have been a first-order phase transition providing expanding bubbles of true Higgs vacua and therefore strong non-equilibrium. At the measured value of the Higgs mass $m_\varphi \approx 125$ GeV [8,9], however, the electroweak transition is only a smooth crossover [10]. Coupling the Higgs doublet to another new scalar field could generate a first-order phase transition despite the large Higgs mass. This idea is at the basis of a class of models called *electroweak baryogenesis* [11], and it relies on additional $\mathcal{CP}$ violation, since the one contained in the CKM matrix in the Standard Model is insufficient [12–14]. For a review of electroweak baryogenesis, see e.g. [15].

---

[2]The quantity $\Omega_B h^2$ has been measured by Planck [4] to a high precision. It is related to the quantity in (1.9) via $n_B/s = 3.887 \cdot 10^{-9} \, \Omega_B h^2$, see, e.g., chapter 5.2 of reference [5]. The baryon density is often conveniently normalized to entropy density, because the resulting quantity is comoving.

The cosmic QCD transition might have been of first order, if the loosely constrained lepton asymmetry was large enough [16]. However, at the QCD temperature baryon number is conserved within the Standard Model, because electroweak sphalerons are frozen out, and therefore this still open possibility for a first-order phase transition is not a very attractive setting for baryogenesis.

1.1.3   Dark matter

The energy content of the Universe, according to best fits to the ΛCDM model [4], consists of only about 5% ordinary matter (the origin of which we do not understand, see section 1.1.2), while another 23% of gravitating matter is invisible *dark matter* which does not interact via the electromagnetic force.

This mysterious type of matter had first been discovered in galaxy clusters in 1933 by making use of the virial theorem [17]. The measurement of rotation curves of galaxies beginning in the early 1970s has shown that the stars' angular velocities approach a finite constant with increasing distance from the galactic center [18], indicating that the gravitating mass also increases with distance. If most of the gravitating mass were concentrated near the galactic center, as it seems to be the case if one considers only ordinary matter, the angular velocity would be expected to fall off with increasing distance. The observed rotation curves can be explained by embedding galaxies in spherical halos of dark matter [19]. Today we have proof of the existence of dark matter also from cosmic microwave background [4, 20] and gravitational lensing [21] measurements. Currently there is a large landscape of viable dark matter models containing not only theories with additional bosonic or fermionic particles, but also primordial black holes, as well as modified theories of gravity. In analogy with ordinary matter it is easily possible for dark matter to be comprised of various constituents, especially since the Universe contains roughly five times as much dark matter as ordinary matter.

1.2   Sterile neutrinos

In this section we introduce the concept of sterile neutrinos. We set up the corresponding Lagrangian density in subsection 1.2.1, and in subsection 1.2.2 we give a short overview of how these hypothetical particles can in principle provide answers to all of the open questions raised in section 1.1, even though not necessarily to full extent at the same time.

In the Standard Model all fermions appear as pairs of left- and right-chiral fields, with the exception of neutrinos, which are incorporated only as exactly massless left-chiral fields. This way their chirality translates into helicity, so that the projection of their spin onto spatial momentum is exclusively negative, in accordance with numerous experiments, possibly most notably the famous Wu experiment[3] [22].

One philosophical question that can naturally be asked is why Nature would single out one species of fermions to appear only left-handedly, generating a somewhat incomplete particle content. A natural extension of the Standard Model would then be the introduction of right-handed neutrinos in accordance with current observational constraints. The right-handed neutrinos need to be uncharged under Standard Model gauge groups, because they have not been detected in weak-interaction experiments. Therefore they are coined *sterile*, as opposed to the left-handed neutrinos in the Standard Model, which are usually called *active* in this context, because they carry weak isospin and hypercharge.

Sterile neutrinos have not been detected at all by now which, if they exist, poses bounds on their parameters. There are generally two scenarios prohibiting a simple detection, which are somewhat contrary. If the sterile-neutrino masses are above energies reached by current accelerators, they cannot be produced in collisions. If, on the other hand, their coupling to the Standard Model is very weak, one needs specifically designed experiments, such as high intensity beam dumps, in order for them to be detected eventually [23]. In principle, a combination of these two complications is possible, but then one of the main problems motivating their introduction, namely the explanation of active neutrino squared mass differences, is not solved,[4] so this corner of parameter space is not attractive and is therefore usually left unconsidered.

1.2.1 Lagrangian

We now consider the Standard Model extended by n_s flavors of sterile neutrinos N_i. For a renormalizable extension, only a Yukawa term is allowed for fermions along with the kinetic term. Since the new fields are not charged under any gauge group, they can couple only to currents that are themselves a gauge singlet, in order not to violate the symmetries of the resulting theory under Standard Model gauge groups. These considerations leave little freedom, and one possibility to

---

[3]In the original experiment *anti*neutrinos with *positive* helicity have been emitted.
[4]We will see this below, around (1.16).

write the full Lagrangian of the system is

$$\mathscr{L} = \mathscr{L}_{\text{SM}} + \frac{1}{2} \sum_{i=1\cdots n_{\text{s}}} \overline{N}_i(i\partial\!\!\!/ - M_i)N_i - \sum_{\substack{i=1\cdots n_{\text{s}} \\ \alpha=e,\mu,\tau}} (\overline{N}_i\, h_{i\alpha}\, J_\alpha + \text{H.c.}) \tag{1.10}$$

with $\mathscr{L}_{\text{SM}}$ the Standard Model Lagrangian and the gauge singlet

$$J_\alpha \equiv \widetilde{\varphi}^\dagger\, \ell_\alpha, \tag{1.11}$$

where $\widetilde{\varphi} \equiv i\sigma^2\varphi^*$ with the Pauli matrix σ^2 is the isospin conjugate SU(2) Higgs doublet, and $\ell_\alpha = \begin{pmatrix} \nu_\alpha, & \alpha \end{pmatrix}_{\text{L}}^\top$ is the left-handed SU(2) lepton doublet of flavor α. We describe the sterile neutrinos by the Majorana spinors N_i, whose charge conjugate fields satisfy $N_i^{\text{c}} = N_i$, in a basis in which the mass matrix is diagonal. In general, the matrix of Yukawa couplings h is then non-diagonal. This is different from the active lepton Yukawa couplings which are usually diagonalized simultaneously with their mass matrix. The latter is possible, because the two are related via the Higgs mechanism. On the other hand, the Majorana masses and (complex) Yukawa couplings of the sterile neutrinos are n_{s} and $6n_{\text{s}}$ free parameters,[5] respectively, which generally leads to misalignment of the eigenbases of the corresponding matrices.

1.2.2 Motivation

Apart from the aesthetical motivation of having both chiral fields for all fermions, the introduction of sterile neutrinos is well-motivated for providing feasible solutions to the three problems discussed in section 1.1, as we show in turn.

In the broken phase of the Standard Model, when the Higgs field acquires the vacuum expectation value v ≈ 174 GeV, the mass term in the full Lagrangian (1.10) reads (for simplicity for one sterile and one active flavor)

$$\mathscr{L}_{\text{mass}} = -\frac{1}{2}\overline{N}MN - (\overline{N}\text{v}h\nu_{\text{L}} + \text{H.c.}). \tag{1.12}$$

Being its own charge conjugate, we can write the Majorana spinor as $N \equiv \nu_{\text{R}} + \nu_{\text{R}}^{\text{c}}$ with a chiral field ν_{R}. Now (1.12) can be written as

$$\mathscr{L}_{\text{mass}} = -\frac{1}{2} \begin{pmatrix} \overline{\nu_{\text{L}}} & \overline{\nu_{\text{R}}^{\text{c}}} \end{pmatrix} \begin{pmatrix} 0 & 2\text{v}h \\ 2\text{v}h & M \end{pmatrix} \begin{pmatrix} \nu_{\text{L}} \\ \nu_{\text{R}} \end{pmatrix} + \text{H.c.} \tag{1.13}$$

---

[5]Note, however, that (1.16) reduces the number of degrees of freedom.

For $M \gg 2\mathrm{v}h$, the eigenvalues of the mass matrix[6] are approximately given by

$$m_{\mathrm{small}} \approx \frac{(2\mathrm{v}h)^2}{M}, \tag{1.14}$$

$$m_{\mathrm{large}} \approx M, \tag{1.15}$$

and the corresponding eigenvectors are mostly left- and right-handed, respectively. Due to the inverse relation between the masses in (1.14) this is known as the *(type-I) see-saw mechanism.* For the original Lagrangian in (1.10), relation (1.14) generalizes to a matrix[7]

$$m \approx (2\mathrm{v})^2 h^\top M^{-1} h, \tag{1.16}$$

thus generating masses for the left-handed neutrinos. In the original idea $M \gtrsim 10^7$ GeV, and then the observed magnitudes of the active neutrino masses are obtained by choosing Yukawa couplings comparable to those of the μ or the τ leptons, which provides for a somewhat natural explanation. However, also smaller M are in principle allowed as long as (1.16) is fulfilled, thus loosening the naturalness argument in favor of introducing sterile neutrinos whose masses are not orders of magnitude away of current accelerator energy limits.[8] It is this potential for detection that has made scenarios with lighter sterile neutrinos more fashionable recently.

Sterile neutrinos could also well be responsible for the observed baryon asymmetry of the Universe [25]. The main idea relies on introduction of $\mathcal{CP}$ violation in the Yukawa couplings h that allows to produce a lepton asymmetry at some high scale, which is why these mechanisms are generically called *leptogenesis.* This lepton asymmetry is subsequently transformed into baryon asymmetry by electroweak sphalerons. These are non-perturbative transition processes between distinct vacua of the chiral SU(2)[9] which together with the chiral anomaly violate the conservation of lepton numbers L_α (with $\alpha = e, \mu, \tau$) and baryon number B individually in such a way that the combinations

$$X_\alpha \equiv L_\alpha - \frac{B}{3} \tag{1.17}$$

---

[6]The small eigenvalue (1.14) is actually negative, but the sign can be absorbed into field redefinitions.

[7]See, e.g., reference [24].

[8]Of course, one could argue that already the hierarchy in Yukawa couplings in the active lepton sector spans over four orders of magnitude, and the overall set of Yukawa couplings present in the Standard Model spans over six, so that an extension down by some orders of magnitude might possibly not raise too much concern.

[9]See, e.g., reference [26] for a review of electroweak sphalerons.

are conserved. Electroweak sphaleron processes are efficient only at temperatures above $T \gtrsim 130$ GeV [27], and are virtually unobservable today, since they are exponentially suppressed. An asymmetry in X_α translates into a baryon asymmetry in the Higgs phase according to [28]

$$B = -\frac{28}{79} \sum_\alpha X_\alpha \qquad (1.18)$$

at leading order in Standard Model couplings.[10]   Due to the small Yukawa couplings the sterile neutrinos equilibrate only slowly, if at all, resulting in thermal non-equilibrium. This way all of the Sakharov conditions are satisfied.

Depending on the masses and couplings of the sterile neutrinos, leptogenesis can be realized in different stages of the evolution of the Universe. *Thermal* (or *high-scale*) *leptogenesis* requires very heavy sterile neutrinos with masses larger than 10^6 GeV [30]. These heavy sterile neutrinos which are produced from the Standard Model plasma via the Yukawa interaction in (1.10) generate a lepton asymmetry by out-of-equilibrium decays, and slowly thermalize. $\mathcal{CP}$ violation enters the matrix of Yukawa couplings via a complex phase only for at least two sterile flavors, and then interference between tree-level and one-loop diagrams gives X_α violating reactions. Assuming a hierarchy in the Majorana masses of these flavors allows to integrate out heavier states and work with an effective $\mathcal{CP}$ violating vertex.[11] Without hierarchy in the Majorana masses, there is the possibility of two nearly mass-degenerate sterile neutrinos, known as *resonant leptogenesis*, which lowers the mass bound to 10^3 GeV [32]. *Leptogenesis through oscillations* [33,34] (or *low-scale leptogenesis*) can work for even smaller masses, below ~ 5 GeV, such that these sterile neutrinos could in principle be experimentally detected [23]. The underlying mechanism is somewhat more involved. Here $\mathcal{CP}$ violation enters already at tree-level through oscillations between at least two sterile states. Since the Majorana masses are very small compared to the temperature (this scenario is usually operative at temperatures somewhere between 130 GeV $\lesssim T \lesssim 10^5$ GeV [35,36]), the sum of lepton numbers in the active and the sterile sectors is nearly conserved. Thus, if one of the sterile states couples weakly enough to the Standard Model such that it does not equilibrate until electroweak sphalerons become inefficient, some of the lepton number gets carried away by sterile neutrinos, and the same

---

[10]All corrections of $\mathcal{O}(g^2)$ to (1.18), where g denotes a generic Standard Model coupling, have been obtained in [29].

[11]See, e.g., reference [31] for a review of thermal leptogenesis.

amount with opposite sign remains in the active sector. Then again by means of (1.18), a net baryon number remains in the Higgs phase.

Dark matter could be comprised of sterile neutrinos with keV masses [37], either partly or completely. Due to mixing in the Higgs phase, these sterile neutrinos can decay into a pair of an active neutrino and a photon. While the original Dodelson-Widrow model [37] cannot generate all of the dark matter given current gamma ray observations and Lyman-α constraints [38], observations still leave open the possibility for all of the dark matter being *resonantly* produced sterile neutrinos via the Shi-Fuller mechanism [39], see e.g. [40] for a review. This mechanism requires a non-vanishing lepton asymmetry which generates a peak in a resummed propagator, therefore boosting the production rate. It is usually effective around the QCD temperature, see e.g. [41].

It has been suggested [42] that with three generations of sterile neutrinos, two nearly degenerate flavors with GeV masses could be responsible for the baryon asymmetry via low-scale leptogenesis, while at the same time providing enough residual lepton asymmetry to fuel the production of a third, lighter flavor with keV mass, which then constitutes the dark matter. A recent study has shown that this model (while at the same time reproducing active neutrino masses in accordance with experimental observations) can generate only about 10% of the dark matter abundance [43]. Keeping in mind that there is no theoretical reason for dark matter to consist of one single species of particles, these sterile neutrinos could still be part of a more complicated composition of the dark matter content of the Universe.

We obtain kinetic equations applicable to scenarios with sterile neutrinos describing low-scale leptogenesis and/or dark matter production in chapter 2.

1.3   Right-handed electrons

On first sight, the right-handed electrons e_{R} contained in the Standard Model might not have too much connection with the problems discussed in section 1.1, let alone with the notion of sterile neutrinos which we have introduced in section 1.2. In this section we shortly recall the place of right-handed electrons in the Standard Model and their evolution in the early Universe and motivate why they might play a role in the generation of the baryon asymmetry of the Universe.

Right-handed electrons e_{R} are charged only under the weak hypercharge U(1) in the Standard Model. Among gauge interactions with the corresponding B bosons,

they also have a Yukawa interaction, such that the part of the Standard Model Lagrangian containing the e_R field reads

$$\mathscr{L}_{SM} \ni \overline{e_R}\,i\slashed{D}\,e_R - (\overline{e_R}\,h_e\,\varphi^\dagger \ell_e + \text{H.c.}) \tag{1.19}$$

with the covariant derivative $D_\mu = \partial_\mu + iy_{e_R}g'B_\mu$, with $y_{e_R} = -1$, and h_e is the electron Yukawa coupling, with the value $h_e = 2.9 \cdot 10^{-6}$ at the Z boson mass [3]. Note that, unlike in the Lagrangian for sterile neutrinos (1.10) containing $\widetilde{\varphi}$ in the Yukawa interaction, φ appears in (1.19). At the classical level, the gauge invariant kinetic term in (1.19) conserves the right-handed electron lepton number

$$L_{eR} \equiv \int d^3x\,\overline{e_R}\gamma^0 e_R, \tag{1.20}$$

which is, on the other hand, violated by the Yukawa interaction in (1.19).

The electron Yukawa coupling h_e is the smallest coupling constant of the Standard Model. Therefore thermal equilibrium between right- and left-handed electrons (the equilibration of the charge L_{eR}) is achieved relatively late in the evolution of the Universe.[12] Nevertheless, it happened in the symmetric phase, while electroweak sphaleron processes were still effective. Because baryogenesis scenarios usually rely on the B violation induced by these processes, the equilibration of right-handed electrons can play an important role in the creation of the matter-antimatter asymmetry of the Universe.

The interplay between right-handed electron equilibration and baryogenesis through neutrino oscillations [33, 34], which we have shortly discussed in section 1.2.2, is one central topic of this work. The exact choice of the sterile-neutrino Yukawa couplings and the Majorana masses in (1.10) determines the temperature regime at which the leptogenesis mechanism operates,[13] and for certain values of these parameters the generation of the matter-antimatter asymmetry and the equilibration of right-handed electrons take place around the same time. Then the latter is part of the leptogenesis process, and the dynamics of the variable L_{eR} must be accounted for in the kinetic equations. At leading order, the equilibration of right-handed electrons proceeds purely via Standard Model interactions. The temperature T_{eq} at which the Yukawa interaction of e_R effectively equilibrates the quantity L_{eR} is among the results of chapter 3.

---

[12]The temperature T_{eq} at which L_{eR} comes into equilibrium is parametrically given by $T_{eq} \sim h_e^2 g^2 m_{Pl}$ with an appropriate Standard Model coupling g and the Planck mass m_{Pl}, see section 2.1.1.

[13]Roughly speaking, increasing the Yukawa couplings leads to the leptogenesis process happening earlier in the evolution of the Universe.

A connection between the equilibration of right-handed electrons and the generation of the matter-antimatter asymmetry had been suggested earlier in the context of baryogenesis at some very high temperature, like e.g. in GUT baryogenesis. If a matter-antimatter asymmetry is created at that temperature, it can be protected from washout if the right-handed electrons are not yet in equilibrium [44, 45].

A lepton asymmetry in right-handed electrons may also generate hypermagnetic fields [46] which is due to the so-called *abelian anomaly* from which the quantity $L_{e\mathrm{R}}$ suffers. It converts the helicity stored in $L_{e\mathrm{R}}$ to circularly polarized modes of the hypercharge gauge field, which is energetically more favorable. In particular this implies that the Yukawa interaction in (1.19) is not the only source of $L_{e\mathrm{R}}$ violation in the Standard Model. Therefore this phenomenon plays a role in the determination of the equilibration rate of $L_{e\mathrm{R}}$ in chapter 3.

Effective kinetic equations for out-of-equilibrium processes

In this chapter we derive general formulae for the rate coefficients appearing in effective kinetic equations of a certain class of non-equilibrium problems which we define in section 2.1. In section 2.1.1 we briefly discuss the emergence of this specific class of problems in the dynamics of the early Universe. We generalize the considerations of reference [47] to include non-linear terms in the kinetic equations and obtain master formulae in terms of real time correlation functions in section 2.2. We discuss the relations between charges and chemical potentials in various temperature regimes in section 2.3, and apply the formalism to sterile neutrinos (section 2.4) and the linearized version which had been obtained in [47] to the dynamics of right-handed electron lepton number L_{eR} (section 2.5).

2.1   General setup

In general, the description of non-equilibrium systems is a complex task which we simplify by making two central assumptions. We consider a situation in which there is a separation of time scales in such a way that some reactions in the plasma happen considerably more often than others. Then these *fast* interactions keep most of the degrees of freedom in equilibrium, with a frequency we call ω_{fast}, while some other quantities relax much more slowly with frequency ω, and we call these quantities *slow*. Then for $\omega \ll \omega_{\text{fast}}$ the time evolution of the departure from equilibrium of the slow quantities, which we denote by y_a, can only depend on the values of the slow quantities themselves and the details of the thermal system. In a canonical description these are the temperature T, the volume V,

and the values of the *strictly conserved* charges $Q_{\bar{c}}$, such that generally

$$\dot{y}_a = \dot{y}_a(\{y_b\}, T, V, \{Q_{\bar{c}}\}). \tag{2.1}$$

Additionally, we assume the situation to be close to full equilibrium, so that the deviations of all slow quantities from equilibrium are small. In this case we can expand (2.1) in departures from equilibrium, yielding

$$\dot{y}_a = -\gamma_{ab}\, y_b - \frac{1}{2}\gamma_{abc}\, y_b\, y_c - \frac{1}{3!}\gamma_{abcd}\, y_b\, y_c\, y_d - \cdots, \tag{2.2}$$

where now the dependence on the details of the thermodynamic state of the fast degrees of freedom enter the coefficients, so that $\gamma_{ab} = \gamma_{ab}(T, V, \{Q_{\bar{c}}\})$ and analogously for the coefficients multiplying the non-linear terms. We assume that the y_a as well as the coefficients in (2.2) are real-valued.

2.1.1 Applicability to early Universe dynamics

In a considerable temperature range during the evolution of the early Universe a large amount of degrees of freedom is in equilibrium. This is due to the fact that the Hubble expansion rate

$$H = \sqrt{\frac{4\pi^3 g_*}{45}} \frac{T^2}{m_{\mathrm{Pl}}}, \tag{2.3}$$

with g_* the number of relativistic degrees of freedom, and $m_{\mathrm{Pl}} = 1.22 \cdot 10^{19}$ GeV the Planck mass, albeit its apparent large size, is actually much smaller than most of the rates mediated by Standard Model interactions, i.e. the ratio ω_{fast}/H is much larger than unity. Let us briefly illustrate this for Standard Model gauge interactions. The frequency of such an interaction with gauge coupling g is given by $\omega_{\mathrm{fast}} = ag^4 T$ with a a numerical prefactor. Then we have

$$\frac{\omega_{\mathrm{fast}}}{H} \approx ag^4 \frac{7 \cdot 10^{17} \text{ GeV}}{T} \tag{2.4}$$

in the symmetric phase of the Standard Model where $g_* = 106.75$. In the following we will be interested mainly in temperatures well below $T \ll 10^9$ GeV so that the ratio (2.4) is indeed large, and all gauge interactions are in equilibrium. Depending on the temperature additional interactions, e.g. Yukawa interactions, may be in equilibrium, and for these interactions one has $\omega_{\mathrm{fast}} = \mathcal{O}(h^2 g^2 T)$, with h the respective Yukawa coupling and g a generic gauge coupling. We elaborate on the fast interactions in section 2.3. If we now consider slowly varying charges

whose deviations from equilibrium are small,[14] the two assumptions facilitating the description of the non-equilibrium system are met. The latter is neither a prediction nor an observation, however, it can be checked for consistency a posteriori. For example, one can compare the linear rates γ_{aa} (no summation over a) in (2.2) to the Hubble rate (2.3). Equating the two gives an expression for the temperature which we call the *equilibration temperature* of the quantity y_a. Due to efficient equilibration around this temperature, the deviations from equilibrium can be assumed to be small, as long as coefficients γ_{ab} much larger than γ_{aa}, efficiently driving the quantity y_a away from equilibrium, are absent.

We will assume spatial homogeneity, in which case the covariant time derivative for occupancies $f(t, \mathbf{k})$ in a Hubble expanding background reads [48]

$$\partial_t f(t, \mathbf{k}) \to \left(\partial_t - H|\mathbf{k}|\partial_{|\mathbf{k}|}\right) f(t, \mathbf{k}). \tag{2.5}$$

By integration by parts the corresponding one for densities $n(t)$ is given by

$$\partial_t n(t) \to (\partial_t + 3H)\, n(t), \tag{2.6}$$

in which the second term on the right-hand side reflects dilution. Hubble expansion enters the effective kinetic equations (2.2) on the left-hand sides through (2.5) and (2.6).

2.2   Derivation of rate coefficients

We make use of Landau's theory of quasi-stationary fluctuations [49] to obtain the coefficients $\gamma_{a\cdots}$ in (2.2). This has been done for the linear case in [47], and the reasoning has been extended to $\mathcal{CP}$ violating rates in [50]. Here we generalize the approach to apply also to (potentially $\mathcal{CP}$ violating) non-linear coefficients.

2.2.1   Correlators in the effective theory

The thermal fluctuations of the slow variables y_a satisfy the same type of equations as (2.2), but with an additional Gaussian noise term on the right-hand side, representing the effect of rapidly fluctuating quantities.[15]

From these equations one can compute real time correlation functions of the fluctuations such as

$$\mathcal{C}_{ab}(t) = \langle y_a(t) y_b(0) \rangle \tag{2.7}$$

---

[14]Deviations from equilibrium are said to be small, if they are smaller than their thermal fluctuations. We discuss this issue in detail in section 2.2.

[15]See, e.g., §118 of reference [49] on correlations of fluctuations in time.

by solving these equations and then averaging over the noise and over initial conditions.[16]

In [47] the rates γ_{ab} have been found by taking the one-sided Fourier transform of the correlator $\mathcal{C}_{ab}$ after the exact solution of the linear equations of motion had been inserted. The non-linear equation of motion (2.2) can generally not be solved analytically. We solve it perturbatively by directly taking the one-sided Fourier transform of the non-linear equation of motion. We encounter the one-sided Fourier transformation of the slow variable y_a,

$$y_a^+(\omega) \equiv \int_0^\infty dt\, e^{i\omega t} y_a(t). \tag{2.8}$$

At linear order in y in (2.2) we obtain

$$y_a^{+(0)}(\omega) = \left[(-i\omega + \gamma)^{-1}\right]_{ab} y_b(0) + \cdots, \tag{2.9}$$

where the ellipsis represents a term linear in the noise. Inserting this into the one-sided Fourier transform of (2.7) one obtains [47]

$$\mathcal{C}_{ab}^+(\omega) = \left[(-i\omega + \gamma)^{-1}\right]_{ac} \Xi_{cb}. \tag{2.10}$$

Here the noise term has dropped out. When averaging over the initial conditions at $t = 0$, one encounters the real and symmetric susceptibility matrix with elements

$$\Xi_{ab} \equiv \langle y_a y_b \rangle, \tag{2.11}$$

i.e., the *equal* time correlators $\mathcal{C}_{ab}(0)$. As in (2.7), the average in (2.11) is canonical, that is, at fixed values of the conserved charges.

The rate matrix γ_{ab} can be extracted from (2.10) by considering frequencies ω which are parametrically much larger than the elements of the matrix γ. Then one can expand (2.10) in γ/ω. For real ω the leading term in this expansion is purely imaginary. Thus by taking the real part of (2.10) one can extract the next term which is linear in γ [47],

$$\operatorname{Re} \mathcal{C}_{ab}^+(\omega) = \frac{1}{\omega^2} \gamma_{ac}\, \Xi_{cb} + \mathcal{O}(\omega^{-3}) \qquad \text{(for real } \omega\text{)}. \tag{2.12}$$

---

[16]Non-linear terms in the equation of motion could potentially lead to non-vanishing expectation values of y_a. Therefore in general one also has to include y-independent terms on the right-hand side to ensure that the expectation values vanish. Eventually we want to describe deviations from thermal equilibrium with (2.2). Then the y_a are much larger than their thermal fluctuations, and the y-independent term will be small compared to the non-linear terms in (2.2) and can be neglected.

Here it is important that we take the one-sided Fourier transform instead of the Fourier transform because the latter only depends on the symmetric part of γ.

Now we go beyond linear order. We include the non-linear terms in the equation motion, and expand

$$y = y^{(0)} + y^{(1)} + y^{(2)} + \cdots \tag{2.13}$$

where $y^{(n)}$ is of order $(y(0))^{n+1}$ and vanishes at the initial time $t = 0$. We will encounter the generalization of (2.11),

$$\Xi_{a_1 a_2 \cdots a_n} \equiv \langle y_{a_1} y_{a_2} \cdots y_{a_n} \rangle_{\mathrm{C}}, \tag{2.14}$$

where the subscript 'C' indicates that we only include the connected part, for which we assume

$$(\Xi_{a_1 \cdots a_m})^{1/m} \ll (\Xi_{a_1 \cdots a_n})^{1/n} \qquad (m > n \geq 2). \tag{2.15}$$

This can be seen as a consequence of our assumption that we can expand the right-hand side of equation (2.2), since the time evolution of the fluctuations also determines their equal time correlations (see, e.g., [51]). For the occupancies of sterile neutrinos we have checked the assumption (2.15) in appendix A. The coefficient γ_{abc} of the quadratic term in equation (2.2) can then be extracted from the correlation function

$$\mathcal{C}_{a(bc)}(t) \equiv \langle y_a(t) y_b y_c(0) \rangle \tag{2.16}$$

as follows (for details see appendix B).[17] We have

$$\mathcal{C}_{a(bc)}(t) = \langle y_a^{(0)}(t) y_b y_c(0) \rangle + \langle y_a^{(1)}(t) y_b y_c(0) \rangle. \tag{2.17}$$

The first term on the right-hand side is very similar to (2.10), one only has to replace (2.11) with the expectation value of three factors of $y(0)$. Again we take the one-sided Fourier transform. Our assumption (2.15) allows us to neglect the contribution from Ξ_{abcd}, which gives

$$\langle y_a^{+(1)}(\omega) y_b y_c(0) \rangle_{\mathrm{C}} = \frac{1}{\omega^2} \gamma_{ade} \, \Xi_{db} \, \Xi_{ec} + \mathcal{O}(\omega^{-3}). \tag{2.18}$$

Thus we obtain

$$\mathrm{Re} \, \mathcal{C}_{a(bc)}^{+}(\omega) = \frac{1}{\omega^2} \left[\gamma_{ade} \, \Xi_{db} \, \Xi_{ec} + \gamma_{ai} \, \Xi_{ibc} \right] + \mathcal{O}(\omega^{-3}), \tag{2.19}$$

---

[17]Note that (2.16) is connected, because the expectation value of a single y vanishes.

which allows us to extract γ_{abc}. Similarly we obtain the coefficient multiplying the cubic term in (2.2) by solving the equation of motion for y_a perturbatively up to linear order in γ_{abc} and γ_{abcd} and successively computing the *connected* correlation function

$$\mathcal{C}_{a(bcd)}(t) \equiv \langle y_a(t) y_b y_c y_d(0) \rangle_{\mathrm{C}} . \tag{2.20}$$

Following the same line of arguments, we obtain

$$\operatorname{Re} \mathcal{C}^+_{a(bcd)}(\omega) = \frac{1}{\omega^2} \left[\gamma_{aijk} \, \Xi_{ib} \, \Xi_{jc} \, \Xi_{kd} + \frac{1}{2} \, \gamma_{aij} \, \Xi_{ijbcd} + \gamma_{ai} \, \Xi_{ibcd} \right] + \mathcal{O}(\omega^{-3}). \tag{2.21}$$

2.2.2 Correlators in the microscopic theory

The one-sided Fourier transforms of the correlators (2.7), (2.16), and (2.20) as well as the susceptibilities (2.14) can also be computed in the microscopic quantum theory. In the range of validity $\omega \ll \omega_{\mathrm{fast}}$ of the effective equations of motion (2.2) they have to match their counterparts in the effective theory. This way the coefficients in (2.2) can be computed from (2.12), (2.19) and (2.21) with the quantum correlators on the right-hand side, evaluated in the regime $\gamma \ll \omega \ll \omega_{\mathrm{fast}}$. In this regime $\mathcal{C}^+_{ab}$ has to match the one-sided Fourier transform of the microscopic correlation function

$$C_{ab}(t) \equiv \frac{1}{2} \langle \{ y_a(t), y_b(0) \} \rangle. \tag{2.22}$$

Since $\omega_{\mathrm{fast}} \lesssim T$,[18] we are dealing with frequencies ω much smaller than the temperature. In this regime the one-sided Fourier transform of (2.22) is approximately given by [50]

$$C^+_{ab}(\omega) = -i \frac{T}{\omega} \left[\Delta_{ab}(\omega) - \Delta_{ab}(0) \right], \tag{2.23}$$

where

$$\Delta_{ab}(\omega) \equiv \int \frac{d\omega'}{2\pi} \frac{\rho_{ab}(\omega')}{\omega' - \omega}. \tag{2.24}$$

The two-point function in (2.24) is an analytic function off the real axis, and

$$\rho_{ab}(\omega) \equiv \int dt \, e^{i\omega t} \langle [y_a(t), y_b(0)] \rangle \tag{2.25}$$

---

[18]Or even $\omega_{\mathrm{fast}} \ll T$ for certain combinations of the process underlying ω_{fast} and the temperature (e.g. processes due to h_μ at temperatures well below 10^9 GeV [52]).

is the spectral function of the bosonic operators y_a and y_b. For real ω, the function $\Delta_{ab}(\omega + i0^+)$ equals the retarded two-point function $\Delta_{ab}^{\rm ret}(\omega)$. Matching $\mathcal{C}^+$ and C^+, and using (2.12) as well as the fact that $\Delta_{ab}(0)$ is real one obtains the master formula [50]

$$\gamma_{ab} = T\omega \operatorname{Im} \Delta_{ac}^{\rm ret}(\omega)(\Xi^{-1})_{cb} \qquad (\gamma \ll \omega \ll \omega_{\rm fast}). \tag{2.26}$$

For real spectral functions it agrees with the Kubo-type relation in [47]. Following the same steps with (2.19) and (2.21) we obtain the master formulae

$$\gamma_{abc} = \Big[T\omega \operatorname{Im} \Delta_{a(de)}^{\rm ret}(\omega) - \gamma_{af}\, \Xi_{fde}\Big](\Xi^{-1})_{db}(\Xi^{-1})_{ec}, \tag{2.27}$$

$$\gamma_{abcd} = \Big[T\omega \operatorname{Im} \Delta_{a(efg)}^{\rm ret}(\omega) - \frac{1}{2}\gamma_{aij}\,\Xi_{ijefg} - \gamma_{ai}\,\Xi_{iefg}\Big](\Xi^{-1})_{eb}(\Xi^{-1})_{fc}(\Xi^{-1})_{gd}, \tag{2.28}$$

where in both cases $\gamma \ll \omega \ll \omega_{\rm fast}$. As in (2.20), we include only the connected piece of the correlator $\Delta_{a(efg)}^{\rm ret}$ in (2.28). In general the operators inside the retarded correlators will not necessarily commute at equal times.

In some cases it is more convenient to compute the correlators of time derivatives of one or both of the operators, and then use the relations

$$\Delta_{AB}^{\rm ret}(\omega) = \frac{1}{\omega}\Big[i\Delta_{\dot{A}B}^{\rm ret}(\omega) + \big\langle[A(0), B(0)]\big\rangle\Big], \tag{2.29}$$

$$\Delta_{AB}^{\rm ret}(\omega) = \frac{1}{\omega^2}\Big[\Delta_{\dot{A}\dot{B}}^{\rm ret}(\omega) + i\big\langle[A(0), \dot{B}(0)]\big\rangle + \omega\big\langle[A(0), B(0)]\big\rangle\Big] \tag{2.30}$$

for bosonic operators A and B which are easily obtained via integration by parts.

2.3 Charges and chemical potentials

In the equations of motion (2.2) the slow charges appear on the right-hand side, along with the susceptibilities (2.11) and (2.14) after the master formulae (2.26), (2.27) and (2.28) have been inserted. Once the susceptibilities and the n-point functions have been determined, the set of equations is closed. Sometimes it can be more comfortable to express the right-hand sides in terms of chemical potentials instead of the charges. Here we make a connection between the two via the susceptibilities, focusing on temperatures in the symmetric phase of the Standard Model.

We restrict ourselves to the determination of the susceptibilities Ξ_{ab}, since the dependence on the generalized susceptibilities Ξ_{abc} and Ξ_{abcd} of Standard

Model charges will drop out once we express our equations in terms of chemical potentials, as we will see in section 2.4. The generalized susceptibilities will play a role, if the indices label sterile neutrino occupancies, see appendix C.

Denoting the slow charges by Q_a and their departures from equilibrium playing the role of the y_a in (2.2) by $\delta Q_a \equiv Q_a - Q_a^{\text{eq}}$, we have the relation

$$\delta Q_a = \Xi_{ab}\frac{\mu_b}{T} + \frac{1}{2}\Xi_{abc}\frac{\mu_b}{T}\frac{\mu_c}{T} + \mathcal{O}(\mu^3). \tag{2.31}$$

The susceptibilities can be obtained by switching from an ensemble in which the conserved charges, which we denote by $Q_{\bar{a}}$, have fixed values to a grand-canonical one [47]. In the latter all charges, collectively denoted by Q_A fluctuate, not only the slowly varying ones. Then we have a relation similar to (2.31), but for *all* charges,

$$Q_A = \sum_B \chi_{AB}\frac{\mu_B}{T} + \mathcal{O}(\mu^3). \tag{2.32}$$

Here χ is the susceptibility matrix in the full grand-canonical ensemble, in which the charges are odd functions of the chemical potentials. Therefore, unlike in (2.31), no terms of order μ^2 and no equilibrium values appear in (2.32). The susceptibility matrix χ is related to the pressure $P(T, \mu)$ via

$$\chi_{AB} = TV \left.\frac{\partial^2 P(T, \mu)}{\partial \mu_A \partial \mu_B}\right|_{\mu=0}. \tag{2.33}$$

Considering $A = a$ in (2.32) and comparing with (2.31), we find that the inverse susceptibilities satisfy

$$(\Xi^{-1})_{ab} = (\chi^{-1})_{ab}, \tag{2.34}$$

where a and b label slowly varying charges only. The equilibrium values are obtained analogously,

$$Q_a^{\text{eq}} = -\,\Xi_{ab}\,(\chi^{-1})_{b\bar{c}}\,Q_{\bar{c}}. \tag{2.35}$$

The computation of the susceptibilities χ in the symmetric phase in terms of the pressure is described in [47], where the leading order (in Standard Model couplings) contributions to the pressure have been obtained. There also the $\mathcal{O}(g)$ corrections and some of the $\mathcal{O}(g^2)$ contributions can be found, and the remaining $\mathcal{O}(g^2)$ contributions have been obtained in [29]. All gauge charges are strictly

conserved, and in principle chemical potentials have to be added for all of them. However, non-abelian gauge charges, i.e. color charge or weak isospin, are not correlated with the slowly varying or the strictly conserved non-gauge charges. Therefore, non-abelian gauge charges decouple from the others (and also among each other), such that they can be neglected. Weak U(1) hypercharge Y, despite being a gauge charge, is correlated with all charges we consider, and therefore has to be considered in the set of strictly conserved charges. In the imaginary time formalism the temporal component of the hypercharge gauge field B_0 is purely imaginary. It has a non-zero expectation value [28] which plays the role of a hypercharge chemical potential,

$$\mu_Y = ig'B_0, \tag{2.36}$$

ensuring hypercharge neutrality of the plasma.

At leading order in Standard Model couplings, and when we have only diagonal charges,[19] the pressure reads [47]

$$\frac{12}{T^2}\left[P(T,\mu) - P(T,0)\right] = 18\mu_Q^2 + 9\mu_{u_\mathrm{R}}^2 + 9\mu_{d_\mathrm{R}}^2$$
$$+ 2\sum_\alpha \mu_{\ell_\alpha}^2 + \sum_\alpha \mu_{\alpha_\mathrm{R}}^2 + 4\mu_\varphi^2 + \mathcal{O}(\mu^4), \tag{2.37}$$

The chemical potentials carried by particles which appear in (2.37) are functions of the chemical potentials of all charges, and therefore depend on the temperature regime. Throughout all temperature regimes in the symmetric phase discussed in the following, we have

$$\mu_\varphi = \frac{\mu_Y}{2}. \tag{2.38}$$

Some quark Yukawa couplings come into equilibrium at temperatures in the regimes we consider, analogous to h_e. However, strong sphalerons are in equilibrium in the symmetric phase up to temperatures well above the ones considered here [53]. They violate the conservation of chiral quark charges like $\int_\mathbf{x} \overline{u_\mathrm{R}}\gamma^0 u_\mathrm{R}$, such that these quantities are fast, and do not enter the sets of slow or conserved charges.

The slow charges we are interested in in the following sections 2.4 and 2.5 are violated by interactions whose scale is set by the temperature T, up to

---

[19]When the Yukawa interaction of the μ or the one of the τ lepton is slow, also flavor non-diagonal charges have to be considered. In this case the particle chemical potentials are matrices, and (2.37) contains traces [47].

dimensionless couplings. The Hubble rate (2.3), on the other hand, behaves like $H \sim T^2$, such that in the evolution of the Universe the slow charges we consider eventually come into equilibrium at the equilibration temperature, they are said to *freeze in* [48]. The opposite is the case for electroweak sphalerons which effectively violate baryon and lepton numbers with a rate much larger than the Hubble rate only above the *freeze out* temperature (see below).

$8.5 \cdot 10^4$ GeV $\ll T \ll 10^9$ GeV The lepton number L_{eR} carried by right-handed electrons is not yet efficiently violated by the electron Yukawa coupling so that it constitutes a strictly conserved charge, and we have to introduce a corresponding chemical potential in (2.32). Interactions mediated by μ and τ Yukawa couplings are in equilibrium [52], and constitute fast processes, which do not give rise to conserved charges. Inserting the particle chemical potentials

$$
\mu_Q = \frac{\mu_Y}{6} - \frac{\mu_X}{3}, \qquad \mu_{u_R} = \frac{2\mu_Y}{3} - \frac{\mu_X}{3}, \qquad \mu_{d_R} = -\frac{\mu_Y}{3} - \frac{\mu_X}{3}
$$

$$
\mu_{\ell_\alpha} = -\frac{\mu_Y}{2} + \mu_{X_\alpha}, \qquad \mu_{e_R} = -\mu_Y + \mu_{X_e} + \mu_{L_{eR}}, \qquad \mu_{\mu_R} = -\mu_Y + \mu_{X_\mu}
$$

$$
\mu_{\tau_R} = -\mu_Y + \mu_{X_\tau}, \qquad \mu_\varphi = \frac{\mu_Y}{2} \tag{2.39}
$$

with $\mu_X \equiv \frac{1}{3}\sum_\alpha \mu_{X_\alpha}$ into the pressure (2.37) and using (2.33), we obtain the inverse susceptibilities

$$
\chi^{-1} = \frac{2}{481\, T^3 V}
\begin{pmatrix}
666 & 0 & 0 & -555 & 111 \\
0 & 533 & 52 & 156 & 156 \\
0 & 52 & 533 & 156 & 156 \\
-555 & 156 & 156 & 2133 & 135 \\
111 & 156 & 156 & 135 & 246
\end{pmatrix}
\tag{2.40}
$$

for the ordering $\{X_e, X_\mu, X_\tau, L_{eR}, Y\}$. If all the X_α are slow the matrix Ξ^{-1} is given by the upper left 3×3 block of (2.40) due to (2.34), and then

$$
\Xi = \frac{T^3 V}{180}
\begin{pmatrix}
65 & 0 & 0 \\
0 & 82 & -8 \\
0 & -8 & 82
\end{pmatrix}
\tag{2.41}
$$

for the ordering $\{X_e, X_\mu, X_\tau\}$. According to (2.35), the equilibrium values read

$$
X_e^{\mathrm{eq}} = \frac{5}{6} L_{eR}, \tag{2.42}
$$

$$
X_\alpha^{\mathrm{eq}} = -\frac{4}{15} L_{eR} \qquad (\alpha = \mu, \tau). \tag{2.43}
$$

Hypercharge neutrality implies

$$\mu_Y = \frac{1}{11}\mu_{L_{e\mathrm{R}}} + \frac{8}{33}\sum_\alpha \mu_{X_\alpha}, \tag{2.44}$$

and the relation between $L_{e\mathrm{R}}$ and its chemical potential reads

$$\mu_{L_{e\mathrm{R}}} = -\frac{5}{6}\mu_{X_e} + \frac{4}{15}\left(\mu_{X_\mu} + \mu_{X_\tau}\right) + \frac{33}{5\,T^2V}L_{e\mathrm{R}}. \tag{2.45}$$

$\boldsymbol{T \sim 8.5 \cdot 10^4}$ **GeV**   Interactions mediated by the electron Yukawa coupling happen at a rate comparable to the Hubble rate, so that $L_{e\mathrm{R}}$ is slowly varying (we obtain the equilibration temperature in chapter 3). The relation between charges and chemical potentials remains the same as in (2.40), and also (2.44) and (2.45) are valid. If all four charges are slowly varying, i.e., if X_α generation and equilibration of right-handed electrons happen at the same time, we have vanishing equilibrium values for all slow variables, because there is no strictly conserved non-zero charge. In this case the matrix Ξ^{-1} is given by the upper left $4{\times}4$ block of (2.40), and then we have

$$\Xi = \frac{T^3V}{594}\begin{pmatrix} 277 & -20 & -20 & 75 \\ -20 & 277 & -20 & -24 \\ -20 & -20 & 277 & -24 \\ 75 & -24 & -24 & 90 \end{pmatrix} \tag{2.46}$$

for the ordering $\{X_e, X_\mu, X_\tau, L_{e\mathrm{R}}\}$. In particular, even though the sterile-neutrino interactions do not violate the conservation of $L_{e\mathrm{R}}$, and the electron Yukawa coupling does not violate the one of X_α, the evolution equations of $L_{e\mathrm{R}}$ and the X_α are coupled through the matrix of susceptibilities. In case the only slow variable is $L_{e\mathrm{R}}$, we have the $1{\times}1$ matrix

$$\Xi = \frac{481}{4266}T^3V, \tag{2.47}$$

and $L_{e\mathrm{R}}$ obtains an equilibrium value for non-vanishing X_α, see section 2.5.

$\boldsymbol{160}$ **GeV** $\boldsymbol{\ll T \ll 8.5 \cdot 10^4}$ **GeV**   Here all Standard Model interactions are in equilibrium. The particle chemical potentials are given by (2.39) with $\mu_{L_{e\mathrm{R}}} = 0$.

Repeating the same steps as above, the inverse susceptibility matrix reads [47][20]

$$\chi^{-1} = \frac{2}{237\,T^3 V} \begin{pmatrix} 257 & 20 & 20 & 72 \\ 20 & 257 & 20 & 72 \\ 20 & 20 & 257 & 72 \\ 72 & 72 & 72 & 117 \end{pmatrix} \tag{2.48}$$

for the ordering $\{X_e, X_\mu, X_\tau, Y\}$. If all X_α are slow, the matrix Ξ^{-1} is given by the upper left $3{\times}3$ block of (2.48), and we have

$$\Xi = \frac{T^3 V}{594} \begin{pmatrix} 277 & -20 & -20 \\ -20 & 277 & -20 \\ -20 & -20 & 277 \end{pmatrix} \tag{2.49}$$

for the ordering $\{X_e, X_\mu, X_\tau\}$. Here hypercharge neutrality imposes [54][21]

$$\mu_Y = \frac{8}{33} \sum_\alpha \mu_{X_\alpha}. \tag{2.50}$$

$T \sim 130$ GeV Around this temperature electroweak sphalerons freeze out [27]. Well below this temperature not only the differences between baryon and lepton numbers X_α, but also their sum is conserved, such that the latter is a slow variable here. As above, there is some freedom in the choice of the slow charges in this temperature regime. We will see in section 2.4.2 that it is convenient to introduce a chemical potential μ_B for baryon number B, instead of a chemical potential for the sum $B + L$. Neglecting the Higgs vacuum expectation value, which is a small quantity at this temperature, the chemical potentials carried by the particles read

$$\mu_Q = \frac{\mu_Y}{6} - \frac{\mu_X}{3} + \frac{\mu_B}{3}, \quad \mu_{u_{\mathrm{R}}} = \frac{2\mu_Y}{3} - \frac{\mu_X}{3} + \frac{\mu_B}{3}, \quad \mu_{d_{\mathrm{R}}} = -\frac{\mu_Y}{3} - \frac{\mu_X}{3} + \frac{\mu_B}{3}$$
$$\mu_{\ell_\alpha} = -\frac{\mu_Y}{2} + \mu_{X_\alpha}, \qquad \mu_{\alpha_{\mathrm{R}}} = -\mu_Y + \mu_{X_\alpha}, \qquad \mu_\varphi = \frac{\mu_Y}{2}, \tag{2.51}$$

again with $\mu_X \equiv \frac{1}{3}\sum_\alpha \mu_{X_\alpha}$, and the inverse susceptibilities are given by

$$\chi^{-1} = \frac{1}{36\,T^3 V} \begin{pmatrix} 88 & 16 & 16 & 28 & 24 \\ 16 & 88 & 16 & 28 & 24 \\ 16 & 16 & 88 & 28 & 24 \\ 28 & 28 & 28 & 79 & 6 \\ 24 & 24 & 24 & 6 & 36 \end{pmatrix} \tag{2.52}$$

---

[20]See equation (63) of reference [47].
[21]See equation (4.2) of reference [54].

for the ordering $\{X_e, X_\mu, X_\tau, B, Y\}$. If all X_α are slow, the matrix Ξ^{-1} is given by the upper left 4×4 block of (2.52), and we have

$$\Xi = \frac{T^3 V}{594} \begin{pmatrix} 277 & -20 & -20 & -84 \\ -20 & 277 & -20 & -84 \\ -20 & -20 & 277 & -84 \\ -84 & -84 & -84 & 360 \end{pmatrix} \tag{2.53}$$

for the ordering $\{X_e, X_\mu, X_\tau, B\}$. In [55] the developing Higgs expectation value is taken into account.[22] Hypercharge neutrality yields the relation [54][23]

$$\mu_Y = \frac{8}{33} \sum_\alpha \mu_{X_\alpha} - \frac{2}{11} \mu_B. \tag{2.54}$$

$T \ll 130$ GeV Deep in the Higgs phase the susceptibilities have a non-trivial temperature dependence because of the fact that not all particles are ultra-relativistic, which is assumed in the approach of [47]. They have been studied in [56].[24]

2.4 Kinetic equations for sterile neutrinos

Leptogenesis through oscillations has been described by Boltzmann equations, and in the relativistic case with several flavors with generalizations thereof [57]. The momentum spectrum of sterile neutrinos is non-thermal and it can be important to keep the full momentum dependence [58], but for parameter space scans usually momentum space averages are considered.[25] There have been various approaches which start from first principles to avoid some ad-hoc assumptions inherent in the Boltzmann equation, and to systematically include medium effects [61–64]. Our generalization of the approach of [47] makes use of the slowness of the sterile neutrino's interaction right from the start. The resulting relations (2.26), (2.27), and (2.28) are valid to all orders in fast Standard Model couplings, and can thus be used to compute higher order corrections allowing to estimate the accuracy of the approximations [50].

In [47] the linear coefficient for X_α equilibration, also called the *washout rate*, has been obtained. It was applied to the production of a single sterile-neutrino

---

[22]See equations (3.8) and (3.9) of reference [55].

[23]See equations (4.5) and (4.6) of reference [54].

[24]See appendix A of reference [56].

[25]For recent work see, e.g., [59, 60].

flavor in [65]. In [58] it has been pointed out that non-linear terms in the kinetic equations may also play an important role. We obtain these non-linear terms in the remainder of this section by applying the formulae (2.27) and (2.28), along with (2.26) for the linear ones. In [54] the rates for leptogenesis including non-linear terms have been obtained using a quite different approach. There the sterile-neutrino masses have been neglected, and in [43] non-linear equations have been obtained also for the massive case.

Kinetic equations for the resonant production of a sterile-neutrino dark matter candidate in the Higgs phase have been obtained, e.g., in [41, 43, 66]. Here the need for non-linear kinetic equations arises naturally because of the dependence of the active neutrino propagator on active lepton number chemical potentials. It is conceivable that the dark matter content of the Universe be comprised of several flavors of sterile neutrinos (either completely, or along other constituents), which has not yet been systematically studied, to the best of our knowledge. The kinetic equations we obtain in this chapter can be applied to sterile neutrinos in such scenarios.

Now we proceed to use the formalism developed in section 2.2 to derive kinetic equations for slow quantities in the Standard Model extended by n_s flavors of sterile neutrinos, as described by (1.10). We consider temperatures at which the muon Yukawa interaction is in equilibrium, which is the case when $T \ll 10^9$ GeV [52]. Then there are two types of slow variables we are interested in. The first type are the charges X_α, see (1.17). In the presence of conserved charges[26] the X_α can have a non-vanishing equilibrium value X_α^eq, so that the y_a in (2.2) correspond to $\delta X_\alpha \equiv X_\alpha - X_\alpha^\text{eq}$. We discuss the equilibrium expectation values in section 2.3. At $T \sim 8.5 \cdot 10^4$ GeV, when the rate of electron Yukawa interactions is comparable to the Hubble rate,[27] the lepton number carried by right-handed electrons $L_{e\text{R}}$ is a slow variable, and at $T \sim 130$ GeV, when electroweak sphalerons freeze out [27], baryon number is slow. The conservation of $L_{e\text{R}}$ and B is not violated by the sterile-neutrino Yukawa interaction. However, the X_α, $L_{e\text{R}}$ and B are individually correlated with U(1) hypercharge Y, see section 2.3, so that their evolution equations are coupled through the matrix of susceptibilities Ξ. When $T \gtrsim 10^9$ GeV the muon Yukawa coupling causes slow interactions and additional,

---

[26]At the temperatures we consider, only right-handed electron number $L_{e\text{R}}$ can be conserved and non-vanishing, if all X_α are violated by the sterile-neutrino Yukawa interaction. This can be the case between $8.5 \cdot 10^4$ GeV $\ll T \ll 10^9$ GeV, see section 2.3.

[27]We obtain the equilibration temperature of right-handed electron number $L_{e\text{R}}$ in section 3.3, see (3.57).

flavor non-diagonal charges have to be taken into account [61]. Specifically, then, the symmetry group of slow charges is non-abelian. In our case, however, all of the charges X_α, $L_{e\mathrm{R}}$, and B commute at equal times.

We consider a finite volume V and take $V \to \infty$ in the end. Without the Yukawa interaction, the sterile neutrino fields N_i in (1.10) would be free and the equation of motion would give

$$N_i(x) = \sum_{\mathbf{k}\,\lambda} \frac{1}{\sqrt{2E_{\mathbf{k}i}V}} \left[e^{i\mathbf{kx}} u_{\mathbf{k}i\lambda} a_{\mathbf{k}i\lambda}(t) + e^{-i\mathbf{kx}} v_{\mathbf{k}i\lambda} a^\dagger_{\mathbf{k}i\lambda}(t) \right] \qquad (2.55)$$

with $a_{\mathbf{k}i\lambda}(t) = \exp(-iE_{\mathbf{k}i}t)a_{\mathbf{k}i\lambda}(0)$ and $E_{\mathbf{k}i} = (\mathbf{k}^2 + M_i^2)^{1/2}$. The spinors u and v are chosen such that $a^\dagger_{\mathbf{k}i\pm}$ creates a sterile neutrino with helicity $\pm 1/2$. The sterile neutrinos can not be expected to be in kinetic equilibrium since kinetic and chemical equilibration are due to the same processes. Therefore the other type of slow variables consists of the phase space densities, or occupancies, of the sterile neutrinos. For each $\mathbf{k}$ and λ the occupation number operators form a matrix, called matrix of densities, or density matrix, with elements[28]

$$(f_{\mathbf{k}\lambda})_{ij} \equiv a^\dagger_{\mathbf{k}i\lambda} a_{\mathbf{k}j\lambda}. \qquad (2.56)$$

In the presence of the Yukawa interaction in (1.10) we *define* the occupation number operators through equations (2.55) and (2.56).[29] Their equilibrium values read

$$(f^{\mathrm{eq}}_{\mathbf{k}\lambda})_{ij} = \delta_{ij} f_{\mathrm{F}}(E_{\mathbf{k}i}). \qquad (2.57)$$

The variables appearing in the effective kinetic equations (2.2) are real, such that the theory in section 2.2 is not applicable to all of the operators in (2.56) for $n_{\mathrm{s}} > 1$. Therefore we consider the Hermitian operators

$$f^a_{\mathbf{k}\lambda} \equiv T^a_{ij} a^\dagger_{\mathbf{k}i\lambda} a_{\mathbf{k}j\lambda}, \qquad (2.58)$$

and go back to kinetic equations for the $(f_{\mathbf{k}\lambda})_{ij}$ in the end. The T^a in (2.58) are the Hermitian $\mathrm{U}(n_{\mathrm{s}})$ generators satisfying the normalization and completeness relations

$$\mathrm{tr}(T^a T^b) = \frac{\delta^{ab}}{2}, \qquad\qquad \sum_a T^a_{ij} T^a_{kl} = \frac{\delta_{il}\delta_{jk}}{2}. \qquad (2.59)$$

---

[28]In the literature there are several conventions for the order of the indices. We use the one of [54].

[29]This definition slightly differs from the one in [65]. The definition in [65] and our present definition are equivalent to the first and the second definition in [54], respectively.

We write $\delta f \equiv f - f^{\text{eq}}$ for both $(f_{\mathbf{k}\lambda})_{ij}$ and $f_{\mathbf{k}\lambda}^a$. The $\delta f_{\mathbf{k}\lambda}^a$ appear as slow variables y_a in the equations of motion (2.2).

We will expand the kinetic equations (2.2) to order h^2, and to second order in the deviations δX of the charges (1.17), including the terms of order $(\delta X)^2 \delta f$. Terms with more than one factor of δf do not enter the kinetic equations at order h^2, as we show in appendix C.

The fluctuations of the occupancies are comparable to the deviation of f from equilibrium, and the higher susceptibilities (2.14) of f do not satisfy (2.15). Strictly speaking, the theory in the preceding sections is therefore not applicable to the occupancy. However, one can coarse-grain the operators f over a certain momentum region, and the resulting operators satisfy the requirements of the framework developed in the above sections. The dependence on the momentum averaging volume drops out in the end. This way we can effectively use the original operators f instead of their smeared versions in our equations. We elaborate on the details of this procedure in appendix A.

2.4.1 Correlation functions

With a certain degeneracy of the vacuum masses in (1.10), the sterile neutrinos undergo oscillations, which appear already at order h^0. They are described by the off-diagonal matrix elements in (2.56). One can obtain the equation of motion simply by taking the time derivative of the operators (2.56) and taking the expectation value. However, it is also instructive to use the Kubo relation (2.26). The equilibrium contribution cancels the disconnected contractions, such that we can replace $\delta f \to f$ in (2.65) and consider only the connected two-point function

$$\Delta_{f_{\mathbf{k}\lambda}^a f_{\mathbf{p}\lambda'}^b}(t) \equiv \left\langle \mathcal{T} f_{\mathbf{k}\lambda}^a(t) f_{\mathbf{p}\lambda'}^b(0) \right\rangle_{\text{C}}. \tag{2.60}$$

The time t in (2.60) is imaginary, $t = -i\tau$ with real τ, and $\mathcal{T}$ denotes time ordering with respect to τ, see (D.2). We encounter the 2-point functions of the operators appearing in (2.55), for which we find (for both positive and negative τ)

$$\left\langle \mathcal{T} a_{i\mathbf{k}\lambda}^\dagger(-i\tau) a_{j\mathbf{p}\lambda'}(0) \right\rangle = \delta_{ij}\, \delta_{\mathbf{k}\mathbf{p}}\, \delta_{\lambda\lambda'}\, T \widetilde{\sum_{p^0}} \frac{e^{p^0 \tau}}{p^0 - E_{i\mathbf{k}}}. \tag{2.61}$$

The retarded correlators appearing in (2.26) are obtained by Fourier transforming (2.60) with imaginary bosonic Matsubara frequency $\omega = i\omega_n \equiv in\pi T$ (with even n), and then continuing ω to the real axis, $\Delta^{\text{ret}}(\omega) = \Delta(\omega + i0^+)$ with real ω.

One encounters factors like $1/(\omega + E_{\mathbf{k}i} - E_{\mathbf{k}j})$. To give a contribution to (2.26) this has to be approximately $1/\omega$ when $\omega \ll \omega_{\text{fast}}$. This requires

$$|\delta M_{ij}^2|/E_{\mathbf{k}i} \sim |\delta M_{ij}^2|/T \ll \omega \qquad (2.62)$$

with

$$\delta M_{ij}^2 \equiv M_i^2 - M_j^2, \qquad (2.63)$$

which means that the frequency for the oscillations between sterile flavors i and j has to be small compared to ω_{fast}. After a simple computation we obtain at order h^0

$$\omega \, \Delta^{\text{ret}}_{f^a_{\mathbf{k}\lambda} f^b_{\mathbf{p}\lambda'}}(\omega) = -\,\delta_{\mathbf{kp}}\,\delta_{\lambda\lambda'} \sum_{(ij)} f'_{\text{F}}(E_{\mathbf{k}i}) \frac{\delta M_{ij}^2}{2E_{\mathbf{k}i}}\, T_{ij}^a T_{ji}^b + \mathcal{O}\big(\omega, h^2, \delta M^4\big), \qquad (2.64)$$

The notation (ij) indicates that we only sum over indices with $|\delta M_{ij}^2|/T \ll \omega_{\text{fast}}$. After expanding in δM^2 and h, the retarded correlator entering (2.26) no longer knows about the scale γ, and we can set $\omega \to 0$.

At order h^2 only the first terms in square brackets in (2.27) and (2.28) survive in the kinetic equations (2.87) and (2.88), if we expand to quadratic order in chemical potentials. Therefore we only discuss these terms in the following. Terms with Ξ_{XXX} are canceled once the slow charges are expressed through their chemical potentials, see (2.31), and the terms containing Ξ_{fff} or Ξ_{ffff} lead to cancellation of the coefficients γ_{fff} and γ_{ffff}, which we demonstrate in appendix C. Since they are defined as the *connected* pieces, the contributions from the susceptibilities (2.14) with mixed indices f and X vanish at leading order in h, since the correlators they multiply in the master formulae are already of order h^2.

We keep the dependence on the absolute Majorana mass scale in all expressions. This is important in order to be able to obtain kinetic equations describing light sterile neutrino dark matter production during the QCD epoch, because here the $\mathcal{O}(h^2)$ terms actually go like $h^2 M^2$ [41]. This dependence emerges from the retarded active neutrino self-energy, which appears in the kinetic equations in the Higgs phase. At order h^2 we neglect terms of order δM^2, because both h^2 and δM^2 are small quantities.

To determine the coefficients γ_{ff}, γ_{ffX}, and γ_{ffXX} we employ (2.26) through (2.28) directly, without making use of (2.30). The latter relation turns out to be very inconvenient here if there is more than one sterile flavor due to a UV divergent

contribution from the commutators, which only cancels against a divergence in the first term in square brackets of (2.30). Thus we consider

$$\Delta_{f_{\mathbf{k}\lambda}^a(f_{\mathbf{p}\lambda'}^b X_{\alpha_1}\cdots X_{\alpha_n})}(t) \equiv \left\langle \mathcal{T} f_{\mathbf{k}\lambda}^a(t) \left(f_{\mathbf{p}\lambda'}^b X_{\alpha_1}\cdots X_{\alpha_n} \right)(0) \right\rangle_{\mathrm{C}}. \qquad (2.65)$$

Again, we were able to replace $\delta f \to f$ and here also $\delta X \to X$ on the right-hand side of (2.65), since we need only the connected correlator. We adopt this procedure in the remainder of this section, understanding that all expectation values are connected. As in (2.60), t is imaginary. $f_{\mathbf{p}\lambda'}^b$ and the charge operators X_{α_i} commute at equal times. The $\mathcal{O}(h^2)$ contribution to (2.65) becomes

$$\Delta_{f_{\mathbf{k}\lambda}^a(f_{\mathbf{p}\lambda}^b X_{\alpha_1}\cdots X_{\alpha_n})}(t) = \int d^4x_1 d^4x_2 \qquad (2.66)$$
$$\times \operatorname{tr}\left\{ h^\dagger \left\langle \mathcal{T} N(x_2)\overline{N}(x_1) f_{\mathbf{k}\lambda}^a(t) f_{\mathbf{p}\lambda}^b(0) \right\rangle_{\mathrm{C}} h \left\langle \mathcal{T} J(x_1)\bar{J}(x_2)(X_{\alpha_1}\cdots X_{\alpha_n})(0) \right\rangle_{\mathrm{C}} \right\},$$

where the trace refers to both spinor and active flavor indices. Since we consider the leading order in h, we can neglect the sterile-neutrino Yukawa interaction in the expectation values on the right-hand side of (2.66). Our definition of a and $a^\dagger$ allows us to substitute them for N and $\overline{N}$ in the path integral, and then work with (2.61). The second expectation value in (2.66) is now a correlation function containing only Standard Model fields. When h is neglected, the charges X_α are conserved, and one can introduce chemical potentials μ_{X_α} such that

$$\left\langle \mathcal{T} J(x_1)\bar{J}(x_2)(X_{\alpha_1}\cdots X_{\alpha_n})(0) \right\rangle_{\mathrm{C}} = \left[T\frac{\partial}{\partial\mu_{X_{\alpha_1}}} \cdots T\frac{\partial}{\partial\mu_{X_{\alpha_n}}} \Delta_{J\bar{J}}(x_1 - x_2, \mu) \right]_{\mu_X = 0} \qquad (2.67)$$

with

$$\Delta_{J_\alpha \bar{J}_\beta}(x, \mu) \equiv Z^{-1} \operatorname{tr}\left\{ \mathcal{T} J_\alpha(x)\bar{J}_\beta(0) \exp\left[\frac{1}{T}\left(\sum_\gamma \mu_{X_\gamma} X_\gamma - H_{\mathrm{SM}} \right) \right] \right\}, \qquad (2.68)$$

where $Z \equiv \operatorname{tr} \exp\left[\left(\sum_\gamma \mu_{X_\gamma} X_\gamma - H_{\mathrm{SM}} \right)/T \right]$ is the partition function at finite chemical potentials of the slowly varying charges, and H_{SM} is the Hamiltonian containing all Standard Model interactions which are in equilibrium at the temperature of interest. The traces in (2.68) and in Z run over states with definite values of the conserved charges, which is why only the slow charges appear in the exponential. Note that one can introduce chemical potentials for the X_γ only *after* expanding in h. Therefore one cannot write $\Delta_{ff}(\omega, \mu)$. We collect some useful formulae for thermal two-point functions at finite chemical potentials in

appendix D. For vanishing h, (2.68) is diagonal in the active flavor indices, so that we can write

$$\Delta_{J_\alpha \bar{J}_\beta} \equiv \delta_{\alpha\beta} \Delta_\alpha. \tag{2.69}$$

The chemical potential of the operator J_α in the sense of (D.5) is $\mu_{J_\alpha} = -\mu_{X_\alpha}$. Therefore the function $e^{\mu_{X_\alpha}\tau} \Delta_\alpha(-i\tau, \mathbf{x}, \mu)$ is anti-periodic in τ, see (D.4), and the Fourier decomposition of (2.68) reads[30]

$$\Delta_\alpha(-i\tau, \mathbf{x}, \mu) = T \widetilde{\sum_{p^0}} e^{-(p^0 + \mu_{X_\alpha})\tau} \Delta_\alpha(p^0, \mathbf{x}, \mu). \tag{2.70}$$

The Matsubara correlator on the right-hand side of (2.70) can be expressed through its spectral function[31] via

$$\Delta_\alpha(-i\tau, \mu) = \int \frac{d\omega'}{2\pi} \, e^{-\omega'\tau} \rho_\alpha(\omega', \mu) \left\{ \Theta(\tau) \left[1 - f_F(\omega' - \mu_{X_\alpha}) \right] \right.$$
$$\left. - \Theta(-\tau) f_F(\omega' - \mu_{X_\alpha}) \right\}. \tag{2.71}$$

The spectral function satisfies

$$\rho_\alpha(k, \mu) = \frac{1}{i} \left[\Delta_\alpha^{\text{ret}}(k, \mu) - \Delta_\alpha^{\text{adv}}(k, \mu) \right], \tag{2.72}$$

and according to (D.8), the retarded and advanced correlators are given by

$$\Delta_\alpha^{\text{ret,adv}}(k, \mu) = \Delta_\alpha\big(k + u[-\mu_{X_\alpha} \pm i0^+], \mu\big) \tag{2.73}$$

with real k^0, where $u = (1, \mathbf{0})$ is the four-velocity of the plasma.

After summing over the Matsubara frequencies we analytically continue ω towards the real axis which gives the $\mathcal{O}(h^2)$ contribution to the retarded correlator

$$\omega \Delta^{\text{ret}}_{f^a_{\mathbf{k}\lambda}(f^b_{\mathbf{p}\lambda'} X_{\alpha_1} \cdots X_{\alpha_n})}(\omega) = - \, \delta_{\mathbf{k}\mathbf{p}} \, \delta_{\lambda\lambda'} \sum_{\beta(ijl)} \frac{f'_F(E_{\mathbf{k}i})}{2E_{\mathbf{k}i}} \left[T \frac{\partial}{\partial \mu_{X_{\alpha_1}}} \cdots T \frac{\partial}{\partial \mu_{X_{\alpha_n}}} \right.$$

$$\times \left\{ h^\dagger_{\beta l} T^b_{lj} T^a_{ji} h_{i\beta} \, \overline{u}_{\mathbf{k}i\lambda} \Delta_\beta^{\text{ret}}(k_j, \mu) u_{\mathbf{k}l\lambda} - h^\dagger_{\beta i} T^a_{ij} T^b_{jl} h_{l\beta} \, \overline{u}_{\mathbf{k}l\lambda} \Delta_\beta^{\text{adv}}(k_j, \mu) u_{\mathbf{k}i\lambda} \right. \tag{2.74}$$

$$\left. \left. + h^\dagger_{\beta i} T^a_{lj} T^b_{ji} h_{l\beta} \, \overline{v}_{\mathbf{k}l\lambda} \Delta_\beta^{\text{ret}}(-k_j, \mu) v_{\mathbf{k}i\lambda} - h^\dagger_{\beta l} T^b_{ij} T^a_{jl} h_{i\beta} \, \overline{v}_{\mathbf{k}i\lambda} \Delta_\beta^{\text{adv}}(-k_j, \mu) v_{\mathbf{k}l\lambda} \right\} \right]_{\mu_X = 0}$$

---

[30] See, e.g., chapter 8.1 of reference [67].

[31] The spectral function for fermionic operators is defined as in (2.25), but with an anticommutator instead of the commutator.

with $k_j \equiv (E_{\mathbf{k}j}, \mathbf{k})$. Here and in the following we take $\omega \to 0$ on the right-hand side, as we did in equation (2.64). Due to

$$
\left[\overline{u}_{\mathbf{k}j\lambda} \Delta^{\mathrm{ret}}_{\bar{J}_\alpha \bar{J}_\beta}(q, \mu) u_{\mathbf{k}'i\lambda'} \right]^* = \overline{u}_{\mathbf{k}'i\lambda'} \Delta^{\mathrm{adv}}_{\bar{J}_\beta \bar{J}_\alpha}(q, \mu) u_{\mathbf{k}j\lambda}, \tag{2.75}
$$

the right-hand side of (2.74) is purely imaginary.

The computation of the correlator entering γ_{fX} is analogous to the one relevant for γ_{fXX}, with a few less extra steps. In the computation of the latter we make use of (2.29), where the commutator vanishes, and obtain the contribution

$$
\omega \operatorname{Im} \Delta^{\mathrm{ret}}_{f^a_{\mathbf{k}\lambda}(X_\alpha X_\beta)}(\omega) = -\operatorname{Re} \left[\Delta^{\mathrm{ret}}_{f^a_{\mathbf{k}\lambda}(\dot{X}_\alpha X_\beta)}(\omega) + \Delta^{\mathrm{ret}}_{f^a_{\mathbf{k}\lambda}(\dot{X}_\beta X_\alpha)}(\omega) + \Delta^{\mathrm{ret}}_{f^a_{\mathbf{k}\lambda}([X_\alpha, \dot{X}_\beta])}(\omega) \right] \tag{2.76}
$$

to the master formula (2.27). Since

$$
\left[\Delta^{\mathrm{ret}}_{AB}(\omega) \right]^* = \Delta^{\mathrm{ret}}_{A^\dagger B^\dagger}(-\omega) \tag{2.77}
$$

for bosonic operators A and B, the rightmost term in (2.76) vanishes for $\omega \to 0$, and we are left with the two terms in which the charge X without time derivative appears to the right of $\dot{X}$. In these terms we can use the same line of arguments as the one below (2.66) after having expanded the correlators to quadratic order in h,[32] relating averages like $\langle \mathcal{T} J \bar{J} X \rangle$ to derivatives with respect to chemical potentials of $\langle \mathcal{T} J \bar{J} \rangle_\mu$. The time derivative of the charge is obtained from the Heisenberg equation of motion and reads

$$
\dot{X}_\alpha(t) = i \sum_j \int d^3x \left[\overline{N}_j(t, \mathbf{x}) h_{j\alpha} J_\alpha(t, \mathbf{x}) - \mathrm{H.c.} \right]. \tag{2.78}
$$

Using (2.75) and omitting terms of order δM^2, we obtain (for $n = 0, 1$)

$$
\operatorname{Re} \Delta^{\mathrm{ret}}_{f^a_{\mathbf{k}\lambda}(\dot{X}_\alpha X^n_\beta)}(\omega) = -\sum_{(ij)} \frac{1}{4E_{\mathbf{k}i}} \frac{f'_{\mathrm{F}}(E_{\mathbf{k}i})}{f_{\mathrm{F}}(E_{\mathbf{k}i})} T^a_{ij} \left[\left(T \frac{\partial}{\partial \mu_{X_\beta}} \right)^n \right. \tag{2.79}
$$

$$
\times \left\{ \frac{f_{\mathrm{F}}(E_{\mathbf{k}i} - \mu_{X_\alpha})}{f_{\mathrm{F}}(-\mu_{X_\alpha})} h^\dagger_{\alpha i} h_{j\alpha} \overline{u}_{\mathbf{k}j\lambda} \rho_\alpha(k_i, \mu) u_{\mathbf{k}i\lambda} \right.
$$

$$
\left. \left. - \frac{f_{\mathrm{F}}(E_{\mathbf{k}i} + \mu_{X_\alpha})}{f_{\mathrm{F}}(\mu_{X_\alpha})} h^\dagger_{\alpha j} h_{i\alpha} \overline{v}_{\mathbf{k}i\lambda} \rho_\alpha(-k_i, \mu) v_{\mathbf{k}j\lambda} \right\} \right]_{\mu_X = 0}.
$$

---

[32] In contrast to the computation of (2.74), here only one additional interaction is needed, because $\dot{X}$ is already of order h, see (2.78).

Analogously, we use (2.29) to relate $\Delta^{\rm ret}_{X(fX\cdots)}$ to $\Delta^{\rm ret}_{\dot{X}(fX\cdots)}$, where the commutator vanishes once again. Using (2.75) and (2.72) we obtain the correlators

$$\omega\Delta^{\rm ret}_{X_\alpha(f^a_{\mathbf{k}\lambda}X_{\beta_1}\cdots X_{\beta_n})}(\omega) = i\sum_{\gamma\,(i\,j)}\frac{f'_{\rm F}(E_{\mathbf{k}i})}{2E_{\mathbf{k}i}}\,T^a_{ij}\left[T\frac{\partial}{\partial\mu_{X_{\beta_1}}}\cdots T\frac{\partial}{\partial\mu_{X_{\beta_n}}}\right. \tag{2.80}$$

$$\left.\times\left\{h^\dagger_{\alpha i}h_{j\alpha}\overline{u}_{\mathbf{k}j\lambda}\rho_\alpha(k_i,\mu)u_{\mathbf{k}i\lambda} - h^\dagger_{\alpha j}h_{i\alpha}\overline{v}_{\mathbf{k}i\lambda}\rho_\alpha(-k_i,\mu)v_{\mathbf{k}j\lambda}\right\}\right]_{\mu_X=0},$$

where once again we have dropped terms of order δM^2.

The correlators containing only charges X are obtained similarly to the steps that yield (2.79). Equation (2.30) gives

$$\Delta^{\rm ret}_{X_\alpha(X_\beta X_\gamma)}(\omega) = \frac{1}{\omega^2}\left[\Delta^{\rm ret}_{\dot{X}_\alpha(X_\beta X_\gamma)^{\textbf{.}}}(\omega) + i\langle[X_\alpha,(X_\beta X_\gamma)^{\textbf{.}}]\rangle + \omega\langle[X_\alpha, X_\beta X_\gamma]\rangle\right]. \tag{2.81}$$

The first commutator on the right-hand side drops out when taking the imaginary part in (2.27). The second one vanishes because the charges (1.17) commute at equal times. We rewrite the first term on the right-hand side as

$$\Delta^{\rm ret}_{\dot{X}_\alpha(X_\beta X_\gamma)^{\textbf{.}}} = \Delta^{\rm ret}_{\dot{X}_\alpha(\dot{X}_\beta X_\gamma)} + \Delta^{\rm ret}_{\dot{X}_\alpha(\dot{X}_\gamma X_\beta)} + \Delta^{\rm ret}_{\dot{X}_\alpha([X_\beta,\dot{X}_\gamma])}\,, \tag{2.82}$$

where the third term on the right-hand side of (2.82) does not contribute to (2.27) due to the relation (2.77). Since $\dot{X} = \mathcal{O}(h)$, at order h^2 the first two terms can be obtained from

$$\Delta^{\rm ret}_{\dot{X}_\alpha(\dot{X}_\beta X_\gamma)}(\omega) = \left[T\frac{\partial}{\partial\mu_{X_\gamma}}\Delta^{\rm ret}_{\dot{X}_\alpha\dot{X}_\beta}(\omega,\mu)\right]_{\mu_X=0}. \tag{2.83}$$

Then we take the thermodynamic limit replacing $\sum_{\mathbf{k}} \to V\int_{\mathbf{k}}$ and we find (the trace runs over spinor indices)

$$\frac{1}{\omega}\,{\rm Im}\,\Delta^{\rm ret}_{\dot{X}_\alpha\dot{X}_\beta}(\omega,\mu) = -\,\delta_{\alpha\beta}\,V\int_{\mathbf{k}}\sum_i|h_{i\alpha}|^2\frac{1}{4E_{\mathbf{k}i}}\frac{f'_{\rm F}(E_{\mathbf{k}i})}{f_{\rm F}(E_{\mathbf{k}i})} \tag{2.84}$$

$$\times{\rm tr}\left\{\slashed{k}_i\left[\frac{f_{\rm F}(E_{\mathbf{k}i} - \mu_{X_\alpha})}{f_{\rm F}(-\mu_{X_\alpha})}\rho_\alpha(k_i,\mu) + \frac{f_{\rm F}(E_{\mathbf{k}i} + \mu_{X_\alpha})}{f_{\rm F}(\mu_{X_\alpha})}\rho_\alpha(-k_i,\mu)\right]\right\}.$$

2.4.2 Kinetic equations

In [47] the washout rate was written in terms of charges. Here we express all kinetic equations in terms of the chemical potentials μ_{X_α} by making use of the relations between charges and chemical potentials from section 2.3. In this case

one does not need the equilibrium values (2.42) and (2.43). This is not true, if the right-hand sides of the kinetic equations are expressed in terms of the charges.

From now on we understand the $\Delta_\alpha(k,\mu)$ to be defined in a grand-canonical description, where the μ label chemical potentials associated with *all* charges.

We expand our kinetic equations to quadratic order in slowly varying chemical potentials, then the higher order terms in (2.31) do not contribute. The term with Ξ_{XXX} on the right-hand side of (2.31) cancels the second term in square brackets in (2.19). The corresponding susceptibility of the occupancies Ξ_{fff}, which appears only in (2.27), leads to cancellation of the coefficient γ_{fff}, see appendix C, and Ξ_{ffff} in (2.28) does the same with the coefficient γ_{ffff}. At order h^0 all other Ξ_{abc} vanish identically, and the only other nonzero Ξ_{abcd} are those with four charges δX which, however, enter (2.28) only for a coefficient multiplying three factors of δX in (2.2), which is beyond our expansion to order μ^2.

The (inverse) susceptibilities of the sterile-neutrino occupancy read (without sum over $\mathbf{k}$ or λ)

$$\Xi_{f^a_{\mathbf{k}\lambda} f^b_{\mathbf{k}\lambda}} = T^a_{ij} T^b_{ji} \, f_{\mathrm{F}}(E_{\mathbf{k}i})[1 - f_{\mathrm{F}}(E_{\mathbf{k}j})] \,, \tag{2.85}$$

$$(\Xi^{-1})_{f^a_{\mathbf{k}\lambda} f^b_{\mathbf{k}\lambda}} = \frac{4 \, T^a_{ij} T^b_{ji}}{f_{\mathrm{F}}(E_{\mathbf{k}i})[1 - f_{\mathrm{F}}(E_{\mathbf{k}j})]} \,. \tag{2.86}$$

Plugging (2.64), (2.74), and (2.79) into the respective master formulae (2.26) through (2.28) we obtain the kinetic equations

$$
\begin{aligned}
(\dot{f}_{\mathbf{k}\lambda})_{mn} = \frac{i}{2E_{\mathbf{k}m}} \bigg\{ & \delta M^2_{mn} \, (f_{\mathbf{k}\lambda})_{mn} \\
& + \sum_{\alpha l} \bigg[\overline{u}_{\mathbf{k}l\lambda} \Big(h_{n\alpha} \Delta^{\mathrm{ret}}_\alpha(k_l, \mu) h^\dagger_{\alpha l} \big[(f_{\mathbf{k}\lambda})_{ml} - \delta_{ml} f_{\mathrm{F}}(E_{\mathbf{k}l} - \mu_{X_\alpha}) \big] \\
& \qquad\qquad - h_{l\alpha} \Delta^{\mathrm{adv}}_\alpha(k_l, \mu) h^\dagger_{\alpha m} \big[(f_{\mathbf{k}\lambda})_{ln} - \delta_{ln} f_{\mathrm{F}}(E_{\mathbf{k}l} - \mu_{X_\alpha}) \big] \Big) u_{\mathbf{k}l\lambda} \\
& + \overline{v}_{\mathbf{k}l\lambda} \Big(h_{m\alpha} \Delta^{\mathrm{ret}}_\alpha(-k_l, \mu) h^\dagger_{\alpha l} \big[(f_{\mathbf{k}\lambda})_{ln} - \delta_{ln} f_{\mathrm{F}}(E_{\mathbf{k}l} + \mu_{X_\alpha}) \big] \\
& \qquad\qquad - h_{l\alpha} \Delta^{\mathrm{adv}}_\alpha(-k_l, \mu) h^\dagger_{\alpha n} \big[(f_{\mathbf{k}\lambda})_{ml} - \delta_{ml} f_{\mathrm{F}}(E_{\mathbf{k}l} + \mu_{X_\alpha}) \big] \Big) v_{\mathbf{k}l\lambda} \bigg] \bigg\} \\
& + \; \mathcal{O}\big(\mu^3, h^2 \delta M^2, \delta M^4, h^4 \big),
\end{aligned}
\tag{2.87}
$$

for those elements of the occupancy matrix for which $|\delta M^2_{mn}|/T \ll \omega_{\mathrm{fast}}$ (including, of course, the diagonal elements). For the other elements the right-hand side

vanishes in our approximation. The sum is over indices l for which $|\delta M_{ml}^2|/T \ll \omega_{\text{fast}}$. $f_{\mathbf{k}+}$ does not appear on the right-hand side of the kinetic equation for $f_{\mathbf{k}-}$, and vice versa.

In equation (2.84) we express $\not{k}$ through the completeness relation of the u or v spinors. Together with equation (2.80), and taking the limit $V \to \infty$, we obtain the kinetic equation for the charge density $n_{X_\alpha} \equiv X_\alpha/V$

$$
\dot{n}_{X_\alpha} = \sum_{(ij)\lambda} \int_{\mathbf{k}} \frac{1}{2E_{\mathbf{k}i}} \Big\{ \bar{u}_{\mathbf{k}i\lambda} h_{i\alpha} \rho_\alpha(k_i, \mu) h_{\alpha j}^\dagger u_{\mathbf{k}i\lambda} \left[(f_{\mathbf{k}\lambda})_{ij} - \delta_{ij} f_{\text{F}}(E_{\mathbf{k}i} - \mu_{X_\alpha}) \right]
$$
$$
- \bar{v}_{\mathbf{k}i\lambda} h_{j\alpha} \rho_\alpha(-k_i, \mu) h_{\alpha i}^\dagger v_{\mathbf{k}i\lambda} \left[(f_{\mathbf{k}\lambda})_{ij} - \delta_{ij} f_{\text{F}}(E_{\mathbf{k}i} + \mu_{X_\alpha}) \right] \Big\}
$$
$$
+ \mathcal{O}\big(\mu^3, h^2\delta M^2, h^4\big). \tag{2.88}
$$

When additional processes are slow, one needs additional kinetic equations. Around $T \sim 130$ GeV, this is the case for the $B + L$ violating electroweak sphaleron processes [27]. Then it is convenient to include a kinetic equation for B [28, 68], since B is not violated by the sterile-neutrino Yukawa interaction so that only the sphaleron rate enters this equation. When $T \sim 8.5 \cdot 10^4$ GeV, the lepton number carried by right-handed electrons evolves slowly, and one has to include the kinetic equation for $L_{e\text{R}}$ which we obtain in section 2.5 and chapter 3.

Using a different approach from ours, an equation similar to (2.87) was derived previously in [54],[33] assuming $M_i \ll T$ for all Majorana masses, so that the condition (2.62) is satisfied. In [54] the chemical potential for L_α appears in f_{F} instead of the one for X_α, which is nevertheless consistent: When electroweak sphalerons are in equilibrium, our statistical operator which determines Δ_α contains $\mu_{X_\alpha} X_\alpha$, but no separate chemical potential for baryon number because the latter is not conserved. In reference [54] $\mu_\alpha L_\alpha + \mu_B B$ appears. However, using the equilibrium conditions one can match the coefficients which gives $\mu_\alpha = \mu_{X_\alpha}$, and $\mu_B = -\sum_\alpha \mu_{X_\alpha}/3$. Therefore the chemical potentials appearing in the distribution functions in our kinetic equations are consistent with those in [54]. This is also true when baryon number B is slow. In the corresponding temperature regime our statistical operator contains $\mu_{X_\alpha} X_\alpha + \mu_B B$, while the one in reference [54] is the same as in the high-temperature regime discussed above. Matching the chemical potentials again yields $\mu_\alpha = \mu_{X_\alpha}$, and this time $\mu_B^{\text{there}} = \mu_B^{\text{here}} - \sum_\alpha \mu_{X_\alpha}/3$, so that again the chemical potentials in the distribution functions appearing in the kinetic equations coincide.

---

[33]See equation (2.29) of reference [54].

Chapter 2 Effective kinetic equations for out-of-equilibrium processes

Unlike the equation in [54], our (2.87) contains not only scattering contributions, see appendix E.1, but also dispersive ones, see appendix E.2. In [54] the latter are incorporated at a later stage. Aside from that, the first term in the curly bracket in (2.87) (which contains the u-spinors) is equivalent to the corresponding one in [54].[34] For vanishing Majorana masses (2.88) coincides with the corresponding equation in [54].[35] Furthermore, for non-vanishing Majorana masses, our contributions containing the u-spinors also appear there. The v-spinor contribution is equivalent, after the replacement described in footnote 34.

In reference [41] kinetic equations for the spin averaged occupancies of sterile neutrinos without near mass degeneracy and for lepton numbers in the Higgs phase have been obtained. There the spin asymmetry of the sterile neutrinos has been neglected.[36] In reference [43] the same authors have obtained equations for a hierarchical system with one light and two heavy sterile neutrinos in the Higgs phase. There the kinetic equations are given in terms of the retarded correlator of J as a function of slowly varying chemical potentials, like in our (2.87). The terms multiplying these correlators are given to linear order in slowly varying quantities. Using the relation[37]

$$\bar{v}_{\mathbf{k}i\lambda}\Delta_\alpha^{\mathrm{ret}}(-q,\mu)v_{\mathbf{k}i\lambda} \ = \ -\,\bar{u}_{\mathbf{k}i,-\lambda}\Delta_\alpha^{\mathrm{adv}}(q,-\mu)u_{\mathbf{k}i,-\lambda}, \tag{2.89}$$

(no sum over repeated indices) which is valid when the Standard Model $\mathcal{CP}$ violation is neglected, together with (2.75), we can reproduce the kinetic equations for the light flavor and the heavy ones,[38] as well as the one for the lepton asymmetries.[39]

2.4.3 Small Majorana masses & low-scale leptogenesis

In low-scale leptogenesis [33, 34] the sterile-neutrino masses are small compared to the temperature, so that typically $M_i \ll |\mathbf{k}|$. Then they can be neglected in the terms containing their (also small) Yukawa couplings, so that the helicity eigenspinors u and v are purely right- and left-handed. Since the operator J is purely left-handed, the terms with v_+ or u_- drop out. Then we also have the

---

[34]The helicity diagonal contribution containing the v-spinors in [54] is not consistent with our equation (2.87). However, it becomes consistent after applying (2.22) of [54].

[35]See equation (2.32) of reference [54].

[36]See equations (2.21) and (2.24) of reference [41].

[37]Since we have made the transition to the grand-canonical description, μ in equation (2.89) now denotes the chemical potentials of all charges.

[38]See equations (2.5) and (2.6) of reference [43].

[39]See equation (2.4) of reference [43].

relations $u_{\mathbf{k}i+}\overline{u}_{\mathbf{k}i+} = v_{\mathbf{k}i-}\overline{v}_{\mathbf{k}i-} = P_R \slashed{k}$ with the chiral projector $P_R \equiv (1+\gamma^5)/2$. Furthermore, condition (2.62) is trivially satisfied, so that the kinetic equations simplify to

$$(\dot{f}_{\mathbf{k}+})_{mn} = \frac{i}{2|\mathbf{k}|}\left\{ \left[M^2, f_{\mathbf{k}+}\right]_{mn} \right. \tag{2.90}$$
$$+ \sum_{\alpha l}\operatorname{tr}\left[\slashed{k}\left(h_{n\alpha}\Delta_\alpha^{\text{ret}}(k,\mu)h_{\alpha l}^\dagger\left[(f_{\mathbf{k}+})_{ml} - \delta_{ml}f_F(|\mathbf{k}| - \mu_{X_\alpha})\right]\right.\right.$$
$$\left.\left.\left. - h_{l\alpha}\Delta_\alpha^{\text{adv}}(k,\mu)h_{\alpha m}^\dagger\left[(f_{\mathbf{k}+})_{ln} - \delta_{ln}f_F(|\mathbf{k}| - \mu_{X_\alpha})\right]\right)\right]\right\},$$

$$(\dot{f}_{\mathbf{k}-})_{mn} = \frac{i}{2|\mathbf{k}|}\left\{ \left[M^2, f_{\mathbf{k}-}\right]_{mn} \right. \tag{2.91}$$
$$+ \sum_{\alpha l}\operatorname{tr}\left[\slashed{k}\left(h_{m\alpha}\Delta_\alpha^{\text{ret}}(-k,\mu)h_{\alpha l}^\dagger\left[(f_{\mathbf{k}-})_{ln} - \delta_{ln}f_F(|\mathbf{k}| + \mu_{X_\alpha})\right]\right.\right.$$
$$\left.\left.\left. - h_{l\alpha}\Delta_\alpha^{\text{adv}}(-k,\mu)h_{\alpha n}^\dagger\left[(f_{\mathbf{k}-})_{ml} - \delta_{ml}f_F(|\mathbf{k}| + \mu_{X_\alpha})\right]\right)\right]\right\},$$

and (again $n_{X_\alpha} \equiv X_\alpha/V$)

$$\dot{n}_{X_\alpha} = \sum_{(ij)}\int_{\mathbf{k}}\frac{1}{2|\mathbf{k}|}\operatorname{tr}\left[\slashed{k}\left\{h_{i\alpha}\rho_\alpha(k,\mu)h_{\alpha j}^\dagger\left[(f_{\mathbf{k}+})_{ij} - \delta_{ij}f_F(|\mathbf{k}| - \mu_{X_\alpha})\right]\right.\right.$$
$$\left.\left. - h_{j\alpha}\rho_\alpha(-k,\mu)h_{\alpha i}^\dagger\left[(f_{\mathbf{k}-})_{ij} - \delta_{ij}f_F(|\mathbf{k}| + \mu_{X_\alpha})\right]\right\}\right]. \tag{2.92}$$

In (2.90) through (2.92) we have $k^0 = |\mathbf{k}|$, the traces refer to spinor indices, and we have neglected terms of order μ^3, as well as terms of order h^2M^2, M^4, and h^4. Similar equations have been obtained in reference [35]. Keeping in mind that they use the index convention of reference [57], we can reproduce their kinetic equation[40] for the sterile neutrino occupancies by setting $\operatorname{tr}\left[\slashed{k}\Delta_\alpha^{\text{ret}}(k,\mu)\right] = \operatorname{tr}\left[\slashed{k}\Delta_\alpha^{\text{adv}}(k,\mu)\right]^* \to -T^2/4 + i|\mathbf{k}|\left(\gamma^{(0)} + \mu_\alpha\gamma^{(2)}\right)$ in our (2.90) and (2.91), and neglecting terms quadratic in chemical potentials. Recalling (2.72), we can also reproduce their kinetic equation[41] corresponding to our (2.92) in the same way. Setting $\mu = 0$ in the spectral function ρ_α in (2.92) and expanding the Fermi distribution to linear order in μ_{X_α}, one obtains the washout term which was found in [47].

---

[40]See equation (2.14) of reference [35].
[41]See equation (2.18) of reference [35].
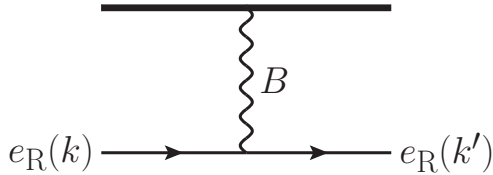
Figure 1: Example of a momentum changing process that keeps right-handed electrons e_{R} in *kinetic* equilibrium. The wiggly line is a U(1) gauge boson, and the thick line represents a generic weak-hypercharged particle in the plasma. This process does *not* involve the electron Yukawa coupling h_e, but only the much larger U(1) gauge coupling g'.

2.5   Kinetic equations for right-handed electrons

Here we apply the formalism of section 2.2 to the equilibration of right-handed electrons. At temperatures T below 10^{13} GeV, weak hypercharge interactions are much faster than the Hubble expansion,[42] and the right-handed electrons are kept in kinetic equilibrium (their spectrum is given by a Fermi-Dirac distribution) by processes like the one in figure 1. This way, unlike for sterile neutrinos, only the total number of right-handed electrons $L_{e\mathrm{R}}$ in (1.20) is a kinetic variable, while the momentum-resolved occupancy is not. Due to the smallness of the electron Yukawa coupling the lepton number $L_{e\mathrm{R}}$ carried by e_{R} takes much longer to equilibrate than the establishment of kinetic equilibrium. For sufficiently small deviations from equilibrium the time evolution of $L_{e\mathrm{R}}$ can be described by the linearized version of (2.2), which generally reads

$$\dot{L}_{e\mathrm{R}} = -\gamma_{L_{e\mathrm{R}}L_{e\mathrm{R}}}\delta L_{e\mathrm{R}} - \gamma_{L_{e\mathrm{R}}X_\alpha}\delta X_\alpha + \cdots \qquad (2.93)$$

without Hubble expansion. If the X_α are not slowly varying at the time when $L_{e\mathrm{R}}$ comes into equilibrium, which is the case if low-scale leptogenesis is not realized,[43] then the terms with $\gamma_{L_{e\mathrm{R}}X_\alpha}$ are absent. A term containing the departure from equilibrium of baryon number δB does not appear in (2.93), because by the time B is a slow variable $L_{e\mathrm{R}}$ has long come into equilibrium, as we will see around (3.57). In principle there are also non-linear terms, like, e.g., the ones we took into account

---

[42]To see this, let us apply our argument from section 2.1.1 to the weak hypercharge gauge coupling g'. Setting the ratio in (2.4) equal to unity and evolving the coupling g' we obtain the equilibration temperature $\sim a\,3.2\cdot 10^{16}$ GeV, such that for a not much smaller than 10^{-3}, the claim holds.

[43]This is also the case, if low-scale leptogenesis is realized, but at temperatures much lower than the equilibration temperature of $L_{e\mathrm{R}}$.

in the kinetic equations for the X_α in section 2.4. Here we work only in the linear regime.

To keep the discussion of the kinetic equation of $L_{e\mathrm{R}}$ as general as possible, it is convenient to strip off the dependence of the susceptibilities in the master formulae, and to work with a kinetic equation that contains chemical potentials on the right-hand side. This is possible by making use of the relation (2.31), such that together with (2.26) the general kinetic equation (2.2) reads at linear order

$$\dot{n}_a = -\Gamma_{ab}\mu_b \tag{2.94}$$

for the charge densities $n_a \equiv Q_a/V$, with

$$\Gamma_{ab} \equiv \frac{1}{V} \lim_{\omega \to 0} \omega^2 \,\mathrm{Im}\Delta_{ab}^{\mathrm{ret}}(\omega). \tag{2.95}$$

For the purpose of determining the rates in (2.93), we will only need the coefficient

$$\Gamma \equiv \Gamma_{L_{e\mathrm{R}}L_{e\mathrm{R}}}, \tag{2.96}$$

which we demonstrate in turn for three scenarios in which the equilibration of $L_{e\mathrm{R}}$ plays a role. Therefore we need the inverse susceptibilities χ^{-1} treated in section 2.3.

1. Only Standard Model interactions, $L_{e\mathrm{R}}$ is the only slow variable. Then the terms $\gamma_{L_{e\mathrm{R}}X_\alpha}$ are absent in (2.93). Assume X_e to be non-zero, and $X_\mu = X_\tau = 0$. Then (2.32) gives

$$\frac{\mu_{L_{e\mathrm{R}}}}{T} = (\chi^{-1})_{L_{e\mathrm{R}}L_{e\mathrm{R}}}(L_{e\mathrm{R}} - L_{e\mathrm{R}}^{\mathrm{eq}}) \tag{2.97}$$

and using (2.35) and (2.47) we obtain

$$L_{e\mathrm{R}}^{\mathrm{eq}} = -\Xi_{L_{e\mathrm{R}}L_{e\mathrm{R}}}(\chi^{-1})_{L_{e\mathrm{R}}X_e}X_e = -\frac{(\chi^{-1})_{L_{e\mathrm{R}}X_e}}{(\chi^{-1})_{L_{e\mathrm{R}}L_{e\mathrm{R}}}}X_e \tag{2.98}$$

Combining this with (2.94) yields

$$\dot{n}_{L_{e\mathrm{R}}} = -\gamma_{L_{e\mathrm{R}}L_{e\mathrm{R}}}(n_{L_{e\mathrm{R}}} - n_{L_{e\mathrm{R}}}^{\mathrm{eq}}) \tag{2.99}$$

with

$$\gamma_{L_{e\mathrm{R}}L_{e\mathrm{R}}} = TV(\chi^{-1})_{L_{e\mathrm{R}}L_{e\mathrm{R}}}\Gamma. \tag{2.100}$$

Collecting the susceptibilities from equation (2.40) then gives

$$\gamma_{L_{e\mathrm{R}}L_{e\mathrm{R}}} = \frac{4266}{481\,T^2}\Gamma, \tag{2.101}$$

$$n_{L_{e\mathrm{R}}}^{\mathrm{eq}} = \frac{185}{711}n_{X_e}. \tag{2.102}$$

2. Only Standard Model interactions, L_{eR} is the only slow variable, so that again terms containing $\gamma_{L_{eR}X_\alpha}$ vanish in (2.93). Now allow for all X_α to be non-vanishing, with the constraint $B - L = \sum_\alpha X_\alpha = 0$. Then, by means of (2.32) and (2.40), we have

$$\dot{n}_{L_{eR}} = -T^{-2}\Gamma \left[\frac{4266}{481} n_{L_{eR}} - \frac{30}{13} n_{X_e} + \frac{24}{37} \left(n_{X_\mu} + n_{X_\tau} \right) \right]. \tag{2.103}$$

This equation can be recast in the form of (2.99) with (2.101) and now

$$n^{\mathrm{eq}}_{L_{eR}} = \frac{1}{3} n_{X_e}, \tag{2.104}$$

which agrees with the result in [45].

3. Type-I see-saw models realizing low-scale leptogenesis, like in section 2.4. We reiterate the fact that if leptogenesis takes place around the same time as the equilibration of right-handed electrons, then both the X_α and L_{eR} have to be treated as slow variables, and both terms appear on the right-hand side of (2.93). We make use of (2.30) to relate the retarded two-point functions of the charges to those of their time derivatives. The one of L_{eR} is due to the Yukawa interaction in (1.19) and reads

$$\dot{L}_{eR} = -i \int d^3x \left(\overline{e_R} h_e \varphi^\dagger \ell_e - \mathrm{H.c.} \right). \tag{2.105}$$

Noting that the two commutators on the right-hand side of (2.30) do not contribute, the time derivatives of X_α in (2.78) are uncorrelated with (2.105), and therefore the rate coefficients $\Gamma_{L_{eR}X_\alpha}$ vanish. Now (2.103) holds again, and so does (2.101). This time the terms with n_{X_α} do not contribute to $n^{\mathrm{eq}}_{L_{eR}}$, but constitute individual source terms, so that $n^{\mathrm{eq}}_{L_{eR}} = 0$ and

$$\gamma_{L_{eR}X_e} = -\frac{30}{13\,T^2}\Gamma, \tag{2.106}$$

$$\gamma_{L_{eR}X_\alpha} = \frac{24}{37\,T^2}\Gamma \qquad (\alpha = \mu, \tau). \tag{2.107}$$

These considerations imply that in the kinetic equation (2.93) for L_{eR} can be written as

$$\dot{n}_{L_{eR}} = -\Gamma\,\mu_{L_{eR}}. \tag{2.108}$$

In order to obtain Γ we make use of (2.30) again to relate the retarded two-point function of $L_{e\mathrm{R}}$ to the one of its time derivative (2.105). Here the commutators on the right-hand side of (2.30) vanish trivially, and we have

$$\Gamma = \frac{1}{V} \lim_{\omega \to 0} \frac{1}{\omega} \operatorname{Im} \Delta^{\mathrm{ret}}_{\dot{L}_{e\mathrm{R}} \dot{L}_{e\mathrm{R}}}(\omega). \tag{2.109}$$

The determination of the coefficient Γ at leading order in Standard Model couplings is the subject of the following chapter 3.

Equilibration rate of right-handed electrons

In this chapter we improve on previous calculations of the equilibration rate $\gamma_{L_{eR}L_{eR}}$ of right-handed electrons e_R by correctly treating various thermal effects, including for the first time contributions from multiple soft gauge interactions in collinear emission processes. We also compute the conversion rates $\gamma_{L_{eR}X_\alpha}$ in the scenario of low-scale leptogenesis around the e_R equilibration temperature. Both of these rates factorize into the mutual rate coefficient Γ in (2.96) and different inverse susceptibilities, see section 2.5. The latter are determined by equilibrium thermodynamics, see section 2.3, and the more intrigued coefficient Γ, which we compute here, encodes the kinematics. According to (2.109), this quantity is determined by the correlator $\Delta^{\text{ret}}_{\dot{L}_{eR}\dot{L}_{eR}}$ which can most generally be visualized as in figure 2. The imaginary part in (2.109) corresponds to cutting the diagram.

The processes contributing to the rate coefficient Γ are very similar to those in the production of ultrarelativistic sterile neutrinos [69, 70], which we briefly discuss in appendix E.1. There are two different types of contributions at leading order, which is $h_e^2 g^2$ where g denotes a generic Standard Model coupling and h_e is the electron Yukawa coupling. The first type includes the (inverse) $1 \leftrightarrow 2$ decay of Higgs bosons into right-handed electrons and lepton doublets, corresponding to including only the thermal mass resummations in the gray blob in figure 2. This decay is kinematically allowed when the thermal Higgs mass is sufficiently large. One also has to take into account $1n \leftrightarrow 2n$ scatterings with soft gauge boson exchanges, which can be visualized as below in figure 4. Due to their collinear nature these processes are not suppressed. On the contrary, they lead to strong enhancement compared to the rate for Higgs decay, because they open several new channels, which also happens in sterile neutrino production [70]. Therefore the multiple scatterings of $1n \leftrightarrow 2n$ particles with arbitrary n have to be included,
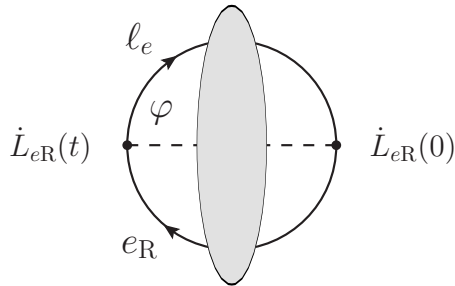
Figure 2: Diagrammatic representation of the correlator entering the rate coefficient Γ. In order to give a contribution, the gray blob must contain additional (self-) interactions. There is also a contribution from the same diagram but with reversed direction of fermion number flow, according to the two terms in (2.105), which we do not show.

which is known as Landau-Pomeranchuk-Migdal (LPM) resummation [71–73]. A complication compared to sterile neutrino production is that right-handed electrons have Standard Model gauge interactions, because they carry weak hypercharge. Therefore they are also affected by multiple scattering, similar to gluons in QCD [74–76]. We discuss the (inverse) $1 \leftrightarrow 2$ Higgs decays and the generalization to multiple soft scattering in section 3.1. The second type of processes are $2 \rightarrow 2$ scattering processes, which we discuss in section 3.2, where we also show the diagrams that result from cutting the corresponding versions of the one in figure 2.[44]

The chiral anomaly violates $L_{e\mathrm{R}}$ conservation in the Standard Model. Therefore $L_{e\mathrm{R}}$ can be converted into hypercharge electromagnetic fields, changing the value of $L_{e\mathrm{R}}$, and leading to terms including the hypercharge gauge fields on the right-hand side of (2.93). In the absence of long-range gauge fields this is a non-linear effect. However, complete equilibration may in fact lead to long-range hypermagnetic fields [77]. These effects can be neglected as long as the growth rate of the gauge fields is smaller than $\gamma_{L_{e\mathrm{R}}L_{e\mathrm{R}}}$ in (2.93). In the Standard Model this requires that the chemical potential conjugate to $L_{e\mathrm{R}}$ satisfies (see appendix F)

$$|\mu_{L_{e\mathrm{R}}}| \lesssim 1.4 \cdot 10^{-3}\, T \tag{3.1}$$

when $\gamma_{L_{e\mathrm{R}}L_{e\mathrm{R}}}$ is comparable to the Hubble rate, i.e. around $T \sim 8.5 \cdot 10^{4}$ GeV, see (3.57).

---

[44]See figure 5 below.

The importance of electron equilibration was first pointed out in [44], where it was noted that the final baryon asymmetry is exponentially sensitive to the equilibration rate. A computation in [44] included only the inverse Higgs decay. The importance of $2 \to 2$ scattering was noted in [45]. The equilibration of heavier lepton flavors in thermal leptogenesis was studied in [61, 78]. It was pointed out that multiple soft $1n \leftrightarrow 2n$ scattering processes also contribute at leading order [78], and the corresponding rate was estimated, but it has not been computed so far.

We evaluate Γ at vanishing chemical potentials, which is appropriate when the charge densities are small. This way we avoid the problem of infrared divergences in processes with Higgs bosons in the initial or final state. In [54] this problem is discussed in the case of rates entering the kinetic equations for sterile neutrinos.

3.1   Higgs decay and multiple soft scattering

The bulk of particles in the plasma have *hard* momenta, $p \sim T$. In the symmetric phase, the Standard Model particles carry thermal masses. For the Higgs boson the thermal mass is momentum independent and is given by [79]

$$m_\varphi^2 = \frac{1}{16} \left[3g^2 + g'^2 + 4h_t^2 + 8\lambda \right] (T^2 - T_0^2), \tag{3.2}$$

with $T_0 = 160$ GeV. For hard fermions one has to use the so-called asymptotic thermal masses [79], which for the left- and right-handed leptons are given by[45]

$$m_{\ell_e}^2 = \frac{1}{16} \left[3g^2 + g'^2 \right] T^2, \tag{3.3}$$

$$m_{e_{\mathrm{R}}}^2 = \frac{1}{4} g'^2 T^2. \tag{3.4}$$

For $T \gg T_0$ the Higgs bosons have the largest mass, and for certain values of the couplings their decay into left-handed electron lepton doublets ℓ_e and the right-handed electrons is kinematically allowed. With increasing temperature the top Yukawa coupling decreases quickly such that above a certain temperature m_φ becomes smaller than $m_{\ell_e} + m_{e_{\mathrm{R}}}$ and the channel closes. Since $m_\varphi > m_{\ell_e} > m_{e_{\mathrm{R}}}$ at any temperature well above the electroweak scale, no other $1 \leftrightarrow 2$ decay channel opens up at a higher temperature.

---

[45]For fermions the asymptotic mass is a factor $\sqrt{2}$ larger than the one at zero momentum [79]. In [45] the zero-momentum fermion masses are used. The thermal lepton doublet mass in (3.3) is actually flavor independent, and the same is true for the singlet mass in (3.4).

Figure 3: The interference of these two exemplary $1n \to 2n$ processes with $n = 2$ needs to be taken into account. The gauge bosons have soft momenta $q \sim gT$, and the short lines at the bottom ends of their wiggly lines represent particles in the plasma.

Since the masses are small compared to T, the particles participating in the decay process are ultrarelativistic. Furthermore, their momenta are nearly collinear, with transverse momenta $p_\perp$ of order gT. The wave packets of the decay products have a width of order $1/p_\perp$. They overlap for a time of order $1/(g^2T)$, the so-called formation time. Here the formation time is of the same order of magnitude as the mean free time between scatterings with *soft* momentum transfer $q \sim gT$. Thus the particles typically scatter multiple times before their wave packets separate, so that the scatterings cannot be treated independently. We show two exemplary diagrams in figure 3. This situation is similar to bremsstrahlung in a medium in QED [71–73, 80] (see also [81]), and in QCD [74–76, 82, 83], where it leads to a suppression of the emission probability. In the case of sterile neutrino production, on the other hand, it gives a strong enhancement, because new kinematic channels are opened [70]. We compute the Higgs decay in section 3.1.1, and include multiple soft scatterings in section 3.1.2.

3.1.1 Higgs decay

We start from the imaginary time correlator

$$\Delta_{\dot{L}_{eR}\dot{L}_{eR}}(i\omega_n) = \int_0^{1/T} d\tau \, e^{i\omega_n\tau} \langle \dot{L}_{eR}(-i\tau)\dot{L}_{eR}(0)\rangle, \tag{3.5}$$

with bosonic Matsubara frequency ω_n. Without soft gauge interactions, the correlator (3.5) reads

$$\Delta_{\dot{L}_{eR}\dot{L}_{eR}}(i\omega_n) = -2Vh_e^2T^2\widetilde{\sum_{p^0,k^0}} \int_{\mathbf{p},\mathbf{k}} \mathrm{tr}\left[S_{\ell_e}(p)S_{e_R}(k)\right]\Delta_\varphi(p - k + i\omega_n u)$$

$$+(i\omega_n \to -i\omega_n), \tag{3.6}$$

with $u = (1, \mathbf{0})$ the four-velocity of the plasma. We write the scalar field propagator as

$$\Delta_a(p) = \frac{-1}{(v \cdot p)(\overline{v} \cdot p) - \mathbf{p}_\perp^2 - m_a^2}. \tag{3.7}$$

Here, $v = (1, \mathbf{v})$ with a unit vector $\mathbf{v}$, which defines the longitudinal direction, and $\overline{v} = (1, -\mathbf{v})$. Chiral symmetry is unbroken, even with thermal masses. Therefore the non-vanishing components of the fermion propagators in the Weyl representation can be written as 2×2 matrices,

$$S_{\ell_e}(p) = \sigma \cdot p \Delta_{\ell_e}(p), \tag{3.8}$$

$$S_{e_{\mathrm{R}}}(p) = \overline{\sigma} \cdot p \Delta_{e_{\mathrm{R}}}(p), \tag{3.9}$$

where σ^μ, $\overline{\sigma}^\mu$ are the usual Pauli matrices. There are two different kinematic situations which we have to take into account: either all momenta satisfy $v \cdot p \sim g^2 T$, $\overline{v} \cdot p \sim T$ or the same but with $v \leftrightarrow \overline{v}$. The second case gives the same result as the first but with $i\omega_n \to -i\omega_n$. For $v \cdot p \sim g^2 T$ the scalar propagator can be approximated as

$$\Delta_a(p) = \frac{1}{2p_\parallel} D_a(p) \tag{3.10}$$

where $p_\parallel \equiv \mathbf{v} \cdot \mathbf{p}$ is the large component of $\mathbf{p}$, and

$$D_a(p) \equiv \frac{-1}{v \cdot p - (\mathbf{p}_\perp^2 + m_a^2)/(2p_\parallel)}. \tag{3.11}$$

Similarly, the fermion propagators can be written as (see e.g. [70])

$$S_{\ell_e}(p) = \eta(\mathbf{p})\eta^\dagger(\mathbf{p}) \, D_{\ell_e}(p), \tag{3.12}$$

$$S_{e_{\mathrm{R}}}(p) = \chi(\mathbf{p})\chi^\dagger(\mathbf{p}) \, D_{e_{\mathrm{R}}}(p) \tag{3.13}$$

with the spinors

$$\eta(\mathbf{p}) = \left[1 - \frac{1}{2p_\parallel}(\boldsymbol{\sigma} \cdot \mathbf{p}_\perp)\right]\begin{pmatrix} 0 \\ 1 \end{pmatrix}, \tag{3.14}$$

$$\chi(\mathbf{p}) = \left[1 + \frac{1}{2p_\parallel}(\boldsymbol{\sigma} \cdot \mathbf{p}_\perp)\right]\begin{pmatrix} 1 \\ 0 \end{pmatrix}. \tag{3.15}$$

In (3.12) through (3.15) we keep only the leading order contributions to the equilibration rate. It is convenient to associate the spinors in (3.12), (3.13) with the adjacent vertices rather than with the propagators.

After performing the sum over Matsubara frequencies we encounter a factor

$$\mathscr{F}(p_{\parallel}, k_{\parallel}) = f_{\mathrm{F}}'(k_{\parallel}) \left[f_{\mathrm{F}}(p_{\parallel}) + f_{\mathrm{B}}(p_{\parallel} - k_{\parallel}) \right]. \tag{3.16}$$

We can then analytically continue $i\omega_n$ to arbitrary complex ω which gives

$$\Delta_{\dot{L}_{e\mathrm{R}}\dot{L}_{e\mathrm{R}}}(\omega) = 2h_e^2 V \int_{\mathbf{k},\mathbf{p}} \frac{\mathscr{F}(p_{\parallel}, k_{\parallel})}{k_{\parallel} - p_{\parallel}} \eta^{\dagger}(\mathbf{p}) \chi(\mathbf{k}) \chi^{\dagger}(\mathbf{k}) \eta(\mathbf{p}) \frac{\delta E}{\delta E - \omega} + (\omega \to -\omega), \tag{3.17}$$

where

$$\delta E = \delta E(\mathbf{p}_{\perp}, \mathbf{k}_{\perp}) \equiv \frac{m_{e\mathrm{R}}^2 + \mathbf{k}_{\perp}^2}{2k_{\parallel}} - \frac{m_{\ell_e}^2 + \mathbf{p}_{\perp}^2}{2p_{\parallel}} - \frac{m_{\varphi}^2 + (\mathbf{k}_{\perp} - \mathbf{p}_{\perp})^2}{2(k_{\parallel} - p_{\parallel})} \tag{3.18}$$

is the change of energy in the decay $\varphi \to \ell_e \bar{e}_{\mathrm{R}}$. When we take the imaginary part of the retarded correlator

$$\Delta_{\dot{L}_{e\mathrm{R}}\dot{L}_{e\mathrm{R}}}^{\mathrm{ret}}(\omega) = \Delta_{\dot{L}_{e\mathrm{R}}\dot{L}_{e\mathrm{R}}}(\omega + i0^+) \tag{3.19}$$

with ω real, δE becomes equal to $\pm\omega$. For both signs one obtains the same imaginary part. Since we need this to compute the rate using (2.26) we can drop terms of order ω^2 and higher. Pulling out a factor $\eta^{\dagger}(\mathbf{p})\chi(\mathbf{k})$, corresponding to the leftmost vertex in figure 4 (without gauge bosons) we may write

$$\mathrm{Im}\,\Delta_{\dot{L}_{e\mathrm{R}}\dot{L}_{e\mathrm{R}}}^{\mathrm{ret}}(\omega) = 8h_e^2 V \omega \,\mathrm{Im} \int_{\mathbf{k},\mathbf{p}} \frac{\mathscr{F}(p_{\parallel}, k_{\parallel})}{k_{\parallel} - p_{\parallel}} \eta^{\dagger}(\mathbf{p}) \chi(\mathbf{k})\, j(\mathbf{p}_{\perp}, \mathbf{k}_{\perp}) \tag{3.20}$$

where j satisfies

$$\left(\delta E - i0^+\right) j(\mathbf{p}_{\perp}, \mathbf{k}_{\perp}) = \frac{1}{2} \chi^{\dagger}(\mathbf{k}) \eta(\mathbf{p}). \tag{3.21}$$

Note that due to the relation

$$\frac{1}{x \pm i0^+} = \mathrm{PV}\frac{1}{x} \mp i\pi\delta(x) \qquad \text{(for real } x\text{)} \tag{3.22}$$

in the integrand of (3.20) the delta function $\delta(\delta E)$ appears which enforces energy conservation for the (inverse) Higgs decay. The coefficient Γ is then obtained by plugging (3.20) into (2.109).
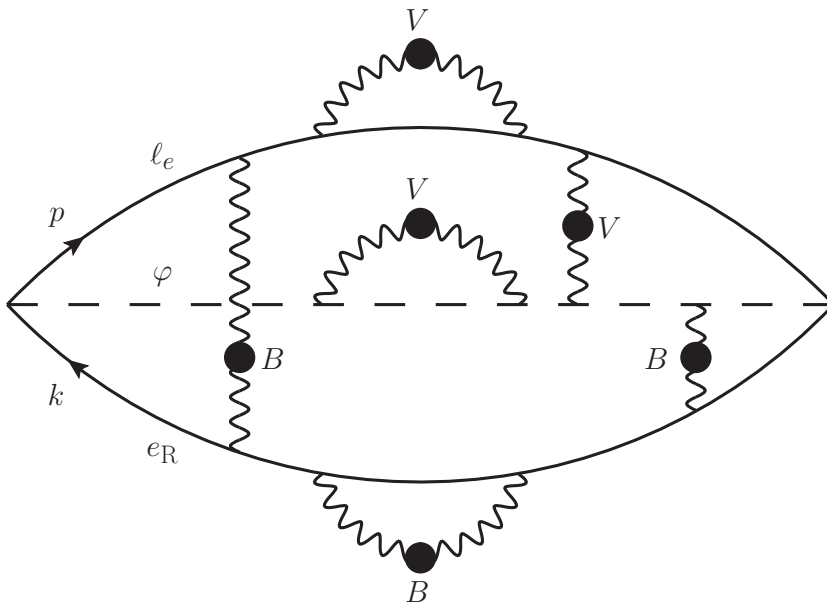
Figure 4: Typical diagram of multiple soft scattering the imaginary part of which gives a contribution to the e_{R} equilibration rate. V stands for either a W or a hypercharge gauge boson B. All gauge bosons are soft and their propagators are hard thermal loop (HTL) resummed, as indicated by the thick dots. This diagram is one of the cases contained in the generic diagram in figure 2.

3.1.2 Multiple soft gauge boson scattering

Now we include the effect of multiple scattering mediated by soft electroweak W or B gauge bosons, as sketched in figure 4.[46] The result can again be described by (3.20), where j now satisfies

$$
\begin{aligned}
\delta E(\mathbf{p}_\perp, \mathbf{k}_\perp)\, j(\mathbf{p}_\perp, \mathbf{k}_\perp) &- i \int \frac{d^2 q_\perp}{(2\pi)^2} \Big\{ \mathscr{C}(\mathbf{q}_\perp^2) \big[j(\mathbf{p}_\perp, \mathbf{k}_\perp) - j(\mathbf{p}_\perp - \mathbf{q}_\perp, \mathbf{k}_\perp) \big] \\
&+ \mathscr{C}'(\mathbf{q}_\perp^2) \Big(y_\varphi\, y_{\ell_e} \big[j(\mathbf{p}_\perp, \mathbf{k}_\perp) - j(\mathbf{p}_\perp - \mathbf{q}_\perp, \mathbf{k}_\perp) \big] \\
&\qquad\qquad + y_{\ell_e}\, y_{e_{\mathrm{R}}} \big[j(\mathbf{p}_\perp, \mathbf{k}_\perp) - j(\mathbf{p}_\perp - \mathbf{q}_\perp, \mathbf{k}_\perp - \mathbf{q}_\perp) \big] \\
&\qquad\qquad - y_\varphi\, y_{e_{\mathrm{R}}} \big[j(\mathbf{p}_\perp, \mathbf{k}_\perp) - j(\mathbf{p}_\perp, \mathbf{k}_\perp - \mathbf{q}_\perp) \big] \Big) \Big\} = \frac{1}{2} \chi^\dagger(\mathbf{k}) \eta(\mathbf{p}). \quad (3.23)
\end{aligned}
$$

---

[46]The range of the gauge interactions is one power of g smaller than the mean free path of the fermions and the Higgs. Therefore crossed gauge bosons, rainbow self-energies, or gauge boson vertex corrections do not contribute at leading order.

Here $\mathbf{q}_\perp$ is the transverse momentum of an exchanged gauge boson. We have introduced

$$\mathscr{C}(\mathbf{q}_\perp^2) \equiv \frac{3}{4} g^2 T \left(\frac{1}{\mathbf{q}_\perp^2} - \frac{1}{\mathbf{q}_\perp^2 + m_{\mathrm{D}}^2} \right), \tag{3.24}$$

$$\mathscr{C}'(\mathbf{q}_\perp^2) \equiv g'^2 T \left(\frac{1}{\mathbf{q}_\perp^2} - \frac{1}{\mathbf{q}_\perp^2 + m_{\mathrm{D}}'^2} \right) \tag{3.25}$$

with the Debye masses [84]

$$m_{\mathrm{D}}^2 = \frac{11}{6} g^2 T^2, \qquad m_{\mathrm{D}}'^2 = \frac{11}{6} g'^2 T^2. \tag{3.26}$$

In the integral in (3.23) the terms containing $j(\mathbf{p}_\perp, \mathbf{k}_\perp)$ correspond to self-energy insertions, which can be easily checked by an explicit calculation.[47] The terms with $\mathscr{C}$ and $\mathscr{C}'$ correspond to interactions mediated by W or B bosons, respectively. By themselves, the self-energies are infrared divergent due to the $1/\mathbf{q}_\perp^2$ term in $\mathscr{C}$ and $\mathscr{C}'$. The subtracted terms in the square brackets in (3.23) correspond to gauge boson exchange between different particles and render the $\mathbf{q}_\perp$-integrals finite. The first two square brackets in (3.23) also appear in the computation of the production rate of ultrarelativistic sterile neutrinos [70]. The other two represent the exchange of weak hypercharge gauge bosons by the right-handed electrons. Replacing the integral in (3.23) by 0^+, one neglects multiple soft scatterings and one recovers the equation (3.21) describing Higgs decay.

Thanks to three-dimensional rotational invariance, the solution to (3.23) can be found as a function of a single transverse momentum [85],

$$j(\mathbf{p}_\perp, \mathbf{k}_\perp) = J(\mathbf{P}), \tag{3.27}$$

with

$$\mathbf{P} \equiv x_k \mathbf{p}_\perp - x_p \mathbf{k}_\perp, \tag{3.28}$$

$$x_k \equiv \frac{k_\parallel}{p_\parallel - k_\parallel}, \qquad x_p \equiv \frac{p_\parallel}{p_\parallel - k_\parallel}. \tag{3.29}$$

In fact, (3.18) now takes the simple form

$$\delta E = \beta \left(\mathbf{P}^2 + M_{\mathrm{eff}}^2 \right) \tag{3.30}$$

---

[47]Note that $y_\varphi y_{\ell_e} + y_{\ell_e} y_{e_{\mathrm{R}}} - y_\varphi y_{e_{\mathrm{R}}} = \left(y_\varphi^2 + y_{\ell_e}^2 + y_{e_{\mathrm{R}}}^2 \right)/2$.

with

$$\beta \equiv \frac{p_{\parallel} - k_{\parallel}}{2p_{\parallel}k_{\parallel}}, \tag{3.31}$$

and

$$M_{\text{eff}}^2 \equiv \beta^{-1} \left[\frac{m_{e_{\text{R}}}^2}{2k_{\parallel}} - \frac{m_{\ell_e}^2}{2p_{\parallel}} - \frac{m_{\varphi}^2}{2(k_{\parallel} - p_{\parallel})} \right]. \tag{3.32}$$

The right-hand side of (3.23) turns into

$$\frac{1}{2}\chi^{\dagger}(\mathbf{k})\eta(\mathbf{p}) = -\frac{\beta}{2}\left(P_x - iP_y\right). \tag{3.33}$$

The function $J(\mathbf{P})$ can be expressed as

$$J(\mathbf{P}) = \frac{i\beta}{4}\left[f_x(\mathbf{P}) - if_y(\mathbf{P})\right], \tag{3.34}$$

where the two-component vector $\mathbf{f}$ is a solution to

$$\begin{aligned}
-i\,\delta E\,\mathbf{f}(\mathbf{P}) - \int \frac{d^2 q_{\perp}}{(2\pi)^2} \Big\{ &\mathscr{C}(\mathbf{q}_{\perp}^2)\big[\mathbf{f}(\mathbf{P}) - \mathbf{f}(\mathbf{P} - x_k \mathbf{q}_{\perp})\big] \\
&+ \mathscr{C}'(\mathbf{q}_{\perp}^2)\Big(y_{\varphi}\,y_{\ell_e}\big[\mathbf{f}(\mathbf{P}) - \mathbf{f}(\mathbf{P} - x_k \mathbf{q}_{\perp})\big] \\
&\quad + y_{\ell_e}\,y_{e_{\text{R}}}\big[\mathbf{f}(\mathbf{P}) - \mathbf{f}(\mathbf{P} + \mathbf{q}_{\perp})\big] \\
&\quad - y_{\varphi}\,y_{e_{\text{R}}}\big[\mathbf{f}(\mathbf{P}) - \mathbf{f}(\mathbf{P} + x_p \mathbf{q}_{\perp})\big]\Big)\Big\} = 2\mathbf{P}.
\end{aligned} \tag{3.35}$$

This is the same integral equation as in [70] (with the appropriate hypercharge assignments), but with two additional terms representing the gauge interaction of right-handed electrons.

Now we choose the unit vector $\mathbf{v}$ in the direction of $\mathbf{k}$. Using $\mathbf{f}(\mathbf{P}) \propto \mathbf{P}$ and integrating over the transverse momentum $\mathbf{k}_{\perp}$, we obtain

$$\Gamma^{\text{LPM}} = \frac{h_e^2}{8\pi^3} \int\limits_0^{\infty} dk \int\limits_{-\infty}^{\infty} dp_{\parallel} \, \frac{(p_{\parallel} - k)^3}{p_{\parallel}^2 k^2} \mathscr{F}(p_{\parallel}, k) \, \text{Re} \int \frac{d^2 P}{(2\pi)^2} \mathbf{P} \cdot \mathbf{f}(\mathbf{P}) \tag{3.36}$$

for the rate coefficient. We solve (3.35) using the algorithm described in [70] and numerically integrate (3.36), see appendix G.
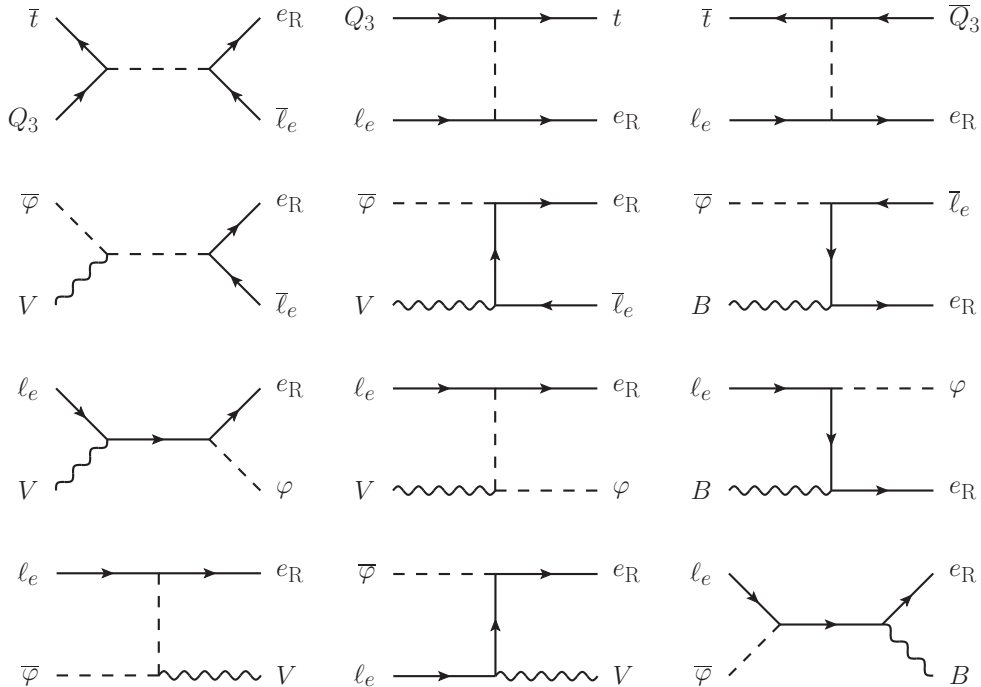
Figure 5: Diagrams for the $2 \to 2$ processes producing an e_R. First line: Quark contributions, second line: $V\overline{\varphi} \to \overline{\ell_e}e_R$, third line: $V\ell_e \to \varphi e_R$, fourth line: $\ell_e\overline{\varphi} \to Ve_R$. Here and in the diagrams we denote $V = B, W$. The exchanged fermion in t-channel is an ℓ_e in the second column and an e_R in the third column. Time runs from left to right.

3.2 $2 \to 2$ processes

At order $h_e^2 g^2$ there are also contributions from $2 \to 2$ scatterings. The corresponding diagrams are shown in figure 5. At leading order all external particles have hard momenta, $p \sim T$, and we can neglect their thermal masses. For s-channel exchange the internal momenta are hard as well, and we can neglect thermal effects on the propagators.[48] However, momenta exchanged in the t-channel become soft at leading order. We treat these contributions in section 3.2.2.

Again, the processes are similar to the ones encountered in relativistic sterile neutrino production in [69]. However, as in the case of the $1n \leftrightarrow 2n$ processes, in e_R equilibration one encounters diagrams in which the produced particle itself

---

[48]In [45] the thermal Higgs mass is included in the Higgs propagator for the process $\bar{t}Q_3 \to \ell_e e_R$. This leads to the complication that the propagator can become on-shell, and a subtraction has to be performed. This problem does not arise in a strict leading order calculation.

couples to a gauge boson B, which leads to additional terms in the matrix elements. In particular, the exchanged particle can be an e_R which can become soft in the t-channel. This contribution has to be treated separately.

3.2.1 Hard momentum transfer

We first consider the case that the exchanged particles have hard momenta. Then the $2 \to 2$ scattering contributions to the equilibration rate can be determined via the Boltzmann equation [86, 87]. We can write the time derivative of the L_{eR} density as

$$\dot{n}_{L_{eR}} = \int_{\mathbf{k}} \frac{\partial}{\partial t} \left[f_{\mathbf{k}} - \bar{f}_{\mathbf{k}} \right] \tag{3.37}$$

where $f_{\mathbf{k}}$ and $\bar{f}_{\mathbf{k}}$ are the occupation numbers of right-handed electrons and positrons, respectively. We replace the time derivatives on the right-hand side by the collision term for $2 \to 2$ particle scattering. It contains the occupancies of the participating particles in the form

$$f_1 f_2 [1 \pm f_3][1 - f_{\mathbf{k}}] - [1 \pm f_1][1 \pm f_2] f_3 f_{\mathbf{k}}, \tag{3.38}$$

corresponding to gain and loss term. The upper and lower signs are for bosons and fermions, respectively.

All Standard Model particles (including the e_R) are in kinetic equilibrium due to their fast gauge interactions. Therefore their occupancies are determined by the temperature and by the chemical potentials of the slowly varying charges and of the strictly conserved ones. To compute Γ at lowest order in chemical potentials, we can set all chemical potentials except $\mu_{L_{eR}}$ equal to zero. For the occupancy of right-handed electrons we can therefore write

$$f_{\mathbf{k}} = f_F(k^0 - \mu_{e_R}) \tag{3.39}$$

with $k^0 = |\mathbf{k}|$, $\mu_{e_R} = \mu_{L_{eR}}$, see (2.39), and for the other Standard Model particles

$$f_i = f_{B,F}(p_i^0) \tag{3.40}$$

where $p_i^0 = |\mathbf{p}_i|$. In thermal equilibrium the gain and the loss term cancel,

$$f_1 f_2 [1 \pm f_3][1 - f_F(k^0)] - [1 \pm f_1][1 \pm f_2] f_3 f_F(k^0) = 0, \tag{3.41}$$

so that the collision term vanishes. Expanding to first order in $\mu_{e_{\mathrm{R}}}$ and making use of (3.41) together with

$$f'_{\mathrm{F}} = -\frac{1}{T} f_{\mathrm{F}}[1 - f_{\mathrm{F}}], \tag{3.42}$$

the contribution to the rate coefficient becomes

$$\Gamma^{2\to2,\mathrm{hard}} = \frac{2}{T} \sum_{\mathrm{processes}} \int_{\mathbf{k},\mathbf{p}_1,\mathbf{p}_2,\mathbf{p}_3} \frac{\sum|\mathcal{M}|^2}{16 p_1^0\, p_2^0\, p_3^0\, k^0} (2\pi)^4 \delta^{(4)}(p_1 + p_2 - p_3 - k)$$
$$f_1 f_2 [1 \pm f_3][1 - f_{\mathrm{F}}(k^0)]\Big|_{\mathrm{hard}}. \tag{3.43}$$

Both terms on the right-hand side of (3.37) give the same contribution which gives rise to the factor 2.

One can write (3.43) in terms of the e_{R} production rate at vanishing e_{R} density,

$$\Gamma^{2\to2,\mathrm{hard}} = \frac{2}{T} \int_{\mathbf{k}} \left[1 - f_{\mathrm{F}}(k^0)\right] (2\pi)^3 \frac{d^4 n_{e_{\mathrm{R}}}}{dt\, d^3 k}\bigg|_{n_{e_{\mathrm{R}}}=0,\,\mathrm{hard}}, \tag{3.44}$$

which is closely related to the production rate of sterile neutrinos computed in [69]. The difference between the two processes is that the sterile neutrinos have no Standard Model gauge interactions, and therefore do not interact once they are produced (at leading order in their Yukawa couplings). In contrast, the right-handed electrons carry weak hypercharge. Scatterings mediated by soft hypercharge gauge bosons contribute to the leading order rate, as discussed in section 3.1. However for the $2 \to 2$ scattering of hard particles the soft scattering is a higher order effect and can be neglected here.

The diagrams contributing to e_{R} production are shown in figure 5. The matrix elements for the processes with quarks and W bosons can be read off from [69] by setting $g' \to 0$,

$$\text{quarks}: \quad \Sigma|\mathcal{M}|^2 = 6\, h_t^2\, h_e^2, \tag{3.45}$$

$$W\overline{\varphi} \to \bar{\ell}_e e_{\mathrm{R}}: \quad \Sigma|\mathcal{M}|^2 = 3g^2\, h_e^2\, \frac{u}{t}, \tag{3.46}$$

$$W\ell_e \to \varphi e_{\mathrm{R}}: \quad \Sigma|\mathcal{M}|^2 = 3g^2\, h_e^2\, \frac{-u}{s}, \tag{3.47}$$

$$\ell_e \overline{\varphi} \to W e_{\mathrm{R}}: \quad \Sigma|\mathcal{M}|^2 = 3g^2\, h_e^2\, \frac{s}{-t}, \tag{3.48}$$

where (3.45) holds for any of the processes $\bar{t}Q_3 \to \ell_e e_{\mathrm{R}}$, $Q_3\ell_e \to te_{\mathrm{R}}$, $\bar{t}\ell_e \to \overline{Q}_3 e_{\mathrm{R}}$. For the processes with hypercharge gauge bosons we find

$$B\overline{\varphi} \to \bar{\ell}_e e_{\mathrm{R}} : \qquad \Sigma|\mathscr{M}|^2 = g'^2 \, h_e^2 \left[4 + \frac{u}{t} + \frac{4t}{u} \right], \tag{3.49}$$

$$B\ell_e \to \varphi e_{\mathrm{R}} : \qquad \Sigma|\mathscr{M}|^2 = g'^2 \, h_e^2 \left[-4 + \frac{-u}{s} + \frac{4s}{-u} \right], \tag{3.50}$$

$$\ell_e\overline{\varphi} \to B e_{\mathrm{R}} : \qquad \Sigma|\mathscr{M}|^2 = g'^2 \, h_e^2 \left[-4 + \frac{s}{-t} + \frac{4(-t)}{s} \right]. \tag{3.51}$$

In (3.45) through (3.51) we have summed over polarizations, color and weak isospin. The Boltzmann equation can now be integrated as in [69], with some additional integrals due to the terms containing a factor 4 in (3.49) through (3.51). We rewrite the contributions proportional to $1/(-u)$ as a process proportional to $1/(-t)$ by interchanging the incoming particles, which may change the statistics of particles 1 and 2.

In the integrals describing lepton exchange in t-channel we need to handle the infrared divergence appearing when the momentum of the exchanged lepton becomes small. We proceed as in [69] by introducing a transverse momentum cutoff q_{cut} for the exchanged particle with $gT \ll q_{\mathrm{cut}} \ll T$. We isolate the piece which is singular for $q_{\mathrm{cut}} \to 0$ and integrate it analytically. Its logarithmic q_{cut} dependence drops out when combined with the soft contribution (see section 3.2.2) which includes only transverse momenta less than q_{cut}. The remaining finite integral is then computed numerically. We treat the integrals appearing on the right-hand side of (3.44) for the various matrix elements (3.45) through (3.51) in appendix H.

3.2.2 Soft momentum transfer

The soft contribution is obtained from the retarded correlator using (2.109), where either of the lepton propagators is HTL resummed. The corresponding diagrams are shown in figure 6. A straightforward computation in imaginary time, in which we make use of the sum rule found in [69], and analytic continuation to real frequency leads to

$$\Gamma^{\mathrm{soft}} = \frac{h_e^2 \, T}{64 \, \pi} \left[m_{\ell_e}^2 \log\left(\frac{q_{\mathrm{cut}}}{m_{\ell_e}} \right) + m_{e_{\mathrm{R}}}^2 \log\left(\frac{q_{\mathrm{cut}}}{m_{e_{\mathrm{R}}}} \right) \right]. \tag{3.52}$$
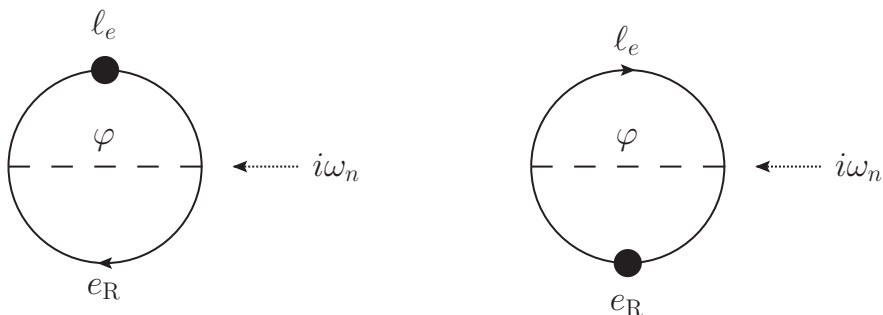
Figure 6: Imaginary time correlator of the time derivative of L_{eR} with one soft fermion. The corresponding propagator has to be HTL resummed, as indicated by the respective blob. The diagrams with $i\omega_n \to -i\omega_n$ are not shown.

3.2.3   Complete $2 \to 2$ rate

Adding the hard singular and finite as well as the soft contributions, q_{cut} drops out, and the contribution from $2 \to 2$ scatterings to the rate coefficient Γ is finite. Evaluating the remaining integrals numerically, we find

$$\Gamma^{2\to2} = \frac{h_e^2 T^3}{2048\,\pi} \left\{ h_t^2 c_t + \left(3g^2 + g'^2\right) \left[c_{\ell_e} + \log \frac{1}{3g^2 + g'^2} \right] \right.$$
$$\left. + 4g'^2 \left[c_{e_R} + \log \frac{1}{4g'^2} \right] \right\} \tag{3.53}$$

with

$$c_t = 2.82, \qquad c_{\ell_e} = 3.52, \qquad c_{e_R} = 2.69. \tag{3.54}$$

3.3   Results

For our numerical results we evaluate the 1-loop running couplings at the renormalization scale πT, which is the first e_R Matsubara mode, see appendix I. We have checked that increasing the renormalization scale by a factor 2, corresponding to renormalization at the first non-zero Higgs Matsubara mode, changes our results by less than 3% in the entire temperature range we consider.

   Figure 7 shows the various contributions to the equilibration rate. The $2 \to 2$ processes are dominant over the entire temperature range considered. The largest contribution comes from scatterings off hard gauge bosons. The $1n \leftrightarrow 2n$
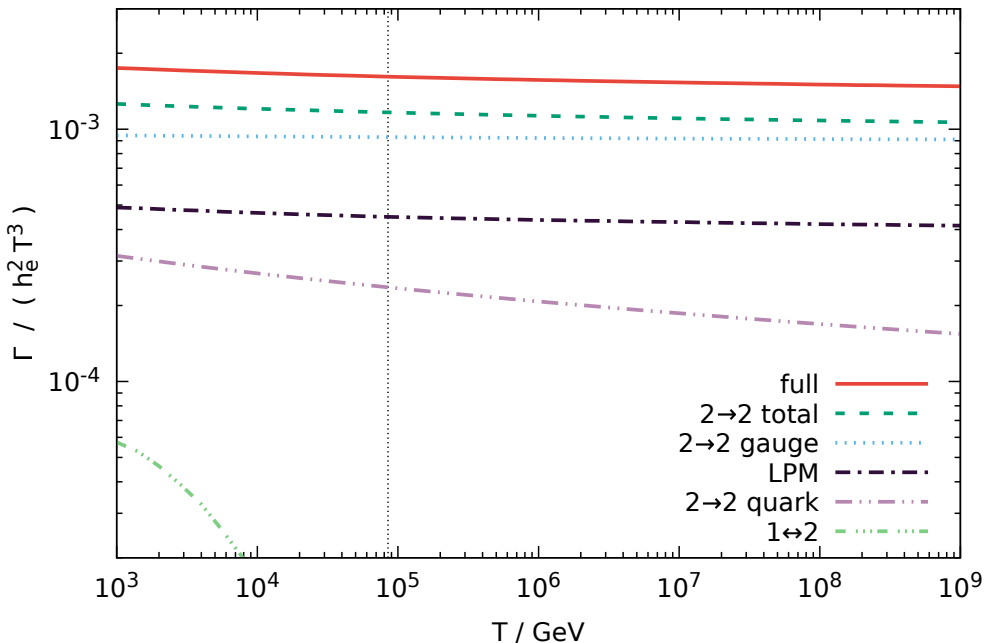
Figure 7: The rate coefficient Γ as function of the temperature. The curve labeled 'full' incorporates all leading order contributions, '$2 \rightarrow 2$ total' shows the full result of (3.53) whose contributions by gauge and quark scattering we show as '$2 \rightarrow 2$ gauge' and '$2 \rightarrow 2$ quark,' respectively. The curve labeled 'LPM' shows the result of (3.36) and is the sum of the resummation of $1n \leftrightarrow 2n$ scatterings by soft gauge boson exchanges and the (inverse) Higgs decay labeled '$1 \leftrightarrow 2$.' The dotted vertical line denotes the equilibration temperature (3.57).

contribution is about a factor 0.4 smaller than the total $2 \rightarrow 2$ rate. Except at very low temperature the (inverse) Higgs decay gives a negligible contribution, and it vanishes completely above $T \simeq 6 \cdot 10^4$ GeV. In table 1 we show numerical values for the total $2 \rightarrow 2$ as well as the LPM resummed contribution along with the full result for Γ.

The LPM resummed rate is a complicated function of the coupling constants and there is not such a simple expression like (3.53) for the $2 \rightarrow 2$ rate. Inspired by the form of (3.53) we have fitted the LPM contribution with a similar expression,

$$\Gamma^{\mathrm{LPM}} \approx \frac{h_e^2 \, T^3}{2048 \, \pi} \left\{ h_t^2 d_t + (3g^2 + g'^2) d_{\ell_e} + 4g'^2 d_{e_{\mathrm{R}}} \right\}. \tag{3.55}$$

Table 1: Numerical values of the contributions from $2 \to 2$ and LPM resummed multiple soft scattering to the equilibration rate coefficient Γ. The numerical uncertainty in the LPM contribution is below 2%.

T/GeV	$\Gamma^{2\to2}/(h_e^2 T^3)$	$\Gamma^{\text{LPM}}/(h_e^2 T^3)$	$\Gamma/(h_e^2 T^3)$
$1.00 \cdot 10^3$	$1.26 \cdot 10^{-3}$	$4.89 \cdot 10^{-4}$	$1.75 \cdot 10^{-3}$
$4.00 \cdot 10^3$	$1.22 \cdot 10^{-3}$	$4.75 \cdot 10^{-4}$	$1.70 \cdot 10^{-3}$
$1.60 \cdot 10^4$	$1.19 \cdot 10^{-3}$	$4.62 \cdot 10^{-4}$	$1.65 \cdot 10^{-3}$
$6.40 \cdot 10^4$	$1.17 \cdot 10^{-3}$	$4.51 \cdot 10^{-4}$	$1.62 \cdot 10^{-3}$
$2.56 \cdot 10^5$	$1.15 \cdot 10^{-3}$	$4.43 \cdot 10^{-4}$	$1.59 \cdot 10^{-3}$
$1.02 \cdot 10^6$	$1.13 \cdot 10^{-3}$	$4.36 \cdot 10^{-4}$	$1.57 \cdot 10^{-3}$
$4.10 \cdot 10^6$	$1.11 \cdot 10^{-3}$	$4.31 \cdot 10^{-4}$	$1.54 \cdot 10^{-3}$
$1.64 \cdot 10^7$	$1.10 \cdot 10^{-3}$	$4.26 \cdot 10^{-4}$	$1.53 \cdot 10^{-3}$
$6.55 \cdot 10^7$	$1.09 \cdot 10^{-3}$	$4.22 \cdot 10^{-4}$	$1.51 \cdot 10^{-3}$
$2.62 \cdot 10^8$	$1.07 \cdot 10^{-3}$	$4.18 \cdot 10^{-4}$	$1.49 \cdot 10^{-3}$
$1.05 \cdot 10^9$	$1.06 \cdot 10^{-3}$	$4.14 \cdot 10^{-4}$	$1.47 \cdot 10^{-3}$

We find that with

$$d_t = 1.48, \qquad d_{\ell_e} = 0.776, \qquad d_{e_\text{R}} = 2.03 \tag{3.56}$$

the relative error between Γ^{LPM} and the fit (3.55) is much smaller than our numerical uncertainty throughout the temperature range $10^3 \text{ GeV} \leq T \leq 10^9 \text{ GeV}$.

We comment on the generalization of our findings to the equilibration of charges carried by the right-handed μ_R or τ_R leptons in appendix J. There we also obtain the fit parameters analogous to the ones in (3.56) for the higher temperature ranges.

The right-handed electron lepton number comes into equilibrium around the temperature T_eq at which $\gamma_{L_{e\text{R}}L_{e\text{R}}}$ equals the Hubble rate[49] (2.3). Using (2.101) we find for the equilibration temperature T_eq of the right-handed electron lepton number in the Standard Model

$$T_\text{eq} = 8.5 \cdot 10^4 \text{ GeV}. \tag{3.57}$$

This value lies in the temperature region in which leptogenesis through neutrino oscillations [33, 34] can take place, see e.g. [35, 36]. In this case X_α and $L_{e\text{R}}$

---

[49]In [45] a different definition of the e_R equilibration temperature is used.

Table 2: Relative increase of Γ when hypercharge gauge interactions are included.

T	10^3 GeV	10^6 GeV	10^9 GeV
LPM	21%	30%	39%
$2 \to 2$	34%	44%	53%
total	30%	40%	49%

are violated on similar time scales, and the kinetic equations must describe the evolution of all four quantities.

It is interesting to see how hypercharge gauge interactions affect the e_R equilibration, since they give rise to diagrams which are not present in sterile neutrino production. We find that they substantially boost the equilibration rate. In table 2 we show the increase in the complete rate compared to the result with $g' = 0$. Despite the relative smallness of g', its effect on the equilibration rate is quite significant, and it increases with the temperature due to the different running of g' and g.

The first calculation of the e_R equilibration rate was performed in [44], where only the $2 \to 1$ inverse Higgs decay is taken into account and thermal fermion masses as well as the final state distribution function are neglected. At $T = 10^3$ GeV our result is about 5 times as large as the one obtained in [44]. Around the equilibration temperature (3.57) the inverse decay is not even kinematically allowed when thermal fermion masses are included, here we obtain a result that is about 6 times the one obtained by the approximations of [44].

Reference [45] includes $2 \leftrightarrow 2$ processes as well as the (inverse) Higgs decays while neglecting $1n \leftrightarrow 2n$ scattering. We can compare the $2 \to 2$ scattering rates involving quarks. Therefore we recompute c_t in (3.53) using Maxwell-Boltzmann statistics for all particles, leading to $c_t^\mathrm{MB} = 2.14$, which is a relative error of 24% compared to the correct quantum statistics, as anticipated in [45]. Our result for classical statistics is 9% larger than the one obtained in [45]. We can also compare the gauge contribution to the $2 \to 2$ scatterings. With the values for the gauge couplings of [45], our result is about 50% larger[50] which could be due to the use of classical statistics and of zero-momentum thermal fermion masses in [45].

The equilibration of right-handed muons and taus in a temperature regime between 10^7 and 10^{13} GeV is considered in [78], by including the (inverse) Higgs decays and $2 \leftrightarrow 2$ scatterings. By removing the inverse susceptibilities and the slow

---

[50]Cf. equations (25) through (27) in [45].

Yukawa couplings, we can compare our results for Γ/h_e^2, because it is lepton-flavor independent. We find our full rate to be 2.8 times their result. The authors also estimate the effect of multiple soft scattering.[51] The relative magnitude of the effect of multiple soft scattering is estimated in [78] as $\gamma_{L_{eR}L_{eR}}^{\mathrm{LPM}}/\gamma_{L_{eR}L_{eR}}^{2\to2} \sim 0.25$, while we obtain about 0.4. Our result for the quark contribution to $2 \to 2$ scattering is 2 times the result in [78], and both our logarithmic contributions to $\Gamma^{2\to2}$ are 2.2 times as large as the ones in [78].

---

[51]See equation (97) in [78].

Chapter 4

Summary & Outlook

We have developed a framework for obtaining non-linear kinetic equations for a type of out-of-equilibrium problems in which certain quantities equilibrate much more slowly than most others. Therefore we have generalized the ideas of [47]. To determine the coefficients in these equations we have matched not only real time two-point functions in the effective kinetic equations for thermal fluctuations to those in thermal field theory, like in [47], but also higher point functions.

We have discussed the strictly conserved charges as well as the susceptibilities providing relations between the slowly evolving charges (the time derivatives of which appear on the left-hand sides of our kinetic equations) and chemical potentials (which we introduce on the right-hand sides) in different temperature regimes, where we have focused on temperatures in the symmetric phase of the Standard Model. We have worked at leading order in Standard Model couplings following the approach of [47].

We have applied the resulting master formulae to sterile-neutrino phase space densities and charge densities carried by Standard Model particles. The sterile neutrinos have been integrated out using a path integral over their Fourier coefficients which correspond to their creation and annihilation operators. We have included only the leading order in their Yukawa coupling, which is h^2, and in their Majorana mass squared differences δM^2, neglecting contributions of order $h^2 \delta M^2$. This way we have obtained relations between the rate coefficients and real time correlation functions of Standard Model fields, evaluated at finite temperature and chemical potentials for charges which are conserved or slowly violated (in the case of $L_{e\mathrm{R}}$ or B for certain temperatures) by the Standard Model interactions. The rate coefficients are infrared safe in the sense that they are well behaved when a parameter characterizing a slow interaction vanishes. Our kinetic equations are

valid to all orders in fast Standard Model interactions, but we have neglected the very small $\mathcal{CP}$ violation inherent in the Standard Model.

The kinetic equations for sterile neutrinos and the relations for the rate coefficients that we have obtained are mostly consistent with the ones obtained in reference [54] the authors of which use a different starting point by making an ansatz with a non-equilibrium density matrix which contains the chemical potentials from the very start, even though we differ at intermediate steps.

Our equations are valid for an arbitrary number of sterile flavors n_s with any mass spectrum, and they can be applied to low-scale leptogenesis and to sterile-neutrino dark matter production, resonant or non-resonant, in the Higgs phase of the Standard Model, as well as to scenarios jointly describing the two.

It would be interesting to apply our equations to theories with more than one sterile neutrino dark matter candidate and to see, e.g., which role oscillations between sterile flavors play in this context, or how much lepton asymmetry (if any) is needed in order to explain all of the dark matter abundance. Ultimately, it would be desirable to conduct parameter space scans, which is possibly quite tedious already for $n_s = 2$.

We have computed the leading order correction of departures from equilibrium of the charges to the dispersion relation of the sterile neutrinos in the symmetric phase. There we have considered only the leading order contribution from Standard Model couplings. It would be interesting to measure the effect of this term in numerical studies of low-scale leptogenesis. Once $\mathcal{O}(g^2\mu)$ terms in this expansion have been obtained, it could be interesting to numerically compare these terms to the one we have obtained and to see whether these terms, despite being suppressed by one additional power of g, have a sizable effect due to their flavor dependence, which is absent in the leading term we have computed.

We have applied the linearized version of our framework, which coincides with an equation found in [50] (and in this case also with the one in [47], since here the spectral function is real), to the dynamics of right-handed electrons. We have subsequently computed their equilibration rate in the symmetric phase by including, for the first time, all Standard Model processes at leading order in the couplings. We have found that the dominant processes are $2 \rightarrow 2$ scatterings. Leading order contributions are also given by (inverse) Higgs decays and additional soft scattering which was included by Landau-Pomeranchuk-Migdal (LPM) resummation. We obtain an equilibration rate which is substantially larger than approximations presented in previous literature. Our result shows that the process

of e_{R} equilibration cannot be neglected in low-scale leptogenesis, if the latter happens at temperatures not too far from $T = 8.5 \cdot 10^4$ GeV.

In the kinetic equation for $L_{e\mathrm{R}}$ we have taken into account only the leading terms $\gamma_{L_{e\mathrm{R}}L_{e\mathrm{R}}}$ and $\gamma_{L_{e\mathrm{R}}X_\alpha}$, where applicable, and it could be interesting to obtain also a non-linear kinetic equation for this variable. In low-scale leptogenesis we expect $L_{e\mathrm{R}} \lesssim X_\alpha$, and the necessity for non-linear kinetic equations for X_α might raise the question whether a non-linear kinetic equation for $L_{e\mathrm{R}}$ is needed as well. In this case one should revisit our argument about the ability to neglect the non-linear dynamics of hypermagnetic fields. Relating the charges to the set of chemical potentials as we have done in section 2.3 will then make a computation analogous to the one in chapter 3 necessary, but this time at finite chemical potentials, which in the context of rates concerning sterile neutrinos is known to be more complicated due to infrared divergencies associated with soft Higgses appearing in the $2 \to 2$ scatterings [54], but we expect the technique of [54] to apply also to the correlators relevant for e_{R} equilibration.

The kinematic considerations entering the rate coefficient Γ for e_{R} equilibration also apply to the equilibration of the heavier lepton flavors μ_{R} and τ_{R}, after stripping off the Yukawa coupling, because the thermal masses in the symmetric phase of the Standard Model are flavor-blind. Therefore, by revisiting the relation between charges and chemical potentials, one can obtain relaxation rates of (non-abelian) charges broken by the Yukawa couplings h_μ and h_τ. This could be especially interesting in scenarios of thermal leptogenesis happening around the respective equilibration temperatures, usually called *flavored leptogenesis*, which are roughly 10^9 GeV (for μ_{R} equilibration) or 10^{12} GeV (for τ_{R} equilibration). The correct results for the respective equilibration rates have not yet been obtained, because the contribution from multiple soft scattering had only been estimated so far, and because, to the best of our knowledge, a correct analysis of the susceptibilities has not yet been presented. We have made a step towards the complete result for these rates by evaluating the contribution from multiple soft scattering also in the corresponding higher temperature regimes. It would be interesting to complete the derivations of the rates for these heavier flavors and to check how correctly including the dynamics of the respective right-handed leptons influences the results of the flavored leptogenesis processes.

Even though we have made a connection between low-scale leptogenesis and the equilibration of right-handed electrons for the first time, we have not investigated the quantitative effect of this intertwinement. The task of solving (momentum

resolved) equations for low-scale leptogenesis is usually more intrigued than solving the ones describing thermal leptogenesis, because due to the oscillations of sterile neutrinos there are multiple time scales present. Therefore involved numerical studies like the one presented in [36] are needed. It would be very interesting to conduct a detailed study to see, e.g., in which temperature regime including the dynamics of right-handed electrons changes the produced baryon asymmetry significantly, how large the effect is maximally, or how it changes the allowed parameter space for successful baryogenesis, which might potentially be a very complex problem. From first principles, it is also not obvious whether the effect of right-handed lepton equilibration on the generation of the baryon asymmetry of the Universe is larger in the case of e_R in low-scale leptogenesis, or in the case of the heavier leptons in flavored leptogenesis, and it would be interesting to compare these scenarios.

Acknowledgments

Appendix A

Smeared occupancies

The theory of quasi-stationary fluctuations and the framework developed in chapter 2 is applicable to quantities with (no summation over a),

$$\sqrt{\Xi_{aa}} = \sqrt{\langle y_a y_a \rangle} \ll y_a, \tag{A.1}$$

where the average is taken in an ensemble with fixed values of the strictly conserved charges. The relation (A.1) is not satisfied by the sterile-neutrino occupancies the fluctuations of which are not small, $\Xi_{ff} \sim \delta f$. In order for the approach in sections 2.2.1 and 2.2.2 to be applicable, we consider occupancies averaged over a certain momentum space region $\Omega_{\mathbf{k}}$ around $\mathbf{k}$,

$$F_{\mathbf{k}} \equiv \frac{(2\pi)^3}{V|\Omega_{\mathbf{k}}|} \sum_{\mathbf{p} \in \Omega_{\mathbf{k}}} f_{\mathbf{p}}. \tag{A.2}$$

The volume of this region $|\Omega_{\mathbf{k}}|$ is taken to be independent of the spatial volume V, with $(2\pi)^3/V \ll |\Omega_{\mathbf{k}}| \ll T^3$. The susceptibilities (2.14) of $F_{\mathbf{k}}$ are of order $(V|\Omega_{\mathbf{k}}|)^{-n+1}$. Now we have $\sqrt{\Xi_{F_{\mathbf{k}}F_{\mathbf{k}}}} \ll \delta F_{\mathbf{k}}$, and the assumption (2.15) is satisfied.

We should also consider smeared occupancies in the microscopic correlators appearing in section 2.4.1. However, since the volume $|\Omega_{\mathbf{k}}|$ is small compared to characteristic momentum scales over which the correlators in (2.26)–(2.28) vary, they can to a good approximation be replaced by

$$\Delta^{\mathrm{ret}}_{F_{\mathbf{k}}(F_{\mathbf{k}'}X\cdots X)}(\omega) = \delta_{\mathbf{k}\mathbf{k}'} \frac{(2\pi)^3}{V|\Omega_{\mathbf{k}}|} \Delta^{\mathrm{ret}}_{f_{\mathbf{k}}(f_{\mathbf{k}}X\cdots X)}(\omega), \tag{A.3}$$

so that the dependence on $V|\Omega_{\mathbf{k}}|$ drops out when plugging (A.3) and Ξ_{FF} into the master formula (2.26), and one can effectively use the unsmeared occupancies f.

Appendix B

Perturbative solution
of the equations of motion for fluctuations

The fluctuations of y_a satisfy (2.2) with an additional Gaussian noise ζ, and a y-independent term that does not play a role once we consider (2.2) for departures from equilibrium (see footnote 16 on page 16). We solve the equation of motion by one-sided Fourier transformation. Neglecting non-linear terms and expanding as in (2.13), one obtains (2.9). Now inserting (2.13) up to $y^{(1)}$ into (2.2), including the term with γ_{abc} and dropping the one with γ_{abcd}, we obtain

$$y_a^{+(1)}(\omega) = -\frac{1}{2}\left[(-i\omega + \gamma)^{-1}\right]_{ab}\,\gamma_{bcd}\int\frac{d\omega'}{2\pi}y_c^{+(0)}(\omega')y_d^{+(0)}(\omega - \omega'), \qquad (\text{B.1})$$

where we have used that

$$y_a(t) = \int\frac{d\omega'}{2\pi}e^{-i\omega't}y_a^+(\omega'). \qquad (\text{B.2})$$

Considering now the correlator $\mathcal{C}_{a(bc)}^+$ and inserting (2.9) yields averages like $\langle\zeta y(0)\rangle$ which vanish. We then consider frequencies much larger than the rates γ_{ab}, approximating $\left[(-i\omega + \gamma)^{-1}\right]_{ab} \approx i\delta_{ab}(\omega + i0^+)^{-1}$. The disconnected contribution vanishes, and we obtain

$$\mathcal{C}_{a(bc)}^+(\omega) \ni -\frac{i}{2\omega}\,\gamma_{ajk}\left[\Xi_{jb}\,\Xi_{kc} + \Xi_{jc}\,\Xi_{kb}\right]\int\frac{d\omega'}{2\pi}\frac{i}{(\omega' + i0^+)}\frac{i}{(\omega - \omega' + i0^+)} \quad (\text{B.3})$$

along with a contribution from γ_{ab}. Solving the integral and making use of the symmetry $\gamma_{ajk} = \gamma_{akj}$, we arrive at (2.18).

The perturbation caused by γ_{abcd} is obtained by inserting (2.13) into (2.2), this time keeping also $y^{(2)}$. Having obtained already $y^{+(0)}$ and $y^{+(1)}$ we can now

solve for $y^{+(2)}$, which reads

$$y_a^{+(2)}(\omega) = -\frac{1}{3!}\left[(-i\omega + \gamma)^{-1}\right]_{ab}\gamma_{bcde}$$
$$\times \int \frac{d\omega'}{2\pi}\int \frac{d\omega''}{2\pi}y_c^{+(0)}(\omega')y_d^{+(0)}(\omega'')y_e^{+(0)}(\omega - \omega' - \omega''). \qquad \text{(B.4)}$$

Considering the same limit $\omega \gg \gamma$, we find contributions of orders 1, γ_{ab}, γ_{abc} and γ_{abcd} in the correlator (2.20). The $\mathcal{O}(1)$ contribution is time-independent and does not contribute to the real part. The contributions from γ_{ab} and γ_{abc} are obtained in the same manner as before. The contribution from γ_{abcd} reads

$$\mathcal{C}_{a(bcd)}^+(\omega) \ni -\frac{i}{3!\,\omega}\,\gamma_{ajkl}\big[\Xi_{jb}\,\Xi_{kc}\,\Xi_{ld} + \Xi_{jb}\,\Xi_{kd}\,\Xi_{lc} + \Xi_{jc}\,\Xi_{kb}\,\Xi_{ld}$$
$$+\,\Xi_{jc}\,\Xi_{kd}\,\Xi_{lb} + \Xi_{jd}\,\Xi_{kb}\,\Xi_{lc} + \Xi_{jd}\,\Xi_{kc}\,\Xi_{lb}\big]$$
$$\times \int \frac{d\omega'\,d\omega''}{2\pi\;2\pi}\frac{i}{(\omega' + i0^+)}\frac{i}{(\omega'' + i0^+)}\frac{i}{(\omega - \omega' - \omega'' + i0^+)}\,. \qquad \text{(B.5)}$$

Because $\mathcal{C}_{a(bcd)}$ contains only the connected pieces, no contractions like $\Xi_{jk}\Xi_{lb}\Xi_{cd}$ appear in the square brackets in (B.5), and because of (2.15) we can neglect the connected part of the six-point function $\langle y_b y_c y_d y_j y_k y_l\rangle$. Making use of the symmetry of γ_{ajkl} under permutations of the last three indices, (B.5) can be solved for the rate coefficient. Carrying out the integrals and collecting the contributions from γ_{ab} and γ_{abc} eventually leads to (2.21).

Appendix C

Cancellation of the rates γ_{fff} and γ_{ffff}

Here we demonstrate that the coefficients γ_{fff} and γ_{ffff} in the equation of motion for f vanish at order h^2. For simplicity we will assume that the a and $a^\dagger$ appearing in all occupancies in this appendix correspond to sterile neutrino generations satisfying (2.62). First consider γ_{fff}. According to (2.27) it consists of two pieces containing only f operators (suppressing momentum indices $\mathbf{k}$),

$$\gamma_{f^a f^b f^c} = T\omega \operatorname{Im}\Big[\Delta^{\text{ret}}_{f^a(f^d f^e)}(\omega) - \Delta^{\text{ret}}_{f^a f^g}(\omega)(\Xi^{-1})_{f^g f^f}\,\Xi_{f^f f^d f^e}\Big] \tag{C.1}$$
$$(\Xi^{-1})_{f^d f^b}(\Xi^{-1})_{f^e f^c}.$$

Classically, the kinematic variables commute at equal times, which is not the case in the microscopic theory. Therefore one should replace the product $f^d f^e$ in (C.1) by its symmetrization $\{f^d, f^e\}/2$. In turn we demonstrate the cancellation of the terms with the ordering as in (C.1), the one with $d \leftrightarrow e$ is analogous.

We obtain the generalized susceptibility

$$\Xi_{f^a f^b f^c} = f_{\text{F}}\,[1 - f_{\text{F}}]\left\{[1 - f_{\text{F}}]\,\operatorname{tr}\Big(T^a T^b T^c\Big) - f_{\text{F}}\,\operatorname{tr}\Big(T^a T^c T^b\Big)\right\}, \tag{C.2}$$

where $f_{\text{F}} = f_{\text{F}}(E_{\mathbf{k}})$. The mass in $E_{\mathbf{k}}$ is one of the relevant (nearly) degenerate masses, and a change in this mass gives only a correction of order $h^2 \delta M^2$, which we neglect. We now consider the correlators as a function of imaginary time $t = -i\tau$, before Fourier transformation and analytic continuation to real frequency. Then, using (2.59) and the susceptibility (2.85), the second expression contains a

term

$$\Delta_{f^a f^g}(t)(\Xi^{-1})_{fg\,ff}\Xi_{ff\,f^d f^e} \ni \frac{1}{4VE_{\mathbf{k}}}T_{ij}^a\Big\{[1 - f_{\mathrm{F}}(E_{\mathbf{k}})]\left(T^d T^e\right)_{lm}$$
$$- f_{\mathrm{F}}(E_{\mathbf{k}})\left(T^e T^d\right)_{lm}\Big\}$$
$$\int_0^{1/T} d\tau_1\,d\tau_2\Big\{\langle a_q^\dagger(t_1)a_m(0)\rangle\langle \mathcal{T}a_r(t_2)a_i^\dagger(t)\rangle\langle a_j(t)a_l^\dagger(0)\rangle$$
$$- \langle \mathcal{T}a_q^\dagger(t_1)a_j(t)\rangle\langle a_r(t_2)a_l^\dagger(0)\rangle\langle a_i^\dagger(t)a_m(0)\rangle\Big\}$$
$$\int d^3x_1\,d^3x_2\,\bar{u}_{q+}h_{q\alpha}\langle J_\alpha(t_1,x_1)\bar{J}_\beta(t_2,x_2)\rangle h_{\beta r}^\dagger u_{r+}. \qquad \text{(C.3)}$$

To meaningfully define the object $\Delta_{f^a(f^d f^e)}(t)$ in the path integral over the sterile neutrino fields, we separate the quantities at $t = 0$ by replacing $f^d(0)$ by $\lim_{t' \to 0^+} f^d(t')$, taking the limit in the end when the ambiguities have resolved, which is the case after the expectation value has been reduced using Wick's theorem. The equivalent expression to the one in (C.3) now contains 8 terms which fall in either of the following two categories: (i) a product of 4 two-point functions of operators a and $a^\dagger$, in which exactly one operator is at time $t = 0$, and the other one at a time that is integrated over, or (ii) a product of 3 two-point functions in which the operators are at different times, multiplied by one f_{F} or $[1 - f_{\mathrm{F}}]$.[52] The 4 expressions of type (i) are t-independent, since operators at t are always to the left of those at time 0 so that they are not affected by time ordering, and the time evolutions of $a_j(t)$ and $a_i^\dagger(t)$ cancel up to effects of order $h^2\delta M^2$, which we neglect. Time-independent parts do not contribute to our master formula. The remaining four terms of type (ii) are canceled by the terms in (C.3). The other contributions which we have not written in (C.3) are canceled in the same way, and we obtain $\gamma_{fff} = 0$.

The master formula for the coefficient γ_{ffff} also contains only f operators at order h^2. The contribution from γ_{fff} vanishes, and the two remaining terms read

$$\gamma_{f^a f^b f^c f^d} = T\omega \,\mathrm{Im}\Big[\Delta_{f^a(f^e ff\,fg)}^{\mathrm{ret}}(\omega) - \Delta_{f^a f^h}^{\mathrm{ret}}(\omega)(\Xi^{-1})_{fh\,fi}\,\Xi_{fi\,fe\,ff\,fg}\Big] \qquad \text{(C.4)}$$
$$\times (\Xi^{-1})_{fe\,fb}(\Xi^{-1})_{ff\,fc}(\Xi^{-1})_{fg\,fd}.$$

---

[52]Here the time-ordering decides which one of the two expressions f_{F} or $[1 - f_{\mathrm{F}}]$ is generated, and the temporal separation of f^d and f^e plays a role.

Using (2.59), we obtain the generalized susceptibilities

$$\Xi_{f^a f^b f^c f^d} = f_{\mathrm{F}} \left[1 - f_{\mathrm{F}}\right] \left\{ \left[1 - f_{\mathrm{F}}\right]^2 \mathrm{tr}\left(T^a T^b T^c T^d\right) - f_{\mathrm{F}} \left[1 - f_{\mathrm{F}}\right] \mathrm{tr}\left(T^a T^b T^d T^c\right) \right.$$
$$- f_{\mathrm{F}} \left[1 - f_{\mathrm{F}}\right] \; \mathrm{tr}\left(T^a T^c T^b T^d\right) - f_{\mathrm{F}} \left[1 - f_{\mathrm{F}}\right] \mathrm{tr}\left(T^a T^c T^d T^b\right)$$
$$\left. - f_{\mathrm{F}} \left[1 - f_{\mathrm{F}}\right] \; \mathrm{tr}\left(T^a T^d T^b T^c\right) + f_{\mathrm{F}}^2 \; \mathrm{tr}\left(T^a T^d T^c T^b\right) \right\}. \quad \text{(C.5)}$$

The cancellation is now analogous to the one above, after replacing $f^e(0)f^f(0)$ by $\lim_{t'' \to 0^+} \lim_{t' \to 0^+} f^e(t'') f^f(t')$ with $t'' > t'$. The rates $\gamma_{fffX}, \gamma_{Xff}, \gamma_{XffX}$, and γ_{Xfff} are canceled in the same fashion.

Appendix D

Green's functions at finite temperature and chemical potentials

Here we present slight generalizations of some relations in [67] for imaginary time correlators which we use in our calculation. In the presence of one conserved charge Q the 2-point function of operators A and B reads

$$\Delta_{AB}(-i\tau) \equiv Z^{-1}\mathrm{tr}\Big\{e^{(\mu Q - H)/T}\mathcal{T}\left[A(-i\tau)B(0)\right]\Big\} \tag{D.1}$$

with the partition function $Z \equiv \mathrm{tr}\,e^{(\mu Q - H)/T}$, and the time ordering $\mathcal{T}$ with respect to τ is defined as

$$\mathcal{T}\left[A(-i\tau)B(0)\right] \equiv \Theta(\tau)A(-i\tau)B(0) \pm \Theta(-\tau)B(0)A(-i\tau). \tag{D.2}$$

The upper/lower sign is for bosonic/fermionic operators. The correlator (D.1) is defined for $-T^{-1} \le \tau \le T^{-1}$. We assume that A carries a definite charge,

$$[Q, A] = q_A A. \tag{D.3}$$

Then

$$\Delta_{AB}(t + i/T) = \pm e^{-\mu_A/T}\Delta_{AB}(t) \tag{D.4}$$

where the chemical potential of A is defined as

$$\mu_A \equiv q_A \mu. \tag{D.5}$$

Therefore the function $e^{-\mu_A \tau}\Delta_{AB}(-i\tau)$ is (anti-) periodic, and can be expanded in a Fourier series with coefficients

$$\Delta_{AB}^{\mathrm{M}}(i\omega_n) \equiv \int_0^{1/T} d\tau\, e^{(i\omega_n - \mu_A)\tau}\Delta_{AB}(-i\tau). \tag{D.6}$$

(D.6) can be analytically continued to arbitrary complex frequencies off the real axis, and we denote the resulting function by Δ_{AB}^{M}. We need to calculate the retarded correlator

$$\Delta_{AB}^{\text{ret}}(\omega) = i \int_0^\infty dt \; e^{i\omega t} \langle [A(t), B(0)]_{\mp} \rangle \tag{D.7}$$

where ω is real. It can be analytically continued to the complex plane. We denote the resulting function by Δ_{AB}, and then we have $\Delta_{AB}^{\text{ret}}(\omega) = \Delta_{AB}(\omega + i0^+)$. The two analytic continuations are related by

$$\Delta_{AB}^{M}(\omega) = \Delta_{AB}(\omega - \mu_A). \tag{D.8}$$

Correlators of Standard Model fields for sterile neutrinos in the symmetric phase

Here we would like to explore the correlators of Standard Model operators that enter the kinetic equations for sterile neutrinos. We restrict ourselves to the symmetric phase of the Standard Model. The processes contributing to the dissipative part share some similarities to the ones responsible for e_R equilibration. However, there are some differences,[53] especially in the LPM contribution which we discuss in the following section. We subsequently discuss the dispersive contributions in section E.2 where we include the modification of the dispersion relation of sterile neutrinos due to non-zero charge densities. These contributions do not appear in the kinetic equations for e_R equilibration.

E.1 Dissipative contributions

Deep in the symmetric phase one has to distinguish two temperature regimes. When $M_i \gg gT$, at leading order in the Standard Model couplings the dissipative (imaginary) part of $\Delta^\mathrm{ret}_\alpha(k_j, \mu)$ is determined by hard $2 \leftrightarrow 2$ scattering processes. For $M_i \lesssim gT$, nearly collinear $1 \leftrightarrow 2$ decays and inverse decays involving a Higgs boson, a SM lepton and a sterile neutrino, plus the same process with additional soft scatterings ($1n \leftrightarrow 2n$ processes), also contribute at leading order [70].

The multiple soft scatterings need to be LPM [71–73] resummed. The result gives an imaginary contribution to $\Delta^\mathrm{ret}_\alpha(k_j, \mu)$ which can be computed along the lines of [66, 70]. It can be expressed in terms of a the 2-component vector function $\mathbf{f}_j(\mathbf{b})$ and the scalar function $\psi_j(\mathbf{b})$. Analogously to [70], they are solutions to two ordinary differential equations which depend on the 2-dimensional impact

---

[53]See also chapter 3.

parameter vector $\mathbf{b}$ (we denote $b \equiv |\mathbf{b}|$),

$$-i\beta \left(\triangle - M_{j,\,\mathrm{eff}}^2\right) \mathbf{f}_j(\mathbf{b}) \;-\; \mathscr{K}_{\mathrm{N}}(b)\, \mathbf{f}_j(\mathbf{b}) \;=\; -2i\,\nabla \delta^{(2)}(\mathbf{b}), \qquad (\mathrm{E}.1)$$

$$-i\beta \left(\triangle - M_{j,\,\mathrm{eff}}^2\right) \psi_j(\mathbf{b}) - \mathscr{K}_{\mathrm{N}}(b)\, \psi_j(\mathbf{b}) = \delta^{(2)}(\mathbf{b}), \qquad (\mathrm{E}.2)$$

with

$$M_{j,\,\mathrm{eff}}^2 \equiv \frac{p_\|(p_\| - |\mathbf{k}|)}{|\mathbf{k}|^2} M_j^2 - \frac{(p_\| - |\mathbf{k}|)}{|\mathbf{k}|} m_{\ell_e}^2 + \frac{p_\|}{|\mathbf{k}|} m_\varphi^2, \qquad (\mathrm{E}.3)$$

and β as in (3.31) and [70]. Here m_{ℓ_e} and m_φ denote the thermal masses of the Standard Model particles [79], see (3.2) and (3.3). In contrast to $\mathscr{K}$ in (G.3), the function $\mathscr{K}_{\mathrm{N}}$ in (E.1) and (E.2) satisfies [70]

$$\mathscr{K}_{\mathrm{N}}(b) \equiv \frac{3g^2 T}{4} \mathscr{D}(m_{\mathrm{D}} b) + y_{\ell_e}^2 g'^2 T \mathscr{D}(m_{\mathrm{D}}' b) \qquad (\mathrm{E}.4)$$

with the Debye masses (3.26) and $\mathscr{D}$ as in (G.4). Only one term with g'^2 appears in (E.4), because only two particles participate in weak hypercharge interactions here, unlike all three in the case of e_{R} equilibration. In the latter case also the analog to the scalar function ψ in (E.2) does not appear, because there is no mass term for the e_{R}, unlike for the sterile neutrinos. It is straightforward to generalize the analysis of [70] to non-zero chemical potentials which gives[54]

$$\Delta_\alpha^{\mathrm{LPM\,ret}}(k_j, \mu) = \frac{i}{2} \int \frac{dp_\|}{2\pi} \frac{1}{|\mathbf{k}| - p_\|} \left[f_{\mathrm{B}}\left(p_\| - |\mathbf{k}| + \frac{\mu_Y}{2}\right) + f_{\mathrm{F}}\left(p_\| - \mu_{X_\alpha} + \frac{\mu_Y}{2}\right) \right]$$

$$\times \mathrm{P_L} \lim_{\mathbf{b}\to 0} \left\{ \left(\gamma^0 - \hat{\mathbf{k}}\cdot\boldsymbol{\gamma}\right) \mathrm{Re}\,\psi_j(\mathbf{b}) + \frac{1}{8p_\|^2} \left(\gamma^0 + \hat{\mathbf{k}}\cdot\boldsymbol{\gamma}\right) \mathrm{Im}\,\nabla_{\mathbf{b}}\cdot\mathbf{f}_j(\mathbf{b}) \right\}. \qquad (\mathrm{E}.5)$$

Here $\mathrm{P_L} \equiv (1 - \gamma_5)/2$ is a chiral projector, and $\hat{\mathbf{k}} \equiv \mathbf{k}/|\mathbf{k}|$. The second term in the curly bracket is of order g^2 times the first. Nevertheless, it has to be kept because when sandwiched between the u- and v-spinors, the first term gets multiplied by M_j^2 which is assumed here to be $\mathcal{O}(g^2 T^2)$ or smaller. The LPM contribution was computed in [54], where the result does not contain a chiral projector.[55] Aside from that, it is consistent with equation (E.5) (the second term in the curly

---

[54]Note that the Higgs and active lepton chemical potentials appear in the distribution functions in (E.5). We were able to translate these to the chemical potentials of slow charges X_α and the one of strictly conserved weak hypercharge Y, because the relation between them is independent of temperature, cf. equations (2.39) and (2.51) as well as the discussion in between. However, the expression of μ_Y in terms of slowly varying chemical potentials does depend on the temperature regime, see (2.44), (2.50), and (2.54).

[55]See equation (3.4) of reference [54].
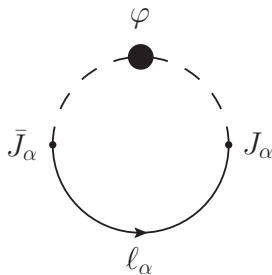
Figure 8: Diagram representing the leading correction of the dispersion relation of sterile neutrinos by non-vanishing charge densities, corresponding to the expression in (E.6). The thick blob indicates that the Higgs propagator is thermal mass resummed.

bracket differs from the corresponding one in [54] only by higher orders in g). Chiral projectors were correctly included in [54] when the result was sandwiched between the u and v spinors which makes it consistent with ours (cf. footnote 34 on page 36). The $2 \to 2$ scattering contributions to the rate coefficients have been computed in [54].

E.2 Dispersive contributions

The imaginary parts of the 2-point functions in (2.90), (2.91) have been computed in [54] at nonzero chemical potentials. Here we compute the real part in the symmetric phase which modifies the dispersion relations of the sterile neutrinos. We include the chemical potentials to linear order and we work at leading order in Standard Model couplings, assuming $M_i \ll |\mathbf{k}|$. The leading order is contained in the 1-loop contribution, which reads

$$\Delta_\alpha(k^0, \mathbf{k}, \mu) = T \widetilde{\sum_{p^0}} \int_{\mathbf{p}} \frac{2 \, \mathrm{P_L}(\slashed{p} + \mu_{\ell_\alpha} \slashed{u})}{(p + \mu_{\ell_\alpha} u)^2 \left[(k - p + \mu_\varphi u)^2 - m_\varphi^2\right]} \qquad \text{(E.6)}$$

in imaginary time. This expression can be visualized as in figure 8, where the four-momentum $(p^0, \mathbf{p})$ runs in the loop. The factor 2 is the dimension of the representation of the weak SU(2). The chemical potentials in (E.6) are the ones carried by the particles. They have the opposite sign compared to the chemical potentials carried by the field operators which annihilate these particles, cf. (D.5). Note instead of $\mu_{\widetilde{\varphi}}$ we have expressed (E.6) in terms of μ_φ (see (2.38)), corresponding to equations (2.39) and (2.51). The relation between

the hypercharge chemical potential μ_Y and the chemical potentials of the slowly varying charges depends on the temperature, see section 2.3.

The leading contribution from (E.6) is due to soft Higgs momenta, which are cut off by the thermal Higgs mass [79] given by (3.2) in the Higgs propagator, which gives rise to an infrared enhancement.

After summing over the imaginary fermionic frequency p^0 we analytically continue to real k^0 according to (2.73), and obtain

$$\operatorname{Re}\operatorname{tr}\left[\not k \Delta_\alpha^{\mathrm{ret}}(k, \mu)\right] = -\frac{T^2}{4} - \frac{m_\varphi T}{4\pi|\mathbf{k}|}\mu_\varphi + \mathcal{O}(g^2\mu, \mu^2), \qquad (\text{E.7})$$

with $k^0 = |\mathbf{k}|$. The g in the higher order terms in (E.7) stands for a generic Standard Model coupling. The first term on the right-hand side of (E.7) gives rise to the thermal mass. The μ-dependent contribution is not simply a correction of the thermal mass, but it depends on momentum. In particular, it is enhanced at small $\mathbf{k}$. The leading correction from chemical potentials is independent of α. We expect higher order, e.g. $\mathcal{O}(g^2\mu_{\ell_\alpha})$, terms in (E.7) to generate an α dependence, but we have not computed those terms. Equations (2.38), (E.6), and (E.7) are consistent with [1], where the Higgs chemical potential is defined as the one carried by the field operators. In reference [56] an expression corresponding to (E.7) in the broken phase has been obtained.[56]

---

[56]See equation (5.7) of reference [56].

Appendix F

Conversion of L_{eR} to hypercharge gauge fields

Even without the Yukawa interaction in (1.19) the conservation of L_{eR} is violated by the chiral anomaly[57]

$$\partial_\mu j_{eR}^\mu = -\frac{y_{eR}^2 g'^2}{32\pi^2} \varepsilon^{\mu\nu\rho\sigma} F_{\mu\nu} F_{\rho\sigma}, \tag{F.1}$$

with

$$j_{eR}^\mu \equiv \overline{e_R}\, \gamma^\mu e_R, \tag{F.2}$$

such that $L_{eR} = \int_{\mathbf{x}} j_{eR}^0(\mathbf{x})$. In (F.1) $F_{\mu\nu}$ denotes the hypercharge field strength, and we use the convention $\varepsilon^{0123} = +1$. This may lead to interesting effects, such as the generation of primordial magnetic fields [46, 89]. In this appendix we want to see when the anomaly can affect the long time and large distance behavior of j_{eR}. Even if there are no gauge fields present initially, there is an instability in the gauge fields for non-zero $\mu_{L_{eR}}$, leading to exponential growth [46]. We compute the maximal growth rate of the unstable modes in order to derive a bound on $|\mu_{L_{eR}}|$ below which the growth is smaller than the equilibration rate $\gamma_{L_{eR}L_{eR}}$ and can be neglected in the kinetic equation (2.93).

The hypercharge electric and magnetic fields $\mathbf{E}$ and $\mathbf{B}$ with wavelengths greater than the particle mean free path are described by magneto-hydrodynamics. In the presence of the anomaly (F.1), in addition to the usual ohmic current $\mathbf{j}_{\mathrm{Ohm}} = \sigma \mathbf{E}$ with the hyperelectric conductivity σ, one has to take into account

---

[57]One can find different prefactors on the right-hand side of (F.1) in the literature, which are related to different conventions for the weak hypercharge. Ours is the same as in [88].

the contribution [46, 90]

$$\mathbf{j}_{\text{anomaly}} = -\frac{y_{e\mathrm{R}}^2 g'^2}{4\pi^2} \mu_{L_{e\mathrm{R}}} \mathbf{B}. \tag{F.3}$$

The fields evolve on time scales much larger than σ^{-1}. Therefore $\dot{\mathbf{E}}$ is much smaller than $\sigma\mathbf{E}$, and can be neglected in the equations of motion which become

$$\mathbf{E} = \frac{1}{\sigma}\left[\nabla\times\mathbf{B} + \frac{y_{e\mathrm{R}}^2 g'^2}{4\pi^2}\mu_{L_{e\mathrm{R}}}\mathbf{B}\right], \tag{F.4}$$

$$\dot{\mathbf{B}} = -\nabla\times\mathbf{E}. \tag{F.5}$$

Using $\nabla\cdot\mathbf{B} = 0$, these can be recast as

$$\dot{\mathbf{B}} + \frac{1}{\sigma}\left[-\triangle\mathbf{B} + \frac{y_{e\mathrm{R}}^2 g'^2}{4\pi^2}\mu_{L_{e\mathrm{R}}}\nabla\times\mathbf{B}\right] = \mathbf{0}. \tag{F.6}$$

Following [46], we Fourier transform $\mathbf{B}(t,\mathbf{x}) = \int_{\mathbf{k}} \mathbf{B}_{\mathbf{k}}(t)e^{i\mathbf{k}\cdot\mathbf{x}}$ to obtain

$$\sigma\dot{\mathbf{B}}_{\mathbf{k}} + \mathbf{k}^2\mathbf{B}_{\mathbf{k}} + i\frac{y_{e\mathrm{R}}^2 g'^2}{4\pi^2}\mu_{L_{e\mathrm{R}}}\mathbf{k}\times\mathbf{B}_{\mathbf{k}} = \mathbf{0}. \tag{F.7}$$

Now decompose $\mathbf{B}_{\mathbf{k}} = \sum_{i=1}^2 b_i \mathbf{e}_i$. The $\mathbf{e}_i$ are an orthonormal basis in the plane orthogonal to $\mathbf{k}$. The equations for $b_\pm \equiv b_1 \pm ib_2$ decouple,

$$\sigma\dot{b}_\pm = -|\mathbf{k}|\left(|\mathbf{k}| \mp \frac{y_{e\mathrm{R}}^2 g'^2}{4\pi^2}\mu_{L_{e\mathrm{R}}}\right)b_\pm. \tag{F.8}$$

For

$$|\mathbf{k}| < \frac{y_{e\mathrm{R}}^2 g'^2}{4\pi^2}|\mu_{L_{e\mathrm{R}}}| \tag{F.9}$$

there is an instability with the growth rate

$$\gamma_{\text{inst}} = \frac{|\mathbf{k}|}{\sigma}\left(\frac{y_{e\mathrm{R}}^2 g'^2}{4\pi^2}|\mu_{L_{e\mathrm{R}}}| - |\mathbf{k}|\right). \tag{F.10}$$

The maximal growth rate is

$$\gamma_{\text{inst}}^{\text{max}} = \frac{\mu_{L_{e\mathrm{R}}}^2 y_{e\mathrm{R}}^4 g'^4}{64\pi^4\sigma}. \tag{F.11}$$

The linear kinetic equation neglecting the dynamics of the long wavelength hypermagnetic fields is valid as long as the magnetic dynamics happen on longer

time scales than the perturbative ones characterized by the equilibration rate $\gamma_{L_{e\mathrm{R}}L_{e\mathrm{R}}}$,

$$\gamma_{\mathrm{inst}}^{\mathrm{max}} < \gamma_{L_{e\mathrm{R}}L_{e\mathrm{R}}}. \tag{F.12}$$

In the leading logarithmic approximation the hyperelectric conductivity is [91]

$$\sigma = C\frac{T}{g'^2 \log(1/g')}, \tag{F.13}$$

with $C = 7.05$ in the Standard Model with one Higgs doublet.[58] At the equilibration temperature (3.57) in the Standard Model, (F.12) translates into the condition (3.1).

Consider again the case of low-scale leptogenesis, corresponding to example 3 of section 2.5. Here the constraint (3.1) implies

$$\left| Y_{L_{e\mathrm{R}}} - \frac{1110}{4266}Y_{X_e} + \frac{312}{4266}\left(Y_{X_\mu} + Y_{X_\tau}\right) \right| \lesssim 3.4 \cdot 10^{-6}. \tag{F.14}$$

for the yield parameters $Y_i \equiv n_i/s$ with the entropy density s. The Y_{X_α} are typically on the order of $10^{-9} \ldots 10^{-8}$ [35, 36]. Since the dominant source terms in the kinetic equation for $L_{e\mathrm{R}}$ are the X_α, we expect $Y_{L_{e\mathrm{R}}}$ to be of similar size, and (F.14) is easily satisfied.

---

[58]Adding further Higgs doublets decreases the conductivity.

Appendix G

Solving the LPM integral equation for $L_{e\mathrm{R}}$ equilibration

Here we elaborate on how the integral equation (3.35) resumming multiple soft gauge boson scatterings contributing to the equilibration of $L_{e\mathrm{R}}$ can be solved. The Fourier transformation

$$\mathbf{f}(\mathbf{B}) \equiv \int \frac{d^2 P}{(2\pi)^2} e^{i\mathbf{P}\cdot\mathbf{B}} \, \mathbf{f}(\mathbf{P}) \tag{G.1}$$

turns the integral equation (3.35) for $\mathbf{f}(\mathbf{P})$ into a differential equation for $\mathbf{f}(\mathbf{B})$,

$$i\beta \left(\triangle - M_{\mathrm{eff}}^2 \right) \mathbf{f}(\mathbf{B}) = \mathscr{K}(B) \, \mathbf{f}(\mathbf{B}) - 2 \, i \, \nabla \delta^{(2)}(\mathbf{B}), \tag{G.2}$$

where the differential operators act on the two-dimensional impact parameter $\mathbf{B}$. We denote $B \equiv |\mathbf{B}|$ and we have introduced

$$
\begin{aligned}
\mathscr{K}(B) &\equiv \frac{3g^2 T}{4} \mathscr{D}(x_k m_{\mathrm{D}} B) \\
&\quad + g'^2 T \big[y_\varphi y_{\ell_e} \, \mathscr{D}(x_k m'_{\mathrm{D}} B) + y_{\ell_e} y_{e_{\mathrm{R}}} \, \mathscr{D}\left(m'_{\mathrm{D}} B \right) - y_\varphi y_{e_{\mathrm{R}}} \, \mathscr{D}\left(x_p m'_{\mathrm{D}} B \right) \big]
\end{aligned}
\tag{G.3}
$$

with

$$\mathscr{D}(y) \equiv \frac{1}{2\pi} \left[\gamma_{\mathrm{E}} + K_0(|y|) + \log \left| \frac{y}{2} \right| \right]. \tag{G.4}$$

γ_{E} is the Euler-Mascheroni constant and K_0 is a modified Bessel function. In terms of the Fourier transform the real part in (3.36) becomes

$$\mathrm{Re} \int \frac{d^2 P}{(2\pi)^2} \mathbf{P} \cdot \mathbf{f}(\mathbf{P}) = \lim_{\mathbf{B}\to\mathbf{0}} \mathrm{Im} \nabla \cdot \mathbf{f}(\mathbf{B}). \tag{G.5}$$

Writing $\mathbf{f}(\mathbf{B}) \equiv \mathbf{B}\, h(B)$, we arrive at the following ordinary differential equation for $h(B)$, valid at $B \neq 0$,

$$i\beta \left\{ \frac{d^2}{dB^2} + \frac{3}{B}\frac{d}{dB} - M_{\text{eff}}^2 \right\} h(B) - \mathscr{K}(B)\, h(B) = 0. \tag{G.6}$$

In terms of h, the relation (G.5) becomes

$$\text{Re} \int \frac{d^2 P}{(2\pi)^2} \mathbf{P} \cdot \mathbf{f}(\mathbf{P}) = 2 \lim_{B \to 0} \text{Im}\, h(B). \tag{G.7}$$

For $B \to 0$ the function h has a singularity which is determined by the delta function in (G.2),

$$h(B) \stackrel{B \to 0}{\sim} -\frac{1}{\pi \beta B^2}, \tag{G.8}$$

and which is insensitive to $\mathscr{K}$. Being purely real, this singularity does not enter (G.7). We write $h = h^{\text{decay}} + h^{\text{scat}}$, where h^{decay} contains only the (inverse) Higgs decay contribution. We obtain it by solving (3.35) with $\int d^2 q_\perp \{\cdots\} \to 0^+ \mathbf{f}(\mathbf{P})$ and then taking the Fourier transform. This gives [92]

$$h^{\text{decay}}(B) = \begin{cases} -\dfrac{m}{\pi \beta B} K_1(mB) & (M_{\text{eff}}^2 > 0) \\[2ex] \dfrac{m}{2\beta B} [Y_1(mB) - i\,\text{sign}(\beta)\, J_1(mB)] & (M_{\text{eff}}^2 < 0) \end{cases} \tag{G.9}$$

with $m \equiv \sqrt{|M_{\text{eff}}^2|}$, and the (modified) Bessel functions K_1, Y_1 and J_1. Then we solve the differential equation for h^{scat} numerically as described in [70].

Appendix H

Integrals appearing in the
$2 \to 2$ *contribution to* e_{R} *equilibration*

In this appendix we handle the integrals describing $2 \to 2$ scattering processes contributing to the $L_{e\mathrm{R}}$ equilibration rate. After summing over all leading order processes the production rate on the right-hand side of (3.44) can be written as

$$\left. \frac{d^2 n_{e_{\mathrm{R}}}}{dt\, dk^0} \right|_{n_{e_{\mathrm{R}}}=0} = \frac{h_e^2 f_{\mathrm{F}}(k^0)}{128\pi^5} \Big[18\, h_t^2\, \mathscr{I}_{\mathrm{fff}}^0$$

$$+ (3g^2 + g'^2) \left\{ \mathscr{I}_{\mathrm{bfb}}^1 + \mathscr{I}_{\mathrm{bbf}}^1 + \mathscr{I}_{\mathrm{fbb}}^1 \right\}$$

$$+ 4g'^2 \left\{ \mathscr{I}_{\mathrm{bfb}}^1 + \mathscr{I}_{\mathrm{bbf}}^1 + \mathscr{I}_{\mathrm{fbb}}^1 + \mathscr{I}_{\mathrm{bbf}}^0 - 2\mathscr{I}_{\mathrm{bfb}}^0 \right\} \Big] \quad \text{(H.1)}$$

with $k^0 = |\mathbf{k}|$. Here we have already integrated over the direction of $\mathbf{k}$. The $\mathscr{I}_{123}^n$ are the different phase space integrals appearing in (3.43). The lower indices refer to the statistics of the particles $1, 2, 3$ and the upper index $n = 0, 1$ is the power of the ratios of Mandelstam variables in equations (3.45) through (3.51). The exact definitions of the $\mathscr{I}$ are given below.

Like in [69] we carry out some integrations analytically until there are two integrals over the variables $q_\pm \equiv (q^0 \pm |\mathbf{q}|)/2$ left. If not stated otherwise, q is the exchanged 4-momentum. For each process we decompose the products of occupancies in (3.43) as

$$f_1 f_2 [1 \pm f_3] = f_{\mathrm{F}}(k^0) \widetilde{f}\widehat{f}, \quad \text{(H.2)}$$

where $\widehat{f}$ is a function of $q_+ + q_-$ and of the energy of one incoming particle only. Most of the integrals appear in sterile neutrino production as well. For the sake of completeness, we list them in this appendix, adopted to our notation. We also give the analytic integrals which were not computed in [69]. The terms

containing $1/t$ are infrared divergent when integrated over $q_{\pm}$. All divergent contributions encountered here already appear in sterile neutrino production (see [69] for details).

The integral $\mathscr{I}_{\mathsf{fff}}$. This integral is exclusive to quark scattering. Since the squared matrix elements do not depend on the Mandelstam variables, we may choose $q = p_3 + k$ for both s- and t-channel. We find

$$\widetilde{f} = f_{\mathrm{B}}(q_+ + q_-) + f_{\mathrm{F}}(q_+ + q_- - k^0) \tag{H.3}$$

$$\widehat{f} = 1 - f_{\mathrm{F}}(q_+ + q_- - E_2) - f_{\mathrm{F}}(E_2), \tag{H.4}$$

and we have

$$\mathscr{I}_{\mathsf{fff}}^0 = \int\limits_{k^0}^{\infty} dq_+ \int\limits_{0}^{k^0} dq_- \, \widetilde{f} \int\limits_{q_-}^{q_+} dE_2 \, \widehat{f}. \tag{H.5}$$

Only $n = 0$ appears, and the integral of $\widehat{f}$ over E_2 is given by equation (A.10) of [69].

The integral $\mathscr{I}_{\mathsf{bfb}}$. This integral appears in s-channel processes, so that $q = p_3 + k$. We have

$$\widetilde{f} = f_{\mathrm{F}}(q_+ + q_-) + f_{\mathrm{B}}(q_+ + q_- - k^0) \tag{H.6}$$

$$\widehat{f} = 1 + f_{\mathrm{B}}(q_+ + q_- - E_2) - f_{\mathrm{F}}(E_2), \tag{H.7}$$

and we need

$$\mathscr{I}_{\mathsf{bfb}}^n = \int\limits_{k^0}^{\infty} dq_+ \int\limits_{0}^{k^0} dq_- \, \widetilde{f} \int\limits_{q_-}^{q_+} dE_2 \, \widehat{f} \left(\frac{\langle -u \rangle}{s} \right)^n \tag{H.8}$$

where $\langle -u \rangle$ is the Mandelstam variable u averaged over angles,

$$\frac{\langle -u \rangle}{s} = \frac{q_+^2 + q_-^2 - (q_+ + q_-)(E_2 + k^0) + 2E_2 k^0}{(q_+ - q_-)^2}. \tag{H.9}$$

The result of the E_2 integration is found in equation (A.13) of [69]. For the $n = 0$ integral we obtain

$$\int\limits_{q_-}^{q_+} dE_2 \, \widehat{f} = -(q_+ - q_-) + T \left[\log \left(-1 + e^{2q_+/T} \right) - \log \left(-1 + e^{2q_-/T} \right) \right]. \tag{H.10}$$

The integral $\mathscr{I}_{\mathbf{bbf}}$. This function arises in t-channel processes, so that $q = p_1 - p_3$. We obtain

$$\widetilde{f} = 1 + f_{\mathrm{B}}(k^0 - q_+ - q_-) - f_{\mathrm{F}}(q_+ + q_-) \tag{H.11}$$

$$\widehat{f} = f_{\mathrm{B}}(E_1) + f_{\mathrm{F}}(E_1 - q_+ - q_-) \tag{H.12}$$

such that

$$\mathscr{I}_{\mathrm{bbf}}^n = \int\limits_0^{k^0} dq_+ \int\limits_{-\infty}^0 dq_- \, \widetilde{f} \int\limits_{q_+}^\infty dE_1 \, \widehat{f} \left(\frac{\langle u \rangle}{t} \right)^n. \tag{H.13}$$

Here we have

$$\frac{\langle u \rangle}{t} = \frac{2q_+ q_- + 2E_1 k^0 - (q_+ + q_-)(E_1 + k^0)}{(q_+ - q_-)^2}. \tag{H.14}$$

The E_1 integral with $n = 1$ is equation (A.24) of [69], while for the case $n = 0$ we get

$$\int\limits_{q_+}^\infty dE_1 \, \widehat{f} = q_+ + q_- + T \left[\log \left(1 + e^{-q_-/T} \right) - \log \left(-1 + e^{q_+/T} \right) \right]. \tag{H.15}$$

The integral $\mathscr{I}_{\mathbf{fbb}}$. We encounter this integral in t-channel, so again $q = p_1 - p_3$. Here

$$\widetilde{f} = 1 + f_{\mathrm{B}}(k^0 - q_+ - q_-) - f_{\mathrm{F}}(q_+ + q_-) \tag{H.16}$$

$$\widehat{f} = f_{\mathrm{F}}(E_1) + f_{\mathrm{B}}(E_1 - q_+ - q_-) \tag{H.17}$$

and we have

$$\mathscr{I}_{\mathrm{fbb}}^1 = \int\limits_0^{k^0} dq_+ \int\limits_{-\infty}^0 dq_- \, \widetilde{f} \int\limits_{q_+}^\infty dE_1 \, \widehat{f} \left(\frac{\langle s \rangle}{-t} \right). \tag{H.18}$$

We write $\langle s \rangle/(-t) = 1 + \langle u \rangle/t$ with $\langle u \rangle/t$ from (H.14). We only need $n = 1$, and the corresponding integral over E_1 is found in [69] in (A.20).

One-loop renormalization group equations

Here we briefly review the renormalization group equations at one-loop level for the various couplings entering the numerical evaluation of the rates in the kinetic equation for L_{eR}. For

$$t \equiv \log\left(\frac{\mu^2}{m_Z^2}\right) \tag{I.1}$$

with the renormalization scale μ and the Z boson mass m_Z, and three fermion generations as well as one complex Higgs doublet, we have the differential equations for the strong and weak gauge couplings [93]

$$\frac{d}{dt}g_{\mathrm{S}}^2(t) = -\frac{7}{16\pi^2}g_{\mathrm{S}}^4(t), \tag{I.2}$$

$$\frac{d}{dt}g^2(t) = -\frac{19}{96\pi^2}g^4(t), \tag{I.3}$$

$$\frac{d}{dt}g'^2(t) = \frac{41}{96\pi^2}g'^4(t). \tag{I.4}$$

Because of the independence of (I.3) and (I.4) of Yukawa couplings and the Higgs self-coupling, these equations can be solved in a first step, yielding

$$g_{\mathrm{S}}^2(t) = g_{\mathrm{S}}^2(0)\left[1 + \frac{7g_{\mathrm{S}}^2(0)}{16\pi^2}t\right]^{-1}, \tag{I.5}$$

$$g^2(t) = g^2(0)\left[1 + \frac{19g^2(0)}{96\pi^2}t\right]^{-1}, \tag{I.6}$$

$$g'^2(t) = g'^2(0)\left[1 - \frac{41g'^2(0)}{96\pi^2}t\right]^{-1}. \tag{I.7}$$

The renormalization group equations for the Yukawa couplings read [94][59]

$$32\pi^2 \frac{d}{dt}U^2(t) = 3\big[U^2(t) - D^2(t)\big]U^2(t) + 2\big[\Sigma(t) - A_U(t)\big]U^2(t), \qquad \text{(I.8)}$$

$$32\pi^2 \frac{d}{dt}D^2(t) = 3\big[D^2(t) - U^2(t)\big]D^2(t) + 2\big[\Sigma(t) - A_D(t)\big]D^2(t), \qquad \text{(I.9)}$$

$$32\pi^2 \frac{d}{dt}L^2(t) = 3L^4(t) + 2\big[\Sigma(t) - A_L(t)\big]L^2(t), \qquad \text{(I.10)}$$

for the matrices $U = \text{diag}(h_u, h_c, h_t)$, $D = \text{diag}(h_d, h_s, h_b)$, $L = \text{diag}(h_e, h_\mu, h_\tau)$. The determination of the running of the lepton Yukawa couplings necessitates including all other fermionic Yukawa couplings as well, since in equations (I.8) through (I.10) we have

$$\Sigma(t) \equiv \text{tr}\big[3D^2(t) + 3U^2(t) + L^2(t)\big], \qquad \text{(I.11)}$$

$$A_U(t) \equiv 8g_S^2(t) + \frac{9}{4}g^2(t) + \frac{17}{12}g'^2(t), \qquad \text{(I.12)}$$

$$A_D(t) \equiv 8g_S^2(t) + \frac{9}{4}g^2(t) + \frac{5}{12}g'^2(t), \qquad \text{(I.13)}$$

$$A_L(t) \equiv \frac{9}{4}g^2(t) + \frac{15}{4}g'^2(t), \qquad \text{(I.14)}$$

and therefore quark Yukawa couplings are not power suppressed in (I.10). The coupled set of renormalization group equations for the Yukawa couplings can only be solved numerically. Finally, neglecting all but the (dominant) top quark Yukawa couplings the Higgs self-coupling λ satisfies the renormalization group equation [93]

$$16\pi^2 \frac{d}{dt}\lambda(t) = 12\lambda^2(t) + 6\lambda(t)h_t^2(t) - 3h_t^4(t) - \frac{3}{2}\lambda(t)\Big[3g^2(t) + g'^2(t)\Big]$$
$$+ \frac{3}{16}\Big[2g^4(t) + \big(g^2(t) + g'^2(t)\big)^2\Big]. \qquad \text{(I.15)}$$

It is now straightforward to solve the system of renormalization group equations with the initial conditions [3]

$$g_S^2(0) = 1.488, \qquad U^2(0) = \text{diag}(1.597 \cdot 10^{-10}, 5.363 \cdot 10^{-5}, 0.9874),$$
$$g^2(0) = 0.4246, \qquad D^2(0) = \text{diag}(7.288 \cdot 10^{-10}, 2.977 \cdot 10^{-7}, 5.764 \cdot 10^{-4}),$$
$$g'^2(0) = 0.1277, \qquad L^2(0) = \text{diag}(8.614 \cdot 10^{-12}, 3.683 \cdot 10^{-7}, 1.042 \cdot 10^{-4}),$$
$$\lambda(0) = 0.1292. \qquad \text{(I.16)}$$

---

[59]It is more useful for our purposes to work with the squared Yukawa couplings and their renormalization group equations. They are easily obtained from the equations in [94] by multiplying with the matrices U, D, L.

The coefficient Γ at temperatures relevant for μ_{R} or τ_{R} equilibration

Our results in chapter 3 can be applied to higher temperatures, corresponding to the coefficient entering the equilibration rates of right-handed charges carried by the heavier leptons, to some extent.

The contribution to Γ from $2 \to 2$ scattering (3.53) remains unchanged, up to trivial exchange of the corresponding Yukawa coupling (which is, of course, also needed for generalization of the LPM resummed rate), and one just has to evolve the large Standard Model couplings appearing in (3.53) to the corresponding scale. This is due to the fact that in the symmetric phase the particles carry only thermal masses and these are flavor-blind. The LPM contribution, however, has to be reevaluated at the higher temperatures, since the couplings enter at various steps in the numerical computation. Table 3 shows the numerical results for temperatures between 10^9 GeV and 10^{13} GeV, and it constitutes the continuation of the results found in table 1.

We now revisit the fit to the LPM contribution in (3.55). For the temperature interval $8.5 \cdot 10^4$ GeV $\leq T \leq 3 \cdot 10^{11}$ GeV which we expect to play a role in the equilibration of charges violated by h_μ, we obtain the fit parameters[60]

$$d_t = 0.600, \qquad d_{\ell_e} = 1.56, \qquad d_{e_{\mathrm{R}}} = 1.08, \qquad \text{(J.1)}$$

while in the range $3 \cdot 10^9$ GeV $\leq T \leq 10^{13}$ GeV which we expect to be relevant for charges carried by the τ_{R}, we find

$$d_t = 0.819, \qquad d_{\ell_e} = 1.44, \qquad d_{e_{\mathrm{R}}} = 1.18. \qquad \text{(J.2)}$$

---

[60]We stick to the notation of (3.55), even though in this context the denomination of the fit parameters d_{ℓ_e} and $d_{e_{\mathrm{R}}}$ might be a bit misleading.

Table 3: Continuation of table 1 to higher temperatures. Again the numerical uncertainty in the LPM contribution is below 2%.

T/GeV	$\Gamma^{2\to2}/(h_e^2 T^3)$	$\Gamma^{\mathrm{LPM}}/(h_e^2 T^3)$	$\Gamma/(h_e^2 T^3)$
$4.19 \cdot 10^9$	$1.06 \cdot 10^{-3}$	$4.11 \cdot 10^{-4}$	$1.47 \cdot 10^{-3}$
$1.68 \cdot 10^{10}$	$1.05 \cdot 10^{-3}$	$4.09 \cdot 10^{-4}$	$1.46 \cdot 10^{-3}$
$6.71 \cdot 10^{10}$	$1.04 \cdot 10^{-3}$	$4.06 \cdot 10^{-4}$	$1.45 \cdot 10^{-3}$
$2.68 \cdot 10^{11}$	$1.03 \cdot 10^{-3}$	$4.04 \cdot 10^{-4}$	$1.43 \cdot 10^{-3}$
$1.07 \cdot 10^{12}$	$1.03 \cdot 10^{-3}$	$4.03 \cdot 10^{-4}$	$1.43 \cdot 10^{-3}$
$4.29 \cdot 10^{12}$	$1.02 \cdot 10^{-3}$	$4.01 \cdot 10^{-4}$	$1.42 \cdot 10^{-3}$
$1.72 \cdot 10^{13}$	$1.02 \cdot 10^{-3}$	$4.00 \cdot 10^{-4}$	$1.42 \cdot 10^{-3}$

Like in the electron case, the fits for the heavier flavors have a way smaller error than our numerical uncertainty in the evaluation of (3.36).

The considerations in this appendix need to be supplied with an analysis of the relevant (flavor non-diagonal) charges and the respective susceptibilities at the higher temperatures in order to obtain results for the complete equilibration rates. We leave this examination to future studies.

List of Figures

List of Tables

References

[1] D. Bödeker and D. Schröder, *Kinetic equations for sterile neutrinos from thermal fluctuations*, *JCAP* **2002** (2020) 033, [`1911.05092`].

[2] D. Bödeker and D. Schröder, *Equilibration of right-handed electrons*, *JCAP* **1905** (2019) 010, [`1902.07220`].

[3] PARTICLE DATA GROUP collaboration, M. Tanabashi et al., *Review of Particle Physics*, *Phys. Rev.* **D98** (2018) 030001.

[4] PLANCK collaboration, N. Aghanim et al., *Planck 2018 results. VI. Cosmological parameters*, `1807.06209`.

[5] V. A. Rubakov and D. S. Gorbunov, *Introduction to the Theory of the Early Universe.* World Scientific, Singapore, 2017, 10.1142/10447.

[6] S. Burles, K. M. Nollett and M. S. Turner, *What is the BBN prediction for the baryon density and how reliable is it?*, *Phys. Rev.* **D63** (2001) 063512, [`astro-ph/0008495`].

[7] A. D. Sakharov, *Violation of CP Invariance, C asymmetry, and baryon asymmetry of the universe*, *Pisma Zh. Eksp. Teor. Fiz.* **5** (1967) 32–35.

[8] ATLAS collaboration, G. Aad et al., *Observation of a new particle in the search for the Standard Model Higgs boson with the ATLAS detector at the LHC*, *Phys. Lett.* **B716** (2012) 1–29, [`1207.7214`].

[9] CMS collaboration, S. Chatrchyan et al., *Observation of a New Boson at a Mass of 125 GeV with the CMS Experiment at the LHC*, *Phys. Lett.* **B716** (2012) 30–61, [`1207.7235`].

[10] K. Kajantie, M. Laine, K. Rummukainen and M. E. Shaposhnikov, *Is there a hot electroweak phase transition at m(H) larger or equal to m(W)?*, *Phys. Rev. Lett.* **77** (1996) 2887–2890, [`hep-ph/9605288`].

[11] V. A. Kuzmin, V. A. Rubakov and M. E. Shaposhnikov, *On the Anomalous Electroweak Baryon Number Nonconservation in the Early Universe*, *Phys. Lett.* **155B** (1985) 36.

[12] M. B. Gavela, P. Hernandez, J. Orloff and O. Pene, *Standard model CP violation and baryon asymmetry*, *Mod. Phys. Lett.* **A9** (1994) 795–810, [hep-ph/9312215].

[13] P. Huet and E. Sather, *Electroweak baryogenesis and standard model CP violation*, *Phys. Rev.* **D51** (1995) 379–394, [hep-ph/9404302].

[14] M. B. Gavela, P. Hernandez, J. Orloff, O. Pene and C. Quimbay, *Standard model CP violation and baryon asymmetry. Part 2: Finite temperature*, *Nucl. Phys.* **B430** (1994) 382–426, [hep-ph/9406289].

[15] D. E. Morrissey and M. J. Ramsey-Musolf, *Electroweak baryogenesis*, *New J. Phys.* **14** (2012) 125003, [1206.2942].

[16] M. M. Wygas, I. M. Oldengott, D. Bödeker and D. J. Schwarz, *Cosmic QCD Epoch at Nonvanishing Lepton Asymmetry*, *Phys. Rev. Lett.* **121** (2018) 201302, [1807.10815].

[17] F. Zwicky, *Die Rotverschiebung von extragalaktischen Nebeln*, *Helv. Phys. Acta* **6** (1933) 110–127.

[18] V. C. Rubin and W. K. Ford, Jr., *Rotation of the Andromeda Nebula from a Spectroscopic Survey of Emission Regions*, *Astrophys. J.* **159** (1970) 379–403.

[19] J. P. Ostriker and P. J. E. Peebles, *A Numerical Study of the Stability of Flattened Galaxies: or, can Cold Galaxies Survive?*, *Astrophys. J.* **186** (1973) 467–480.

[20] PLANCK collaboration, Y. Akrami et al., *Planck 2018 results. I. Overview and the cosmological legacy of Planck*, 1807.06205.

[21] R. Massey, T. Kitching and J. Richard, *The dark matter of gravitational lensing*, *Rept. Prog. Phys.* **73** (2010) 086901, [1001.1739].

[22] C. S. Wu, E. Ambler, R. W. Hayward, D. D. Hoppes and R. P. Hudson, *Experimental Test of Parity Conservation in Beta Decay*, *Phys. Rev.* **105** (1957) 1413–1414.

[23] S. Alekhin et al., *A facility to Search for Hidden Particles at the CERN SPS: the SHiP physics case*, *Rept. Prog. Phys.* **79** (2016) 124201, [`1504.04855`].

[24] M. Drewes et al., *A White Paper on keV Sterile Neutrino Dark Matter*, *JCAP* **1701** (2017) 025, [`1602.04816`].

[25] M. Fukugita and T. Yanagida, *Baryogenesis Without Grand Unification*, *Phys. Lett.* **B174** (1986) 45–47.

[26] V. A. Rubakov and M. E. Shaposhnikov, *Electroweak baryon number nonconservation in the early universe and in high-energy collisions*, *Usp. Fiz. Nauk* **166** (1996) 493–537, [`hep-ph/9603208`].

[27] M. D'Onofrio, K. Rummukainen and A. Tranberg, *Sphaleron Rate in the Minimal Standard Model*, *Phys. Rev. Lett.* **113** (2014) 141602, [`1404.3565`].

[28] S. Yu. Khlebnikov and M. E. Shaposhnikov, *Melting of the Higgs vacuum: Conserved numbers at high temperature*, *Phys. Lett.* **B387** (1996) 817–822, [`hep-ph/9607386`].

[29] D. Bödeker and M. Sangel, *Order g^2 susceptibilities in the symmetric phase of the Standard Model*, *JCAP* **1504** (2015) 040, [`1501.03151`].

[30] K. Moffat, S. Pascoli, S. T. Petcov, H. Schulz and J. Turner, *Three-flavored nonresonant leptogenesis at intermediate scales*, *Phys. Rev.* **D98** (2018) 015036, [`1804.05066`].

[31] S. Davidson, E. Nardi and Y. Nir, *Leptogenesis*, *Phys. Rept.* **466** (2008) 105–177, [`0802.2962`].

[32] A. Pilaftsis and T. E. J. Underwood, *Resonant leptogenesis*, *Nucl. Phys.* **B692** (2004) 303–345, [`hep-ph/0309342`].

[33] E. K. Akhmedov, V. A. Rubakov and A. Yu. Smirnov, *Baryogenesis via neutrino oscillations*, *Phys. Rev. Lett.* **81** (1998) 1359–1362, [`hep-ph/9803255`].

[34] T. Asaka and M. Shaposhnikov, *The nuMSM, dark matter and baryon asymmetry of the universe*, *Phys. Lett.* **B620** (2005) 17–26, [`hep-ph/0505013`].

[35] P. Hernández, M. Kekic, J. López-Pavón, J. Racker and J. Salvado, *Testable Baryogenesis in Seesaw Models*, *JHEP* **08** (2016) 157, [`1606.06719`].

[36] J. Ghiglieri and M. Laine, *GeV-scale hot sterile neutrino oscillations: a numerical solution*, *JHEP* **02** (2018) 078, [`1711.08469`].

[37] S. Dodelson and L. M. Widrow, *Sterile-neutrinos as dark matter*, *Phys. Rev. Lett.* **72** (1994) 17–20, [`hep-ph/9303287`].

[38] A. Boyarsky, J. Lesgourgues, O. Ruchayskiy and M. Viel, *Lyman-alpha constraints on warm and on warm-plus-cold dark matter models*, *JCAP* **0905** (2009) 012, [`0812.0010`].

[39] X.-D. Shi and G. M. Fuller, *A New dark matter candidate: Nonthermal sterile neutrinos*, *Phys. Rev. Lett.* **82** (1999) 2832–2835, [`astro-ph/9810076`].

[40] J. F. Cherry and S. Horiuchi, *Closing in on Resonantly Produced Sterile Neutrino Dark Matter*, *Phys. Rev.* **D95** (2017) 083015, [`1701.07874`].

[41] J. Ghiglieri and M. Laine, *Improved determination of sterile neutrino dark matter spectrum*, *JHEP* **11** (2015) 171, [`1506.06752`].

[42] M. Shaposhnikov, *The nuMSM, leptonic asymmetries, and properties of singlet fermions*, *JHEP* **08** (2008) 008, [`0804.4542`].

[43] J. Ghiglieri and M. Laine, *Sterile neutrino dark matter via GeV-scale lepto-genesis?*, *JHEP* **07** (2019) 078, [`1905.08814`].

[44] B. A. Campbell, S. Davidson, J. R. Ellis and K. A. Olive, *On the baryon, lepton flavor and right-handed electron asymmetries of the universe*, *Phys. Lett.* **B297** (1992) 118–124, [`hep-ph/9302221`].

[45] J. M. Cline, K. Kainulainen and K. A. Olive, *Protecting the primordial baryon asymmetry from erasure by sphalerons*, *Phys. Rev.* **D49** (1994) 6394–6409, [`hep-ph/9401208`].

[46] M. Joyce and M. E. Shaposhnikov, *Primordial magnetic fields, right-handed electrons, and the Abelian anomaly*, *Phys. Rev. Lett.* **79** (1997) 1193–1196, [`astro-ph/9703005`].

[47] D. Bodeker and M. Laine, *Kubo relations and radiative corrections for lepton number washout*, *JCAP* **1405** (2014) 041, [`1403.2755`].

[48] E. W. Kolb and M. S. Turner, *The early universe*, vol. 69 of *Frontiers in physics*. Addison-Wesley, Redwood City, 1990.

[49] L. D. Landau and E. M. Lifshitz, *Statistical Physics, Part 1*, vol. 5 of *Course of Theoretical Physics*. Butterworth-Heinemann, Oxford, 1980.

[50] D. Bodeker and M. Sangel, *Lepton asymmetry rate from quantum field theory: NLO in the hierarchical limit*, *JCAP* **1706** (2017) 052, [`1702.02155`].

[51] J. Zinn-Justin, *Quantum field theory and critical phenomena*, *Int. Ser. Monogr. Phys.* **77** (1989) 1–914.

[52] R. Barbieri, P. Creminelli, A. Strumia and N. Tetradis, *Baryogenesis through leptogenesis*, *Nucl. Phys.* **B575** (2000) 61–77, [`hep-ph/9911315`].

[53] G. D. Moore and M. Tassler, *The Sphaleron Rate in SU(N) Gauge Theory*, *JHEP* **02** (2011) 105, [`1011.1167`].

[54] J. Ghiglieri and M. Laine, *GeV-scale hot sterile neutrino oscillations: a derivation of evolution equations*, *JHEP* **05** (2017) 132, [`1703.06087`].

[55] S. Eijima, M. Shaposhnikov and I. Timiryasov, *Freeze-out of baryon number in low-scale leptogenesis*, *JCAP* **1711** (2017) 030, [`1709.07834`].

[56] J. Ghiglieri and M. Laine, *Precision study of GeV-scale resonant leptogenesis*, *JHEP* **02** (2019) 014, [`1811.01971`].

[57] G. Sigl and G. Raffelt, *General kinetic description of relativistic mixed neutrinos*, *Nucl. Phys.* **B406** (1993) 423–451.

[58] T. Asaka, S. Eijima and H. Ishida, *Kinetic Equations for Baryogenesis via Sterile Neutrino Oscillation*, *JCAP* **1202** (2012) 021, [`1112.5565`].

[59] S. Eijima, M. Shaposhnikov and I. Timiryasov, *Parameter space of baryogenesis in the νMSM*, *JHEP* **07** (2019) 077, [`1808.10833`].

[60] A. Abada, G. Arcadi, V. Domcke, M. Drewes, J. Klaric and M. Lucente, *Low-scale leptogenesis with three heavy neutrinos*, *JHEP* **01** (2019) 164, [`1810.12463`].

[61] M. Beneke, B. Garbrecht, C. Fidler, M. Herranen and P. Schwaller, *Flavoured Leptogenesis in the CTP Formalism*, *Nucl. Phys.* **B843** (2011) 177–212, [`1007.4783`].

[62] J.-S. Gagnon and M. Shaposhnikov, *Baryon Asymmetry of the Universe without Boltzmann or Kadanoff-Baym equations*, Phys. Rev. **D83** (2011) 065021, [1012.1126].

[63] M. Drewes and B. Garbrecht, *Leptogenesis from a GeV Seesaw without Mass Degeneracy*, JHEP **03** (2013) 096, [1206.5537].

[64] M. Drewes, B. Garbrecht, D. Gueter and J. Klaric, *Leptogenesis from Oscillations of Heavy Neutrinos with Large Mixing Angles*, JHEP **12** (2016) 150, [1606.06690].

[65] D. Bödeker, M. Sangel and M. Wörmann, *Equilibration, particle production, and self-energy*, Phys. Rev. **D93** (2016) 045028, [1510.06742].

[66] J. Ghiglieri and M. Laine, *Neutrino dynamics below the electroweak crossover*, JCAP **1607** (2016) 015, [1605.07720].

[67] M. Laine and A. Vuorinen, *Basics of Thermal Field Theory*, Lect. Notes Phys. **925** (2016) pp.1–281, [1701.01554].

[68] Y. Burnier, M. Laine and M. Shaposhnikov, *Baryon and lepton number violation rates across the electroweak crossover*, JCAP **0602** (2006) 007, [hep-ph/0511246].

[69] D. Besak and D. Bodeker, *Thermal production of ultrarelativistic right-handed neutrinos: Complete leading-order results*, JCAP **1203** (2012) 029, [1202.1288].

[70] A. Anisimov, D. Besak and D. Bodeker, *Thermal production of relativistic Majorana neutrinos: Strong enhancement by multiple soft scattering*, JCAP **1103** (2011) 042, [1012.3784].

[71] L. D. Landau and I. Pomeranchuk, *Limits of applicability of the theory of bremsstrahlung electrons and pair production at high-energies*, Dokl. Akad. Nauk Ser. Fiz. **92** (1953) 535–536.

[72] L. D. Landau and I. Pomeranchuk, *Electron cascade process at very high-energies*, Dokl. Akad. Nauk Ser. Fiz. **92** (1953) 735–738.

[73] A. B. Migdal, *Bremsstrahlung and pair production in condensed media at high-energies*, Phys. Rev. **103** (1956) 1811–1820.

[74] R. Baier, Y. L. Dokshitzer, A. H. Mueller, S. Peigne and D. Schiff, *Radiative energy loss of high-energy quarks and gluons in a finite volume quark - gluon plasma*, Nucl. Phys. **B483** (1997) 291–320, [`hep-ph/9607355`].

[75] B. G. Zakharov, *Fully quantum treatment of the Landau-Pomeranchuk-Migdal effect in QED and QCD*, JETP Lett. **63** (1996) 952–957, [`hep-ph/9607440`].

[76] P. B. Arnold, G. D. Moore and L. G. Yaffe, *Photon and gluon emission in relativistic plasmas*, JHEP **06** (2002) 030, [`hep-ph/0204343`].

[77] D. G. Figueroa and M. Shaposhnikov, *Anomalous non-conservation of fermion/chiral number in Abelian gauge theories at finite temperature*, JHEP **04** (2018) 026, [`1707.09967`].

[78] B. Garbrecht, F. Glowna and P. Schwaller, *Scattering Rates For Leptogenesis: Damping of Lepton Flavour Coherence and Production of Singlet Neutrinos*, Nucl. Phys. **B877** (2013) 1–35, [`1303.5498`].

[79] H. A. Weldon, *Effective Fermion Masses of Order gT in High Temperature Gauge Theories with Exact Chiral Invariance*, Phys. Rev. **D26** (1982) 2789.

[80] P. B. Arnold, G. D. Moore and L. G. Yaffe, *Photon emission from ultrarelativistic plasmas*, JHEP **11** (2001) 057, [`hep-ph/0109064`].

[81] P. Aurenche, F. Gelis, G. D. Moore and H. Zaraket, *Landau-Pomeranchuk-Migdal resummation for dilepton production*, JHEP **12** (2002) 006, [`hep-ph/0211036`].

[82] R. Baier, Y. L. Dokshitzer, A. H. Mueller, S. Peigne and D. Schiff, *Radiative energy loss and p(T) broadening of high-energy partons in nuclei*, Nucl. Phys. **B484** (1997) 265–282, [`hep-ph/9608322`].

[83] B. G. Zakharov, *Radiative energy loss of high-energy quarks in finite size nuclear matter and quark - gluon plasma*, JETP Lett. **65** (1997) 615–620, [`hep-ph/9704255`].

[84] M. E. Carrington, *The Effective potential at finite temperature in the Standard Model*, Phys. Rev. **D45** (1992) 2933–2944.

[85] P. Arnold and S. Iqbal, *The LPM effect in sequential bremsstrahlung*, JHEP **04** (2015) 070, [`1501.04964`].

[86] H. A. Weldon, *Simple Rules for Discontinuities in Finite Temperature Field Theory, Phys. Rev.* **D28** (1983) 2007.

[87] M. Laine, *Thermal 2-loop master spectral function at finite momentum, JHEP* **05** (2013) 083, [`1304.0202`].

[88] K. Kamada and A. J. Long, *Baryogenesis from decaying magnetic helicity, Phys. Rev.* **D94** (2016) 063501, [`1606.08891`].

[89] A. J. Long, E. Sabancilar and T. Vachaspati, *Leptogenesis and Primordial Magnetic Fields, JCAP* **1402** (2014) 036, [`1309.2315`].

[90] D. T. Son and P. Surowka, *Hydrodynamics with Triangle Anomalies, Phys. Rev. Lett.* **103** (2009) 191601, [`0906.5044`].

[91] P. B. Arnold, G. D. Moore and L. G. Yaffe, *Transport coefficients in high temperature gauge theories. 1. Leading log results, JHEP* **11** (2000) 001, [`hep-ph/0010177`].

[92] I. S. Gradshteyn and I. M. Ryzhik, *Table of integrals, series, and products.* D. Zwillinger (editor), Academic Press, San Diego, CA, 8. ed., 2014.

[93] J. F. Gunion, H. E. Haber, G. L. Kane and S. Dawson, *The Higgs Hunter's Guide, Front. Phys.* **80** (2000) 1–404.

[94] N. Cabibbo, L. Maiani, G. Parisi and R. Petronzio, *Bounds on the Fermions and Higgs Boson Masses in Grand Unified Theories, Nucl. Phys.* **B158** (1979) 295–305.